POLITECNICO DI TORINO

Corso di Laurea
in Ingegneria Matematica percorso Modellistico

Tesi di Laurea Magistrale

Derivation and travelling wave analysis of partial integro-differential equation models for EMT-mediated immunosuppression in cancer

Relatori
prof. Tommaso Lorenzi
prof. Luigi Preziosi
firma dei relatori

. . . . . .
. . . . . .

Candidato
Jacopo Mensa

firma del candidato

. . . . . .

Anno Accademico 2023-2024

alla mia famiglia
ai miei amici

Summary

The work presented here deals with the derivation and travelling wave analysis of partial integrodifferential equation models for EMT-mediated immunosuppression in cancer with phenotypic heterogeneity, including also the dynamics of killer and regulatory immune cells. Existing literature addresses models of cancer invasion with phenotypic variability, primarily focusing on aspects such as the movement of cancer cells by chemotaxis or haptotaxis. However, none of these specifically cover the dynamics of regulatory and killer cells during the EMT transition and their impact on the immune response to cancer progression. This knowledge gap is one of the reasons why we have chosen to explore this topic.

To gain a better understanding of the phenomenon, we conducted bibliographic research, examining various biological studies. This led to the development of a mathematical model that is both accurate and biologically consistent, yet simple enough to be tackled using appropriate mathematical tools to yield results. Experimental evidence shows that mesenchymal cancer cells promote the recruitment of regulatory cells, which, in turn, inhibit the immune response of killer cells, creating an immunosuppressive microenvironment that protects the tumor. Conversely, epithelial cancer cells are associated with lesser recruitment of regulatory cells, resulting in a higher presence of killer cells and thus a more pronounced immune action. This is particularly evident in carcinomas, where the roles of regulatory and killer cells are respectively played by T cells and CD8+ T cells.

In this work, we assume that cancer cells could have a phenotypic state ranging from totally epithelial to completely mesenchymal, which we model through the structure variable y. Including the phenotypic trait allows us to take into account intrapopulation heterogeneity in cancer, which is a key factor influencing various dynamic aspects. Specifically, a mesenchymal phenotype is characterized by high mobility and low proliferative ability, while an epithelial phenotype prioritizes reproduction over movement, reflecting the biological principle of "go or grow". Mesenchymal cells show a high production of chemical attractant, which is responsible for recruiting regulatory cells. Indeed, regulatory cells undergo chemotactic movement, migrating towards areas with greater attractant concentration. On the other hand, killer cells move up the density gradient of cancer cells and their activity is inhibited in the presence of a sufficient concentration of regulatory cells. These biological considerations are expressed mathematically by carefully choosing functions to model the phenotype-dependent mobility, production, and growth of cancer cells, as well as the chemical-dependent growth of regulatory and killer cells. Using these functions, we can define jump probabilities in branching random walks on a lattice in both

physical and phenotypic space, formulating three coupled discrete agent-based models for the densities of cancer, regulatory and killer cells. These are also coupled with a discrete finite difference equation for the concentration of the chemical attractant.
Through limit procedures and under appropriate regularity assumptions, we formally derive the corresponding continuous model, composed of two partial integrodifferential equations (IPDE) for the density of cancer and killer cells, coupled with two partial differential equations (PDE) for the concentration of the chemical attractant and the density of regulatory cells. Despite the system's complexity, we show through formal asymptotic techniques that a detailed analysis within the framework of the travelling wave can be performed, obtaining invasion fronts with phenotypic structure.
As a preliminary step, we rescale the continuous model with appropriate powers of a small parameter ε, according to the biological relevance of the terms within the equations.
Then we introduce the WKB ansatz for the density of cancer cells. Combining this approach with asymptotic expansions of the involved quantities, we derive an equation and a constraint for u as $\varepsilon \to 0$. Through several mathematical steps, we obtain a transport equation for $\bar{y}$, that is the value of the dominant phenotypic trait at position x and time t. We can conclude that the density of cancer cells converges to a Dirac delta distribution centred at the maximum phenotype $\bar{y}$.
Shifting our focus to the traveling wave framework, we investigate the monotonicity of traveling front solutions, the wavefront position and the minimum propagation speed. We conclude that the maximum phenotypic trait $\bar{y}$ presents a monotonically increasing profile along the wave variable $z = x - ct$ while the density of cancer cells ρ has a decreasing behaviour. Using these results within the remaining equations, we can finally derive the profiles of the chemical concentration and densities of killer and regulatory cells.
As expected from biological evidence, mesenchymal cells dominate the wavefront while epithelial cells reside at the rear, following a leader-stalker cell dynamics. Various scenarios are proposed to investigate how the emergence of a spatial organisation influences the degree of infiltration of killer cells into the tumour via the concentration of attractant and regulatory cells.

Acknowledgements

Un ringraziamento particolare a tutti quelli che mi sono stati accanto in questo percorso lungo, a tratti travagliato ma bellissimo che mi ha portato al conseguimento della Laurea Magistrale. Alla mia famiglia che è la cosa più importante che ho, che non mi ha mai fatto mancare nulla e mi ha sempre sostenuto e consigliato correttamente anche nei momenti più difficili, mostrandomi la giusta strada e spronandomi a dare il massimo sempre, senza di voi non ce l'avrei fatta. Un ringraziamento speciale anche a tutte le persone che hanno alleggerito questo viaggio: ai miei amici storici del mio paese che ci sono sempre stati, ai miei amici del liceo con cui sono felice di essere rimasto in stretto contatto, cosa non scontata e infine ai nuovi e preziosi amici che ho conosciuto tra i banchi dell'università, con cui ho condiviso gioie e dolori e tante vicissitudini in questi anni e con cui spero di mantenere una duratura amicizia una volta terminata questa esperienza. Spero di aver dato a tutti voi almeno una piccola parte di quello che voi avete dato a me. Ringrazio anche i professori che ho conosciuto durante questo percorso e che hanno contribuito a rendere unica la mia esperienza all'interno del Politecnico. In particolare ci tengo a ringraziare il professor Lorenzi per la grande competenza, enorme disponibilità, gentilezza e simpatia dimostrate in più occasioni. Per me è stato un piacere averla come relatore per i miei lavori di tesi magistrale e triennale. Collaborare con Lei mi ha permesso di mparare tantissime cose e scoprire un ramo della matematica che non conoscevo e di cui mi sono appassionato. Ringrazio anche il professor Preziosi per la simpatia, la disponibilità e i consigli fornitemi per il prosequio della mia carriera accademica.

Contents

List of Figures

Part I

First Part

Chapter 1

Introduction

1.1 Biological Background

In the following paragraph, we give a detailed biological description of the EMT program [150] with particular interest in its role in cancer invasion and its immunosuppressive implications. Focusing on the biological assumptions on which our mathematical model relies, we underline the main features that are the basis of our work. A brief and general description of cancer metastasis and invasion process is also given.

1.1.1 Metastasis and Invasion Process in Cancer

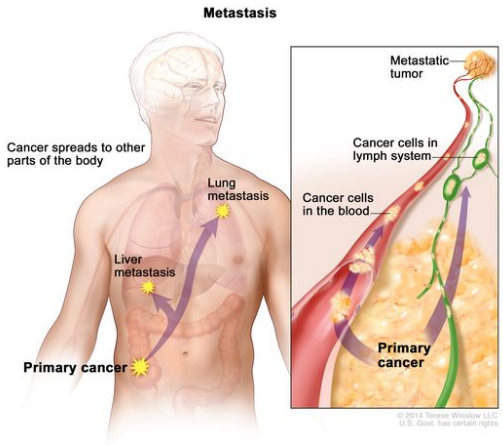

Figure 1.1. Metastasis is defined as the biological process leading to the formation of a secondary neoplasm far from the primary tumour site. Reproduced from "NCI Dictionary of Cancer Terms" [43].

According to [43], cancer metastasis is defined as the process leading to the spread and dissemination of cancer cells from their original location (i.e., the primary tumor site,

where they first formed) to another organ of the body [99].

The development of carcinoma metastases involves a complex sequence of biological events called the "invasion-metastasis cascade" [47]. We refer to Figure 1.3 for a schematic representation of the several steps composing this complex process, which are explained more in detail in the following [139].

Local Invasion

At first, epithelial cells composing the primary tumour locally invade the surrounding extracellular matrix (ECM) and stromal cell layers (local invasion step). In order to facilitate invasion, carcinoma cells increase the production of metalloproteinases, which in turn degrade the basement membrane (BM) and the surrounding extracellular matrix (ECM). Depending on the microenvironmental conditions, cancer cells can migrate as cohesive units (collective invasion) or as "single cells"(mesenchymal or ameboid invasion) [144]. In the latter case, cancer cells undergo the epithelial-to-mesenchymal (EMT) transition to facilitate invasion. As a result, intercellular junctions that hold together the epithelial tissue are dissolved, increasing cell invasiveness [134]. Furthermore, EMT is orchestrated by some transcription factors that also lower E-cadherin levels, the milestone of the epithelial phenotype.

Intravasation, Transport and Survival in Circulation

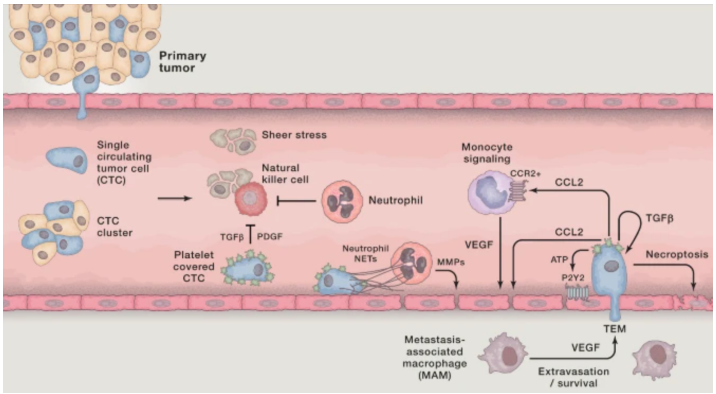

Figure 1.2. The travel of cancer cells in the circulation system. After intravasation, some mechanisms help cancer cells during their path (e.g. neutrophils that facilitate extravasation and metalloproteinases secretion) while others factors act to destroy them (e.g. mechanical stresses, immune attacks by NK cells). Reproduced from Lambert et al. [78]

At some point during the local invasion, cancer cells reach the vasculature and penetrate the walls of microvessels, which are made of endothelial cells. If this first step is successful, cancer cells are transported through the vasculature, disseminating via circulation (intravasation and transport step). The complexity of the intravasation step highly depends on the geometry and topology of blood vessels. Tumor cells could also promote the

formation of new, tortuous, and inefficient blood vessels through the secretion of vascular endothelial growth factors (VEGFs) [27]. This process is called "neoangiogenesis". Circulating tumor cells (CTCs) have an estimated life of several hours [93] before dying due to the leak of adhesion to ECM (anoikis) [60]. In addition, CTCs have a larger diameter than the blood vessels, resulting in the majority of CTCs being trapped in the capillary shortly after entering the circulation. Furthermore, cancer cells resist the hemodynamic shear forces and cooperate to face immune attacks of killer cells by forming large clusters called "emboli" [72].

Arrest at distant locations and extravasation

During their travel through the vasculature, CTCs stop at certain locations due to topological restrictions of the vessels or the detection of specific signals indicating favourable conditions (arrest step). Thus, metastases are formed by carcinomas only on a limited set of organs [47]. At this point, CTCs cross from vessels into the surrounding tissues (extravasation step). To facilitate this process, the primary tumor is able to secrete factors that enhance vascular permeability, for example in the extravasation of breast cancer cells into the lungs [62, 102]. We highlight that intravasation and extravasation steps are not simply the "inverse" mechanism, but they are very different since they involve different microenvironments, macrophage populations [117] and vasculature [27].

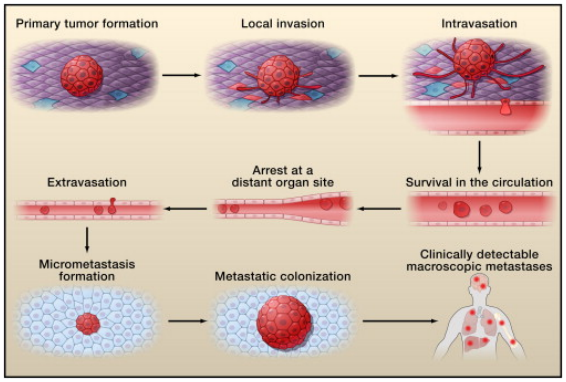

Figure 1.3. The invasion-metastasis cascade. Initially, tumor cells depart from their primary growth sites through local invasion and intravasation processes. Subsequently, these cells undergo systemic translocation, including survival in the circulatory system, arrest within a distant organ site, and extravasation. Upon reaching a new location, these cells adapt to and thrive within the foreign microenvironments of remote tissues, forming micrometastases and establishing metastatic colonization. Reproduced from Valastyan et al. [139]

Micrometastasis Formation and Metastatic Colonization

After extravasation, cells struggle to survive in the new hostile microenvironment to form micrometastases (micrometastasis formation step). In some instances, primary tumors

secrete signals that convert this hostile microenvironment into a more hospitable one before the arrival of cancer cells [115]. In this way, the death rate of the new unadapted cancer cells is lowered, and the chances of surviving increase. Finally, the surviving cells proliferate at metastatic sites, creating macroscopic neoplasms (colonization step). Of note is that micrometastasis could enter a state of dormancy due to the incompatible microenvironment and proliferate only a long time after their first establishment [31], for example in mammary carcinoma [12]. Alternatively, the metastatic colony could stay the same in number also because its continuous proliferation is counterbalanced by apoptosis caused by immune actions [31], like in prostate tumor [73]. The most successful cells in metastatic colonization are called "tumor-initiating cells" (TICs), which have great self-renewal capacity and are only a few within a tumor. Once again, EMT is essential since its transcription factors stimulate the conversion of carcinoma cells into TICs, conferring replication properties [134]. In conclusion, metastasis is a challenging and inefficient process, given that only a very low percentage (around 0.01% [31]) of initial CTCs successfully complete all metastasis steps and generate macroscopic neoplasms (secondary tumor establishment step).

1.1.2 The Epithelial-to-Mesenchymal Transition (EMT)

Basics of the EMT program

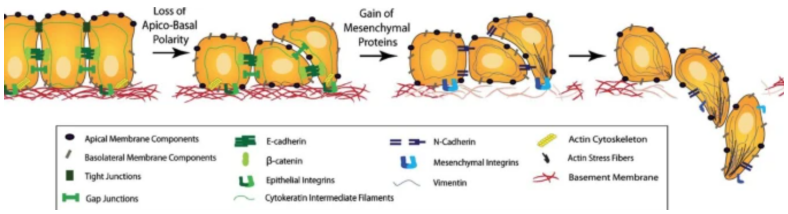

Figure 1.4. Essential representation of the main features linked with the EMT program. Epithelial cells undergoing EMT lose cell-cell adhesion and acquire mesenchymal features, increasing their invading power. Reproduced from Michelizzi et al. [94]

The epithelial-to-mesenchymal transition (EMT) is a cell program occurring in various biological scenarios. Shortly, EMT is the process through which epithelial cells change their structure, assuming mesenchymal characteristics [96] (see Figure 1.4). This means migrating from E to M along the phenotypic axis. This process is not a "black or white" situation since evidence proves that the transition from E to M could also be partial. In this sense, a spectrum of intermediate states is generated, in which cells acquire many but not all mesenchymal features (see Figure 1.5). In this sense, carcinosarcomas are an "exception" since there's a net separation between mesenchymal and epithelial cells with no intermediate states assumed [135]. Of note, the EMT program has multiple variants, depending on the type of cells involved, triggering TFs factors and cellular microenvironment. Specific indicators called EMT biomarkers are involved in EMT transition, allowing us to monitor this process. One of the most important epithelial markers is E-cadherin, which maintains cell-to-cell and cell-to-matrix adhesion. The downregulation of

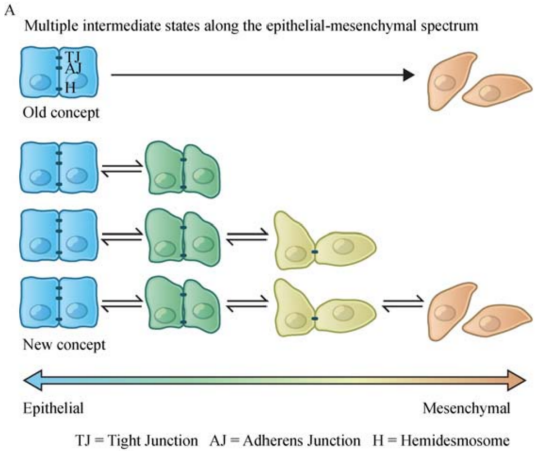

Figure 1.5. The plasticity of the EMT transition. The EMT program is not the unidirectional transition from epithelial to mesenchymal phenotype but intermediate states are also generated between the two extremes in which the cell only partially exhibits mesenchymal characteristics. Reproduced from Zhang et al. [150]

E-cadherin results in the up-regulation of N-cadherin, a mesenchymal marker enhancing cellular motility [89]. Transcriptor factors linked with the EMT program and affecting the regulation of E-cadherin are Slug and Snail (SNAI1), ZEB-1 and TWIST. In particular, these TFs inhibit the expression of the E-cadherin, facilitating EMT transition and promoting invasion [89]. A more detailed dissertation on the contexts in which TFs work is given below.

EMT program has a key role in a wide range of biological processes. In embryonic morphogenesis, EMT plays a fundamental role in the differentiation of metazoan into various cell types [81, 96]. In fact, significant developmental deficits arise when EMT factors are suppressed [28, 35, 69, 71, 140]. From tissue fibrosis and cancer progression to wound healing, EMT is involved in a wide range of pathological processes [96, 125]. During wound healing, epithelial cells at the edge of the wound undergo the EMT transition in order to acquire motility and rebuild the tissue. Subsequently, these cells reverse the process (MET) to accelerate growth and reinstate the integrity of the sheet [124].

In tumor progression, EMT-acquired mesenchymal features are fundamental for carcinoma cells to complete invasion and metastasis steps (invasion in the primary site, intravasation in blood vessels, and extravasation) [78, 133]. In the metastasis colonization process, the EMT reversibility into MET is crucial (see Figure 1.6). At early stages, cells undergo EMT, acquiring mesenchymal features like enhanced motility. This allows tumor cells to disseminate better (dissemination step). Afterwards, cells reverse the process into MET, acquiring epithelial features like high growth ability. This facilitates the formation of macroscopic metastases and promote the establishment of a secondary tumor [80, 98, 136].

In multiple types of cancer, stem-like cells could be generated by the EMT transition. A cancer stem cell (CSC) has some peculiar features, like high self-renewal and the ability to

regenerate the tumor tissue [23, 107, 125]. When it comes to the development of metastases, drug resistance, tumor growth and relapse, CSCs play an important role. In some experiments, cancer cells undergoing EMT acquire stemness (e.g. in mammary tissue [61, 88]) and increase their ability to form tumorspheres and initiate tumors (e.g. in breast cancer [88]). In mice, non-CSC cells often transform into CSCs as a consequence of EMT [29, 30]. However, other researches suggest that stemness might be linked to a transitional state between the mesenchymal and epithelial phenotypes, a tradeoff between the two opposed traits. Indeed, carcinoma cells completing a full EMT transition lose stem-like properties, allowing us to conclude that a mesenchymal trait does not always imply increased stemness [23, 39, 88].

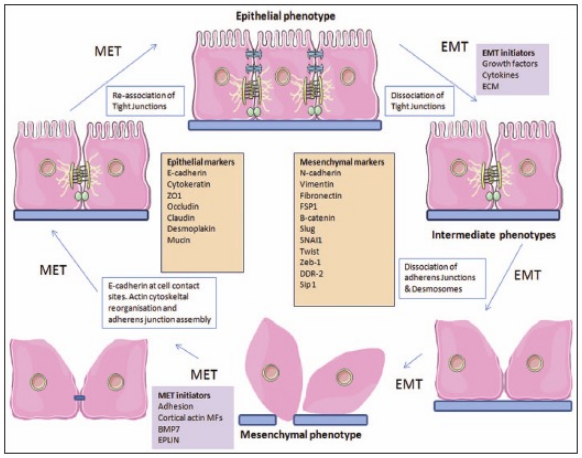

Figure 1.6. The reversibility of the EMT program into MET is fundamental in many invasion steps. Many factors are involved in this complex process, from chemicals triggering the two programs (EMT and MET initiators) to factors that identify the single phenotypic state (epithelial and mesenchymal markers) and facilitate the acquisition/loss of mesenchymal characteristics. Reproduced from "Madame Curie Bioscience Database" [89].

EMT in cancer progression

EMT and metastasis

Metastasis is one of the most dangerous aspects of cancer: almost 90 % of oncologic patients die due to complications related to metastasis rather than primary tumors [78, 91]. Epithelial-to-mesenchymal transition (EMT) plays an important role in all metastasis and invasion steps. EMT converts epithelial cells into mesenchymal ones, which are characterised by enhanced motility and higher secretion of ECM-degrading factors. In this sense, EMT increases cell invasiveness (see Figure 1.7 (A)). When the primary tumor is established, migration towards adjacent tissues could happen as a single cell [76, 91, 98, 136] but more often in a collective way [1, 36, 50, 51]. Experimental evidence shows a great presence of the E-cadherin (epithelial) marker in the bulk of the tumor, where cells also maintain cell-cell junctions. On the contrary, cells at the leading edges of the cancer

mass express mesenchymal features like enhanced motility and high secretion of matrix-degrading proteases, promoting invasion [116, 119, 147, 148]. This evidence suggests that epithelial cells reside in the bulk of the tumor while mesenchymal cells stay at the front, leading cancer invasion. This process reflects a leader-stalker cell dynamic, with the more mesenchymal cells acting as leaders and the more epithelial as followers. During the intravasation step, carcinoma cells penetrating the vasculature (called CTCs i.e. circulating tumor cells) show partial EMT activation, residing in an intermediate state between epithelial and mesenchymal endpoints [149], see Figure 1.7 (B)). Following extravasation, tumor cells may be eliminated by the immune system or enter a dormant state in response to the new hostile microenvironment [67, 92, 95]. In this context, the plasticity of the EMT transition is essential for the outgrowth of macrometastases from disseminated dormant cells (see Figure 1.7 (B)).

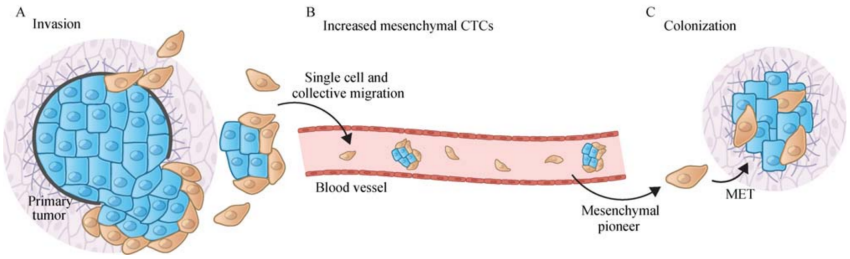

Figure 1.7. The EMT program is important during multiple steps of metastasis and invasion. (A) At the primary tumor location, EMT is induced to increase cell invasiveness. Indeed, migration and dissemination are supported by mesenchymal features like enhanced cell motility and increased secretion of ECM-degrading enzymes. (B) Cells involved in intravasation (CTCs) undergo a partial EMT transition, showing both mesenchymal and epithelial characteristics. (C) During extravasation, cells reverse the EMT program into MET to reacquire epithelial features that promote the colonization process and the growth of secondary metastases. Reproduced from Zhang et al. [150]

At this stage, cells often reverse EMT program into MET, reacquiring epithelial features that are useful to create secondary tumors, like enhanced ability to duplicate and grow (see Figure 1.7 (C)). For instance, primary tumor cells in mouse models of breast and skin cancers undergo EMT transition to disseminate into the lungs and then reverse EMT into MET to form macroscopic metastases at periferic sites [98, 136]. Although the reconversion into a fully epithelial phenotype is helpful for the growth of metastases, it is not strictly necessary in all cases. For example, macrometastases in invasive lobular carcinoma of the breast originate from fully mesenchymal cells [17]. Since EMT generates cells residing in almost all the phenotypic states along the E-M axis, we can say that EMT is a major contributor to phenotypic heterogeneity within a tumor. This heterogeneity is a significant obstacle to the success of cancer therapies [38, 56, 90, 122].

Relation between EMT and therapeutic resistance

The EMT program also increases the resistance of cancer cells to death. For instance, EMT causes cancer cells to become resistant to multiple drugs [125, 134] through various mechanisms such as slow proliferation rate, increased secretion of anti-apoptotic proteins and regulation of ABC transporters that facilitate drug efflux (see Figure 1.8 (A)) [40, 120, 141]. As a result of the EMT program, cancer cells modify their phenotypic trait, acquiring resistance to targeted therapies. For example, EMT transition induces lung and ovarian cancer carcinoma cells to switch from the EGFR to the AXL receptor, acquiring resistance to EGF-targeted therapy [25, 59] (see Figure 1.8 (B)). Moreover, the genetic variability produced by the EMT transition could also lead to the emergence of an advantageous drug-tolerant phenotypic trait. Due to his high fitness, this variant will establish itself as the dominant phenotype due to natural selection. For example, a mesenchymal drug-resistant state emerges in lung cancer as a genetic mutation in response to EGFR-inhibiting treatments [65].
However, the aspect that is of utmost importance for our objectives is that the EMT program leads to the creation of an immunosuppressive tumour microenvironment, which confers resistance to immunotherapies (see Figure 1.8 (C)) [131]. The mechanisms leading to EMT-mediated resistance to immunotherapy include both cell-autonomous and non-autonomous pathways.
From a cellular point of view, carcinoma cells undergoing EMT acquire mesenchymal characteristics, such as less susceptibility to apoptosis, thereby becoming less vulnerable to cytotoxic T cell-mediated lysis [3, 64]. Compared to epithelial cells, mesenchymal cells in mouse mammary tumour models show lower levels of MHC-I molecules and β2-microglobulin, leading to a higher immune resistance [42]. According to [34, 97], the immune response can be hindered in cases of breast and lung carcinomas due to the upregulation of ZEB1 EMT-TF, which in turn causes the expression of PD-L1 that suppresses the functions of T cells.
From a cellular environmental point of view, the EMT program is responsible for remodelling of the tumour microenvironment into an immunosuppressive state (see Figure 1.8 (C)). In melanoma cells, the SNAIL-induced EMT process amplifies the influx of immunosuppressive regulatory T cells into the tumor microenvironment. This is facilitated by the heightened secretion of TGF-β and thrombospondin-1 by the quasi-mesenchymal cancer cells [77]. In models of breast cancer, tumors originating from a higher proportion of epithelial carcinoma cells exhibit an increased presence of M1 anti-tumor macrophages as well as CD8+ T lymphocytes. Conversely, neoplasms initiated from more mesenchymal cells show a higher concentration of regulatory T cells (T-regs) and M2 pro-tumorigenic macrophages and a reduced number of CD8+ cytotoxic T cells, which also exhibit exhaustion. Of note, a small subset of quasi-mesenchymal cancer cells within a breast tumor can foster an immunosuppressive microenvironment which, in turn, safeguards the coexisting majority of epithelial cancer cells from immune assaults [42].

Summarising, epithelial-mesenchymal transition (EMT) significantly reduces the effectiveness of current anticancer treatments, which predominantly focus on eradicating epithelial non-cancer stem cells (non-CSCs) within the tumor mass, but fail to address the

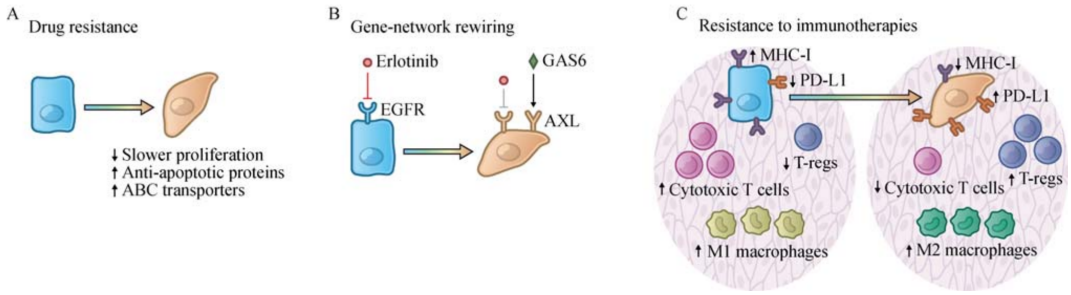

Figure 1.8. The EMT program provides resistance to therapies. (A) The EMT induces multidrug resistence on tumor cells through various mechanisms such as slow proliferation rate, increased secretion of anti-apoptotic proteins and regulation of ABC transporters that facilitate drug efflux. (B) EMT program causes cancer cells to change their phenotypic trait, acquiring resistance to targeted therapies. As a result of EMT transition, lung and ovarian cancer carcinoma cells switch from the EGFR to the AXL receptor, gaining resistance to EGF-targeted therapies. (C) The EMT program modifies tumor microenvironment into a more immunosuppressive one, conferring resistance to immune action and therapies. This involves cell-autonomous and non-autonomous processes, upregulating and downregulating specific molecules. Of note, in carcinoma, the tumour microenvironment is remodelled by recruiting M2 protumorigenic macrophages and regulatory T cells and suppressing the infiltration of "killer" cytotoxic T cells. Reproduced from Zhang et al. [150]

mesenchymal CSC component. Within the realm of immunotherapy, an immunosuppressive tumor microenvironment induced by EMT may confer protection not only to mesenchymal CSCs but also to epithelial non-CSCs. Moreover, due to their tumour-initiating capabilities, the surviving cancer stem cells (CSCs) possess the potential to generate new tumors, subsequently contributing to the manifestation of clinical diseases.

Complexity of the EMT-induced phenotypic spectrum

Throughout the multistep progression of carcinomas, Epithelial-Mesenchymal Transition (EMT) plays a pivotal role across the entire cellular population residing in the intermediate phases between fully epithelial and fully mesenchymal states. This phenomenon contributes to the emergence of a continuum of phenotypic states along the E versus M axis. Each intermediate state displays unique characteristics, including varying levels of invasiveness and drug resistance, which may support cancer growth and spread during specific stages of tumour invasion. Given the complexity of the phenotypic spectrum, considering the EMT program as universal and unique would be an error [105]. Indeed, there is a wide range of EMT versions, each acting on a certain phenotypic state along the E-M axis.

The phenotypic heterogeneity originated by the EMT program is influenced by several mechanisms. As previously elucidated, the execution of the EMT program is facilitated by a select group of EMT-Transcription Factors (EMT-TFs) including SNAIL, TWIST,

SLUG, and ZEB1. These regulators possess divergent capacities in mediating the conversion of epithelial cells into mesenchymal phenotypes [79, 108]. For example, SLUG maintains stemness in mammary stem cells and SNAIL generates CSCs and triggers metastasis in breast cancer [148]. The regulatory mechanism represented by SNAIL can elicit disparate responses across various carcinoma models. SNAIL is of paramount importance in facilitating metastasis within the context of a breast cancer mouse model, yet it proves unnecessary for metastatic processes in pancreatic cancer mouse models [2, 148, 151]. Moreover, the initiation of EMT is triggered by the assimilation of different heterotypic signals, which are detected with varying intensity by each cancer cell. This variation in signal perception is contingent upon the heterogeneous nature of the tumour microenvironment and the specific positioning of the cell relative to the sources of these signals [118]. Intuitively, different combinations of signals result in cancer cells assuming distinct EMT intermediate states along the E-M axis. As a consequence, a topological localization of traits induced by EMT could emerge within neoplasms. For instance, cells exhibiting partial-EMT characteristics are concentrated at the forefront of the primary tumor and promote invasion in head-and-neck squamous cell carcinomas [116].

Therapeutic strategies targeting EMT

In conclusion, EMT transition plays a fundamental role in cancer progression and invasion. Of particular importance is the plastic nature of the EMT program, which results in the emergence of intermediate phenotypic states on the E-M axis. Given his contribution to the development of resistance to immuno- and chemo-therapies, further in-depth study of the EMT program is necessary to develop efficient treatments for cancer. Some potential strategies could include:

- Targeting cancer cells with mesenchymal/CSC characteristics, which are responsible for the immunosuppressive action. In lung cancer patients, evidence shows that the EMT-induced resistance to EGFR-targeted treatment is lost by inhibiting the AXL tyrosine kinase (an EMT-induced receptor conferring resistance to EGFR-targeted therapies) [25].
- Reversing the EMT program at specific stages of tumour development, limiting invasiveness and tumour-initiating ability. In mammary tumour cells, MET is triggered by cholera toxin and forskolin [106].
- Reducing the plasticity of cancer cells, targeting specific signals that trigger and sustain mesenchymal states (for instance, TGF-β inhibitors counteract the EMT) [68].

1.1.3 Summary of Relevant Biological Assumptions for our mathematical model

Briefly, in our work we focus on the collective migration of cancer cells during the invasion and metastasis cascade. Invading fronts are characterised by great phenotypic

heterogeneity which results in the emergence of a leader-follower cell dynamic. In this context, mesenchymal cells act as leaders. Located at the invading edge, mesenchymal cells possess favourable features that promote invasions, like enhanced mobility and significant production of ECM-degrading proteases and chemical signals attracting follower cells. As an energetic tradeoff, more mesenchymal cells exhibit lower proliferative ability than more epithelial ones. On the other hand, epithelial cells reside in the bulk of the tumour and act as followers. Being less motile and showing enhanced cell-to-cell adhesion, epithelial cells are more proliferative but also produce growth-inducing factors targeting mesenchymal cells in order to maintain a global balance in the overall number of cells. In this sense, collective invasion is an ensemble process in which different phenotypic subpopulations of cancer cells cooperate to promote cancer invasion. A great interchange exists between these phenotypic subpopulations, given that cancer cells could change their phenotype due to EMT or MET transition. Of particular interest for our dissertation is the immunosuppressive effect of the EMT program, which remodels the cellular microenvironment to protect cancer cells from immune response [150]. We will focus on the specific cases of melanoma and breast cancer, in which we can detect two types of cells, regulatory T cells and immune killer cells, having an essential role in regulating the immune response to cancer. In the first case, evidence shows that EMT-induced mesenchymal cells produce specific molecules (TGF-β and thrombospondin-1) that promote the infiltration of immunosuppressive regulatory T cells within cancer [77]. In the second case, tumours emerging from more epithelial cells show a high concentration of M1 anti-tumour macrophages and $CD8^{+}T$ cells, resulting in a relevant immune action. Conversely, neoplasms initiated from more mesenchymal cells contain more M2 pro-tumorigenic macrophages and regulatory T cells and fewer $CD8^{+}T$ cells, inhibiting the immune response. Furthermore, only few mesenchymal cells are sufficient to create an immunosuppressive microenvironment which also protects the epithelial population [42]. To conclude, the mesenchymal trait is associated with increased secretion of chemicals that attract regulatory T-cells, which in turn repel immune killer cells, resulting in an immunosuppressive effect that safeguards and promotes tumour growth. On the other hand, epithelial cells are unable to produce enough T-regs-attracting chemicals to confer protection to cancer cells, which are now heavily targeted and killed by immune cells.

1.2 Mathematical Modeling Background

From the mathematical point of view, various models dealing with the biological processes of tumour metastasis and invasion have been proposed over the years. Of note, useful reviews of the state of the art are given in [5, 49, 121].
Particular attention has been given to haptotaxis-driven invasion. In this case, the prototype model consists of a coupled system of two PDEs and ODEs, governing the temporal and spatial evolution of some quantities that are typically the cancer cell density, the concentration of matrix-degrading enzymes (MDE) and the density of extra-cellular-matrix (ECM). Cancer cells migrate due to various factors, including random motion (linear diffusion term) and haptotaxis (advection term depending on the ECM gradient), and also proliferate (non-local reaction term). For the sake of simplicity, early models assume a

homogeneous population of cancer cells like in [10]. More precisely, in [10], Chaplain et al. present two haptotaxis-fuelled invasion models: the first is a continuous homogeneous model at the macroscale, and the second is an individual-cell (discrete) model at the microscale. A detailed analytical study of these models is performed, including proofs of local and global existence, boundness and uniqueness of the solutions. The blow-up of solutions [123] and the radially symmetric case [123] are also investigated. Various extensions of this prototype have been studied: in [7, 32], the focus is on the role of uPA (urokinase plasminogen) activation system in ECM degradation, in [53, 104] non-local terms are included to model cell-cell adhesion while in [37] mechanics aspects and interaction forces are incorporated in the particular case of melanoma. This prototype has also been generalized to a non-homogeneous cancer population, taking into account phenotypic heterogeneity, which is a key factor in the invasion process. Binary models consider only two phenotypic states, typically one "migrating" and the other "proliferating" according to the "go or growth" paradigm. Models of this type have been applied in glioma growth [74, 113, 128] and acid-mediated invasion [130]. Another approach is to include a continuous structure variable representing the phenotypic trait of the single tumor cell [110]. This approach has been employed in chemotaxis/proliferation scenarios [83] to study growth processes driven by chemotaxis but also in mobility/proliferation scenarios to investigate growth processes induced by density [84] or pressure [87]. Regarding cancer, we highlight models dealing with the avascular growth of tumors [45] and the phenotypic variability emerging within neoplasms [46, 85, 143]. Of note, many studies rely on a discrete rather than a continuous approach. Individual base models (IBM) have the advantage of tracking the single-cell behaviour [145, 146] and are widely used also in cancer invasion [10]. Of note, the passage from a discrete to a continuous model could be done directly or inversely. The "inverse" way is to build the continuous model and then derive the discrete one through discretization, defining suitable movement probabilities for the random walks and obtaining the governing rules at the single-cell level. This approach is employed in [10] starting from the prototype model mentioned above. Further extensions of this model have been developed to study the effect of hypoxia on metastatic growth [9], including phenotypic heterogeneity and oxygen-depending proliferation, and also to investigate the role of epithelial and mesenchymal phenotypes during invasion-metastasis cascade [49]. However, the "direct" and more natural way is first to postulate the discrete model and then derive the corresponding continuous model through limiting procedures. This approach is employed to study chemotaxis-driven self-organization processes [103], non-linear diffusion in crowded environments [109] and aggregation, collapse, and blow-up dynamics [129].

Mathematical modelling applied to the study of populations with heterogeneous mobility has recently gained importance, thanks to its various applications in biomedicine, especially in cancer evolution. These models are usually formulated as reaction-diffusion equations with non-local reaction terms. In [11], Arnold A. et al. focus on reaction-diffusion equations with a structure parameter (that is the typical framework in selection-mutation-competition-migration models) and demonstrate the existence of nontrivial steady states. One of the milestones in this field is the cane toad invasion model [15], which explains mathematically the emergence of accelerating invading fronts [114, 126, 127, 138]. These

analytical results perfectly match biological evidence showing a spacial sorting with more motile individuals residing at the leading edge. More in general, the existence of solutions in the travelling wave framework has been proved [19, 20, 21, 137], and the acceleration of invading fronts has also been widely studied [16, 20, 22]. Of note, Bouin,E et al. in [20] derive a dispersion relation between the wave speed and the spatial decay. Using these results, an equation governing the evolution of the dominant phenotypic trait is also obtained.
Of particular relevance for our purpose are [83, 84], which inspired us and constitute the basis for the work presented here. In [84], Lorenzi et al. formulate a continuous model for the growth of a phenotype-structured population characterized by heterogeneous proliferation and mobility, which is particularly relevant for glioma growth. Here, the evolution of cancer cell density is governed by a non-local advection-reaction-diffusion equation, which models random movement (linear spacial-diffusion term) with heterogeneous motility (phenotype-dependent diffusion coefficient), phenotypic and density-dependent growth (non-local reaction term) and spontaneous heritable genetic mutations (linear phenotypic-diffusion term). Using the Hamilton-Jacobi approach, a detailed asymptotic analysis is performed in the travelling-wave framework, investigating travelling-front solutions and their properties. In [83], Lorenzi T. and Painter K.J. extend the classical chemotaxis model of Keller and Segel to include intra-population heterogeneity. The evolution of the population density is now governed by a non-local advection-reaction-diffusion equation coupled with an integro-differential equation for the chemical factor. Even in this case, long-time solutions appear as travelling fronts with a precise biological meaning.
Our work can be seen as an extension of the model presented in [84] to take into account the dynamics of regulatory cell and killer cells in order to study the EMT-induced immunosuppressive effects. In particular, the equation governing the evolution of cancer cell density shears similarity to the one presented in [84] since we consider a population with heterogeneous motility and proliferation ability through a structure variable representing the phenotypic trait. Our model also includes three additional equations. The first one governs the evolution of a chemical factor that attracts regulatory cells and that is secreted by cancer cells with a phenotypic-dependent production rate. This equation is inspired by the one for the attractant in the generalized Keller-Siegel model [83] or by the one for the evolution of the MDE in the haptotaxis model [82]. The second and third additional equations govern the evolution of two types of cells involved in regulating the immunity response: regulatory and killer cells. These equations do not depend on the phenotypic structure variable and take the form of advection-reaction-diffusion equations, representing biological migration processes driven respectively by chemotaxis and local differences in cancer cell density. If we look only at the first three equations composing our model, we find out some formal similarities with haptotaxis models like [82] (same equations but with different biological meanings). This motivates the extensive review of haptotaxis models with particular focus on their mathematical analysis given in this section.

Chapter 2

The Individual Based Model

2.1 Preliminary assumptions

In this section, we build on the approaches developed in [24, 82, 87] to formulate an individual-based model with phenotype structure for cancer invasion.
In this model, we consider a population of cancer cells which are able to secrete a chemical factor attracting regulatory cells. These cells, in turn, inhibit killer cells responsible for the immune action (i.e., the attack and elimination of the cancer cells), conferring immunity to the population. Further details of the mathematical formalization are provided in the respective sections.
Tumor cells, regulatory cells and killer cells are represented as agents, while the concentration of chemical attractant is described by a non-negative function. We allow cancer cells to move in a phenotype-dependent way toward areas with lower density, neglecting random undirected movement (i.e. spatial diffusion). In addition, tumor cells can undergo heritable spontaneous phenotypic changes (randomly, not biased by the surrounding microenvironment) and phenotype-dependent proliferation (division/death). A further cause of death for cancer cells is the encounter with killer cells. We put ourselves in a scenario in which the chemical factor is secreted by the cancer cells at a phenotype-dependent rate, then diffuses following Fick's Law and decays spontaneously. Both regulatory and killer cells undergo random undirected movement and proliferation. While regulatory cells migrate due to chemotaxis in response to the concentration of the chemical attractant, killer cells move up the gradient of cancer cell density. Furthermore, regulatory cells are produced by a chemical-dependent source, while killer cells come from a source depending on the density of regulatory cells. Both types of cells die spontaneously at a constant rate. More details about the dynamics are given below.
We consider a 1D scenario in which cancer, regulatory, and killer cells and the attractant concentration are distributed along the real line $\mathbb{R}$. The phenotypic state of each cell is represented by the structure variable $y \in [0, Y] \in \mathbb{R}^+$, which allows us to take into account the intra-population heterogeneity existing in proliferation, chemical secretion and mobility. We assume that small values of the structure variable ($y \to 0$) are associated with an epithelial phenotype characterized by high proliferation, low motility and low chemical

production. On the contrary, for high values of the phenotypic variable ($y \to Y$) cancer cells show more mesenchymal features like enhanced mobility, high secretion of attractant and low proliferation rate (see Figure 2.1). On one hand, these assumptions reflect the "go or growth" dynamic which governs cellular life due to energetic factors. On the other hand, these hypotheses reflect the immunosuppressive action of the EMT transition. Indeed, evidence shows that cancer cells entering an EMT-induced mesenchymal state can modify the tumoral microenvironment into a more immunosuppressive one. This results in protecting even the epithelial cells in the surroundings from the immune response. In the particular case of melanoma [77] and breast tumor [42], mesenchymal cells promote the infiltration of regulatory T cells into cancer, while a significant presence of epithelial cells attracts T $CD8^+$ anti-tumoral killer cells. Here, a more mesenchymal trait results in greater secretion of chemical factor, attracting more regulatory cells, whose presence reduces the tendency of killer cells to move towards the cancer cells, inhibiting the immune response and protecting them.

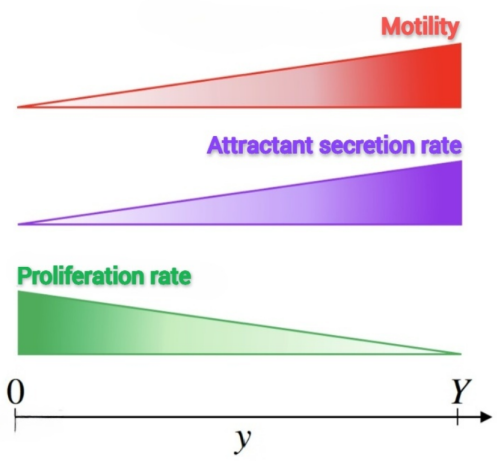

Figure 2.1. The main features linked with epithelial and mesenchymal states: proliferation,attractant secretion and motility.

2.2 Discretized variables and governing rules

We discretise the continuous variables of time $t \in \mathbb{R}^+$ and space $x \in \mathbb{R}$, obtaining the discrete variables of time $t_k = k\tau$ and space $x_i = i\ \Delta_x$ with $k \in \mathbb{N}_0$, $\tau \in \mathbb{R}_*^+$, $i \in \mathbb{Z}$, and $\Delta_x \in \mathbb{R}_*^+$. We use the notation $\mathbb{R}_*^+$ to denote the set of positive real numbers. Furthermore, the phenotypic variable y is also discretized as $y_j = j\ \Delta_y \in [0, Y]$ with $j \in \mathbb{N}_0$ and $\Delta_y \in \mathbb{R}_*^+$. The quantities τ, Δ_x and Δ_y are, respectively, the time step, space step, and phenotype step.
Each agent (i.e. each cancer cell) occupies a certain position in the lattice $\{x_i\}_{i\in\mathbb{Z}} \times \{y_j\}_{j\in\mathbb{N}_0}$. We introduce the dependent variable $N_{i,j}^k \in \mathbb{N}_0$, which represents the number

of cancer cells in the phenotypic state y_j at spacial position x_i and time t_k. Using this definition, we can express quantities like the cell population density (i.e. the density in space and phenotype)

$$n_{i,j}^k \equiv n(t_k, x_i, y_j) := \frac{N_{i,j}^k}{\Delta_x \Delta_y}, \tag{1.1}$$

and the cell density (i.e. population density integrated over the phenotype, depending only on the space variable)

$$\rho_i^k \equiv \rho(t_k, x_i) := \Delta_y \sum_j n_{i,j}^k. \tag{1.2}$$

Similarly, we define ${M_K}_i^k \in \mathbb{N}_0$ and ${M_R}_i^k \in \mathbb{N}_0$ respectively as the number of killer and regulatory cells in position x_i at time t_k. We assume these two populations have no phenotypic heterogeneity, so variable y is not involved in these quantities. We can write the density of regulatory cells

$${m_R}_i^k \equiv m_R(t_k, x_i) := \frac{{M_R}_i^k}{\Delta_x}, \tag{1.3}$$

and the density of killer cells

$${m_K}_i^k \equiv m_K(t_k, x_i) := \frac{{M_K}_i^k}{\Delta_x}. \tag{1.4}$$

Finally, we let

$$S_i^k \equiv S(t_k, x_i) \tag{1.5}$$

be the concentration of the chemotaxis factor at position x_i and time t_k . Our model relies on some biological rules and mechanisms summarized in the figures below and described more precisely in the specific sections. In the remainder of this work, when we refer to cell density (or simply density), we are talking about the density ρ of cancer cells. Whereas, if we want to indicate n, m_K, m_R we will use the terms, respectively: cell population density, density of killer cells and density of regulatory cells.

2.3 Cancer cells dynamics

During a time step $[t_k, t_{k+1}]$, cancer cells in the phenotypic state $y_j \in (0, Y)$ in spacial position $x_i \in \mathbb{R}$ can undergo:

- density-dependent movement towards regions with lower concentration of tumor cells
- heritable spontaneus phenotypic changes
- proliferation
- death, either spontaneous or caused by the immune action of killer cells

Now we consider each of these cases, formalizing them in a mathematical way through the definition of suitable probabilities.

2.3.1 Movement towards less crowded regions

We employ a biased random walk along the spacial dimension to model the movement of cancer cells in response to density variations. To capture the fact that cells move towards regions with lower cell density (i.e. in the opposite direction to the density gradient), we let the movement probabilities depend on the difference between the density at the current location and the one at nearby positions.
In our model, cancer cells with a higher value of phenotypic variable y (i.e. more mesenchymal) exhibit greater mobility than the ones with a lower value of y (i.e. more epithelial). To take into account this biological fact, the function $\mu(y)$, representing the mobility of a cell with phenotype y , is taken as an increasing function of y:

$$\mu(0) \geq 0, \quad \frac{\mathrm{d}\mu(y)}{\mathrm{d}y} > 0 \quad \text{for } y \in (0, Y]. \tag{1.6}$$

Defining $P^k_{DL_{i,j}}$ the probability that a cancer cell with phenotype y_j at time t_k and position x_i moves leftwards to x_{i-1}, and $P^k_{DR_{i,j}}$ the probability to move rightwards to x_{i+1}, we write:

$$P^k_{DL_{i,j}} := \eta\mu(y_j)\frac{(\rho^k_i - \rho^k_{i-1})_+}{2\rho_{\max}}, \quad P^k_{DR_{i,j}} := \eta\mu(y_j)\frac{(\rho^k_i - \rho^k_{i+1})_+}{2\rho_{\max}} \quad \text{con } (\cdot)_+ = \max(0, \cdot), \tag{1.7}$$

where $\rho_{\max} \in \mathbb{R}^+_*$ is the maximum value of density (see also Section 2.3.3) and $\eta \in \mathbb{R}^+_*$ is a scaling factor, small enough to ensure that $\eta\mu(y_j) \leq 1$.
In this way

$$0 < P^k_{DL_{i,j}} + P^k_{DR_{i,j}} < 1 \quad \forall i, j, k.$$

Furthermore, the probability of not moving is given by:

$$P^k_{DS_{i,j}} := 1 - (P^k_{DL_{i,j}} + P^k_{DR_{i,j}}). \tag{1.8}$$

2.3.2 Phenotipic changes

In order to include the heritable sponaneous phenotypic changes that a cancer cell could undergo, we consider a random walk along the phenotypic dimension. After a single time step $[t_k, t_{k+1}]$ a cancer cell could change its phenotypic state with a probability $0 < \beta \leq 1$ or keep the same phenotype with probability $1 - \beta$.
A tumor cell in the phenotypic state y_j could switch into the state y_{j-1} with probability $P^k_{D_{i,j}}$ or into y_{j+1} with probability $P^k_{U_{i,j}}$. Since we consider spontaneous phenotypic changes, both phenomena are equally likely to happen:

$$P^k_{D_{i,j}} = P^k_{U_{i,j}} := \frac{\beta}{2}. \tag{1.9}$$

The probability of not undergoing any phenotypic variation is then:

$$P^k_{N_{i,j}} := 1 - (P^k_{D_{i,j}} + P^k_{U_{i,j}}). \tag{1.10}$$

2.3.3 Cell division and death

If we look at the proliferation events, we assume that a dividing cancer cell is instantaneously replaced by two cancer cells which inherit its phenotypic trait y_j and spacial position x_i. Furthermore, when a cell dies, it is instantaneously removed from the system. To include phenotypic heterogeneity and contact inhibition of growth, we assume that proliferation and death probabilities for a cancer cell at position x_i depend both on the phenotypic state y and the cell density ρ, through a suitable function $G(y, \rho)$. The dependence on ρ is included to take into account volume-filling effects, which reflect the natural tendency of cancer cells to limit their proliferation if the surroundings are densely populated. Since death could be either spontaneous or caused by the encounter with a killer cell that happens at rate γ, the total proliferation rate R must also be a function of $m_{_K}$. In summary, we can define:

$$R(y, \rho(t,x), m_{_K}(t,x)) = G(y, \rho(t,x)) - \gamma\ m_{_K}(t,x), \tag{1.11}$$

that is the net density growth rate of cancer cells with phenotype y at position x and time t as a result of duplication and death events, which are also influenced by the density of killer cells $m_{_K}$. Here, $G(y, \rho)$ is a function that represents the fitness (i.e. the net proliferation rate) of cancer cells with phenotype y surrounded by density $\rho(t, x)$. It also makes sense to impose a saturating condition on the growth function G so that proliferation is totally inhibited when the maximum density value $\rho_{\max}$ is reached:

$$G(\ 0,\ \rho_{\max}) = 0, \quad \partial_\rho G(\cdot,\ \rho) < 0 \quad \text{for } (y,\rho)\ \in (0, Y] \times \mathbb{R}^+, \tag{1.12 a}$$

where $0 < \rho_{\max} < \infty$ is the local carrying capacity of the population (i.e., the system's maximum capacity in terms of cell density).
Building on the biological observations, a more mesenchymal phenotype (high y) entails lower proliferation compared to a more epithelial one (low y). This happens due to the energetic cost of migration, which tends to establish the so-called "go or growth" mechanism for the cell dynamics [4, 5, 52, 54, 55, 57, 58, 63, 66, 100]. These considerations bring to the following modelling assumptions:

$$G(\ Y,\ 0) = 0, \quad \partial_y G(\ y, \cdot) < 0 \quad \text{for } (y,\rho)\ \in (0, Y] \times \mathbb{R}^+. \tag{1.12 b}$$

In particular, we focus on the case:

$$G(y,\rho) := r(y) - \rho \quad \text{with} \quad r(Y) = 0, \quad r(0) = \rho_{\max}, \quad \frac{\mathrm{d}r(y)}{\mathrm{d}y} < 0 \quad \text{for } y\ \in (0, Y], \tag{1.13}$$

where $r(y)$ is a smooth and bounded function that models the net proliferation rate of cancer cells with phenotype y. In the following, we will assume $\rho_{\max} = 1$.
Finally, denoting by $P^k_{A_{i,j}}$ the death probability and by $P^k_{B_{i,j}}$ the division probability of a cancer cell in the phenotypic state y_j at position x_i between time steps t_k and t_{k+1}, we have:

$$\begin{aligned} &P^k_{A_{i,j}} = \tau\ R(y_j, \rho^k_i, {m_{_R}}^k_i)_-, \quad P^k_{B_{i,j}} = \tau\ R(y_j, \rho^k_i, {m_{_R}}^k_i)_+, \\ &\text{with} \quad (\cdot)_- := -\min(0, \cdot), \quad (\cdot)_+ := \max(0, \cdot). \end{aligned} \tag{1.14}$$

Thus, the probability that a cancer cell remains quiescent, without dying or duplicating, will be:

$$P^k_{Q_{i,j}} := 1 - (P^k_{A_{i,j}} + P^k_{B_{i,j}}). \tag{1.15}$$

Choosing τ small enough, ensure that $P^k_{A_{i,j}} + P^k_{B_{i,j}} \leq 1 \quad \forall i, j, k$.
Assumptions (1.12 a),(1.12 b) together with (1.14), ensure that if $\rho^k_i \geq \rho_{\max}$ then cancer cells in position x_i could either enter a state of dormancy or die during the time interval $[t_k, t_{k+1}]$. In turn this ensures that

$$\text{if} \quad \max_{i\in\mathbb{Z}} \rho^0_i \leq \rho_{\max} \quad \Rightarrow \quad \text{then} \quad \rho^k_i \leq \rho_{\max} \quad \forall (k,i) \in \mathbb{N}_0 \times \mathbb{Z}.$$

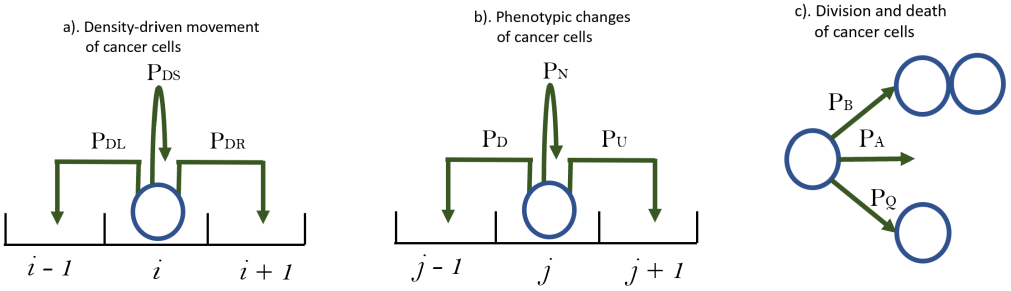

Figure 2.2. Schematic summary of the mechanisms included in the individual-based model for cancer cells. In a time step $[t_k, t_{k+1}]$ a cancer cell with phenotype $y_j \in (0, Y)$ at position $x_i \in \mathbb{R}$: **a)** can move down the density gradient to positions x_{i-1} or x_{i+1} with probabilities $P^k_{DL_{i,j}}$ and $P^k_{DR_{i,j}}$ given by (1.7) or does not move with probability $P^k_{DS_{i,j}}$ given by (1.8) **b)** changes its phenotypic state into y_{j-1} or y_{j+1} with probabilities $P^k_{D_{i,j}}$ and $P^k_{U_{i,j}}$ given by (1.9) or remains in the same phenotypic state with probability $P^k_{S_{i,j}}$ given by (1.10) **c)** dies or divides with probabilities $P^k_{A_{i,j}}$ and $P^k_{B_{i,j}}$ given by (1.14) or remains quiescent with probability $P^k_{Q_{i,j}}$ given by (1.15).

2.4 Chemical factor dynamics

As already mentioned in the previous part, between time steps $[t_k, t_{k+1}]$ the concentration of the chemical factor in spacial position $x_i \in \mathbb{R}$ changes due to:

- spacial diffusion according to the classical Fick's Law of diffusion with coefficient $D_s \in \mathbb{R}^+_*$,
- natural decay with elimination rate λ,
- production by the cancer cells with phenotype-dependent production rate $P(y_j)$.

As mentioned, mesenchymal cells (high y) give cancer immunity by recalling many regulatory cells. Since regulatory cells move up the chemical gradient, the previous scenario

could happen only if the mesenchymal phenotype is associated with a larger production of $S(x,t)$ than the epithelial one (low y). In other words, low chemical production by ephitelial cells implies low attraction of regulatory cells, which means less immunity. These considerations inspire us to model the production rate $P(y)$ as an increasing function of the phenotypic variable y:

$$P(0) > 0, \quad P(Y) < \infty, \quad \frac{\mathrm{d}P(y)}{\mathrm{d}y} > 0. \tag{1.16}$$

Naming S_i^k the concentration of attractant at position x_i and time t_k, the mass conservation principle allows us to write a difference equation for the evolution of the chemoattractant concentration:

$$S_i^{k+1} = S_i^k + \tau \left[D_S \ (\mathcal{L}\ S^k)_i - \lambda S_i^k + \frac{\mathbb{1}_{\mathrm{supp}(\rho_i^k)}}{\rho_i^k} \sum_j \Big(\ P(y_j)\ n_{i,j}^k \Big) \ \Delta_y \right] \ , \tag{1.17}$$

where $\mathcal{L}$ refers to the discrete Laplacian (in the finite-difference sense) that is:

$$(\mathcal{L}S^k)_i := \frac{S_{i+1}^k + S_{i-1}^k - 2S_i^k}{\Delta_x^2}.$$

Of note, we divide it all by ρ_i^k in order to have a kind of integral average of the chemoattractant produced by cancer cells at position x_i and time t_k .

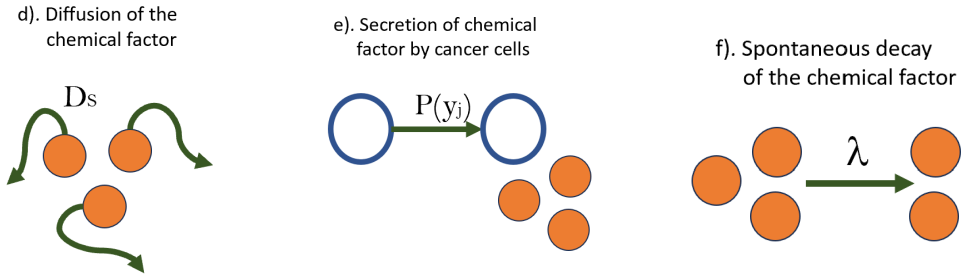

Figure 2.3. Schematic summary of the mechanisms influencing the evolution of the chemical concentration over time. In a time step $[t_k, t_{k+1}]$, the concentration of the attractant is subject to: **d)** diffusion at rate D_S **e)** production by cancer cells in the phenotypic state y_j at a phenotypic-dependent rate $P(y_j)$ **f)** spontaneous decay at rate λ.

2.5 Regulatory cells dynamics

Since we assume no heterogeneity within the population of regulatory cells, the phenotypic variable y is not included in the following formulation. This means that we neglect the contribution of phenotypic changes. In the following, these assumptions will also be true for the killer cells. Biologically, we assume that regulatory cells could undergo:

- chemotaxis-driven movement in response to the concentration S of the chemical attractant,
- undirected random movement ,
- chemical-dependent proliferation and spontaneous death

2.5.1 Chemotactic Movement

Following the approach in [24, 33], we employ a biased random walk to model the chemotactic cell movement, with probabilities expressed as a function of the difference of chemical concentration between the point occupied by the cell and the neighbourhood. This allows us to include the fact that regulatory cells move towards regions with a higher concentration of the attractant, i.e. up the direction of the gradient of S. Calling $P^k_{CL_i}$ the probability that a regulatory cell in position x_i at time t_k ends up in position x_{i-1} and $P^k_{CR_i}$ the probability to jump in position x_{i+1}, it results:

$$P^k_{CL_{i,j}} := \nu \frac{(S^k_{i-1} - S^k_i)_+}{2S_M}, \quad P^k_{CR_{i,j}} := \nu \frac{(S^k_{i+1} - S^k_i)_+}{2S_M} \quad \text{with } (\cdot)_+ = \max(0, \cdot), \tag{1.18}$$

where $\nu > 0$ is a parameter related to the chemotactic sensitivity, and S_M is proportional to the maximum value assumed by the chemoattractant. The probability of not moving by chemotaxis is given by:

$$P^k_{CS_{i,j}} = 1 - (P^k_{CL_{i,j}} + P^k_{CR_{i,j}}). \tag{1.19}$$

2.5.2 Random Movement

We model the random cell movement through a biased random walk in the spacial variable with a movement probability ϑ so that $0 < \vartheta \leq 1$. We call $P^k_{L_i}$ the probability that a regulatory cell at time t_k in position x_i ends up in position x_{i-1} and $P^k_{R_i}$ the probability that the cell jumps in position x_{i+1}. Since the movement is undirected, the two cases have the same probability of happening:

$$P^k_{L_i} = P^k_{R_i} := \frac{\vartheta}{2}, \tag{1.20}$$

Complementary, the probability of not undergoing random movement is :

$$P^k_{S_i} := 1 - \left(P^k_{L_i} + P^k_{R_i} \right) . \tag{1.21}$$

2.5.3 Cell division and death

We assume an instantaneous division, generating two regulatory cells identical to the mother cell and in the same spatial position x_i. After death, the regulatory cell is instantaneously removed from the system. We introduce a function $\Gamma_{_R}(m_{_R}, S)$ which represents the net density proliferation rate of regulatory cells in position x_i at time t_k due to external

production and cellular death, which are processes influenced by the chemical concentration S and the density of regulatory cells itself $m_{_R}$. We assume that regulatory cells are produced by a so-called "diffuse source" at a chemical-dependent rate $\Lambda(S)$ and are eliminated at a constant rate $\gamma_{_R}$. This occurs, for example, if we consider a scenario in which a network of capillaries transports regulatory cells (thus T-regs are potentially available everywhere instantaneously) that can extravasate only at specific locations where the chemical signal is sufficiently strong. As a consequence, we can define:

$$\Gamma_{_R}(m_{_R}, S) = \Lambda(S) - \gamma_{_R} m_{_R}, \tag{1.22}$$

where $\gamma_{_R}$ is the elimination rate of regulatory cells while $\Lambda(S)$ is the chemical-dependent proliferation rate. Since a higher concentration of chemical factor S implies a greater attraction of regulatory cells, the chemical-dependent proliferation rate $\Lambda(S)$ has to be modeled as a non-negative function preserving the monotonicity of its argument S, that is:

$$\frac{\mathrm{d}\Lambda(S)}{\mathrm{d}S} \geq 0 \quad \text{for } S \ \in \mathbb{R}^+ \quad \text{with} \quad \Lambda(0) = 0. \tag{1.23}$$

We let $P^k_{AR_i}$ be the death probability of a regulatory cell at position x_i between time steps t_k and t_{k+1}. An explicit formulation is:

$$P^k_{AR_i} = \tau \ \gamma_{_R}. \tag{1.24}$$

As a consequence, the probability of a regulatory cell to remain quiescent is given by

$$P^k_{QR_i} := 1 - P^k_{AR_i} \ . \tag{1.25}$$

Choosing the time step τ small enough ensure that $P^k_{AR_i} \leq 1 \quad \forall i, j, k$.
Furthermore, the total number of regulatory cells entering the balance in position x_i during the time step $[t_k, t_{k+1}]$ due to the chemical-dependent source is given by

$$\tau \ \Lambda(S^k_i), \tag{1.25b}$$

since $\Lambda(S^k_i)$ is the chemical-dependent rate at which regulatory cells enter the system at position x_i per unit time.

2.6 Killer cells dynamics

Similarly to regulatory cells, killer cells can undergo:

- density-dependent movement towards regions with a higher concentration of cancer cells in order to eliminate them,
- random undirected movement,
- regulatory-dependent proliferation and spontaneous death

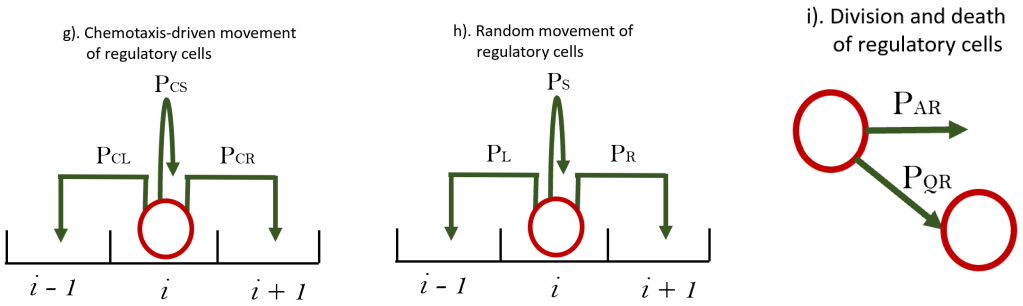

Figure 2.4. Schematic summary of the mechanisms included in the individual-based model for regulatory cells. In a time step $[t_k, t_{k+1}]$ a regulatory cell at position $x_i \in \mathbb{R}$: **g)** can move due to chemotaxis to positions x_{i-1} or x_{i+1} with probabilities $P^k_{CL_{i,j}}$ and $P^k_{CR_{i,j}}$ given by (1.18) or does not move with probability $P^k_{CS_{i,j}}$ given by(1.19) **h)** undergoes random movement to x_{i-1} or x_{i+1} with probabilities $P^k_{L_{i,j}}$ and $P^k_{R_{i,j}}$ given by (1.20) or does not move with probability $P^k_{S_{i,j}}$ given by(1.21) **i)** dies with probability $P^k_{AR_{i,j}}$ given by (1.24) or remains quiescent with probability $P^k_{QR_{i,j}}$ given by (1.25) **j)** can originate from an external chemical-dependent source in the number given by (1.25b)

.

2.6.1 Movement towards regions with higher density of cancer cells

The approach is similar to the one employed in Section 2.3.1 for the density-dependent movement of cancer cells. The difference is that now we want to model a movement up to the cell density gradient, so in the opposite direction if compared with the previous discussion. Similarly, we employ a biased random walk in the spatial dimension with jump probabilities depending on the density difference between the lattice point occupied by the cell and the neighbourhood.
Calling $P^k_{FL_i}$ the probability that a killer cell in position x_i at time t_k ends up in position x_{i-1} and $P^k_{FR_i}$ the probability to jump in position x_{i+1}, we can define:

$$P^k_{FL_i} := \sigma \frac{(\rho^k_{i-1} - \rho^k_i)_+}{2\rho_{\max}}, \quad P^k_{FR_i} := \sigma \frac{(\rho^k_{i+1} - \rho^k_i)_+}{2\rho_{\max}} \text{ with } (\cdot)_+ = \max(0, \cdot), \tag{1.26}$$

where $\sigma > 0$ is a parameter related to the sensitivity to density-driven movement and ρ_M is the carrying capacity of the cancer cell density. Consistently, the probability to not move to cell density gradient is given by:

$$P^k_{FS_i} = 1 - (P^k_{FL_i} + P^k_{FR_i}). \tag{1.27}$$

2.6.2 Random Movement

Regarding the undirected random movement, the approach is exactly the same as the one presented in Section 2.5.2 for the regulatory cells. For this reason, we briefly recall that

even in the case of killer cells, the probability to move leftwards or rightwards is given by

$$P_{L_i}^k = P_{R_i}^k := \frac{\vartheta}{2}, \tag{1.28}$$

whereas the probability of not undergoing random movement is

$$P_{S_i}^k := 1 - \left(P_{L_i}^k + P_{R_i}^k \right) , \tag{1.29}$$

with ϑ being the movement probability of the biased random walk for the random undirected motion.

2.6.3 Cell division and death

Under the same assumptions of instantaneous proliferation and death made in Section 2.3.3 and Section 2.5.3, we now introduce a function $\Gamma_{_K}(m_{_R}, m_{_K})$ which represents the net density proliferation rate of killer cells in position x_i at time t_k due to external production or cellular death. We let Γ_k depend on both $m_{_K}$ and $m_{_R}$ to include the antagonistic behaviour of killer and regulatory cells. This reflects, even in this case, a "diffuse source " approach: killer cells are diffused everywhere in the vasculature but are instantaneously available only at specific locations where the concentration of regulatory cells is favourable to extravasation. We can take:

$$\Gamma_{_K}(m_{_R}, m_{_K}) = B(m_{_R}) - \gamma_{_K} m_{_K}, \tag{1.30}$$

where $\gamma_{_K}$ is the elimination rate for killer cells and $B(m_{_R})$ is the non-negative proliferation function, representing the effect of the density of regulatory cells on the proliferation of the killer ones. Consistently with the evidence showing EMT-induced immunity in cancer, we can consider different biological scenarios through different formulations of the function $B(m_{_R})$.
One possible option is to assume that a large number of regulatory cells result in inhibiting the production of killer cells. So, we expect $B(m_{_R})$ to vanish for high value of $m_{_R}$, that is:

$$\lim_{m_{_R} \to +\infty} B(m_{_R}) = 0 \tag{1.31a}$$

On the other hand, we expect $B(m_{_R})$ to vanish even for low value of $m_{_R}$ since that's the case of a reduced-size cancer which does not trigger a strong immune response. So it holds:

$$\lim_{m_{_R} \to 0} B(m_{_R}) = 0 \tag{1.31b}$$

Another option is to consider the inhibition of killer cell proliferation as a process that goes hand in hand with an increase in the presence of regulatory cells. In other words, the greater the number of regulatory cells, the higher the immunosuppressive inhibition and, thus, the lower the production of killer cells. This translates into assuming $B(m_{_R})$ as a non-negative increasing function of $m_{_R}$, that is:

$$\frac{\mathrm{d}B(m_{_R})}{\mathrm{d}m_{_R}} \geq 0 \quad \text{for } m_{_R} \in \mathbb{R}^+ \quad \text{with} \quad B(0) > 0. \tag{1.31c}$$

We denote by $P^k_{AK_i}$ the death probability of a killer cell in position x_i between time steps t_k and t_{k+1}. Explicitly, we define:

$$P^k_{AK_i} = \tau\ \gamma_K. \tag{1.32}$$

Consequently, the probability of a killer cell to remain quiescent is given by

$$P^k_{QK_i} := 1 - P^k_{AK_i}. \tag{1.33}$$

Choosing the time step τ small enough, ensure that $P^k_{AK_i} + P^k_{BK_i} \leq 1 \quad \forall i, j, k.$
Furthermore, the total number of killer cells entering the balance in position x_i during the time step $[t_k, t_{k+1}]$ due to the regulatory-dependent source is given by

$$\tau\ B(m_{Ri}^{\ k}) \tag{1.34}$$

since $B(m_{Ri}^{\ k})$ is the regulatory-dependent rate at which killer cells enter the system at position x_i per unit time.

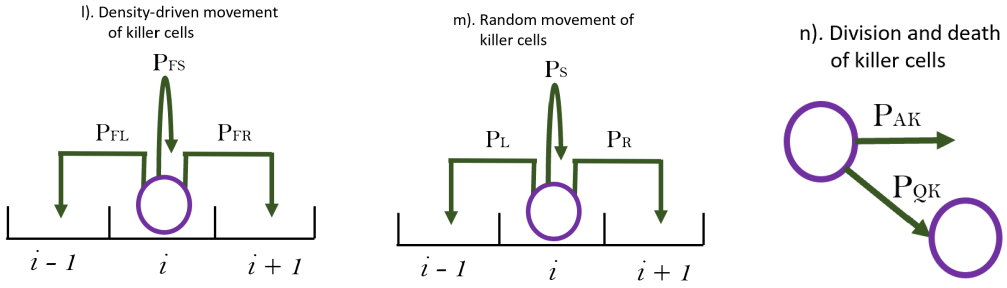

Figure 2.5. Schematic summary of the mechanisms included in the individual-based model for killer cells. In a time step $[t_k, t_{k+1}]$ a killer cell at position $x_i \in \mathbb{R}$: **l)** can move via density-driven motion to positions x_{i-1} or x_{i+1} with probabilities $P^k_{FL_{i,j}}$ and $P^k_{FR_{i,j}}$ given by (1.26) or does not move with probability $P^k_{FS_{i,j}}$ given by(1.27) **m)** undergoes random movement to x_{i-1} or x_{i+1} with probabilities $P^k_{L_{i,j}}$ and $P^k_{R_{i,j}}$ given by (1.28) or does not move with probability $P^k_{S_{i,j}}$ given by(1.29) **n)** dies with probability $P^k_{AK_{i,j}}$ given by (1.32) or remains quiescent with probability $P^k_{QK_{i,j}}$ given by (1.33) **o)** can originate from an external regulatory-dependent source in the number given by (1.34)

.

Chapter 3

Formal derivation of the continuum model from the individual-based model

In this section, we present a formal derivation of the continuum model, starting from the individual-based one. Building on the rules presented on Chapter 2, we first formulate discrete balance equations for the evolution of the cancer cell density n, the chemoattractant concentration S and the regulatory and killer densities $m_{_R}$ and $m_{_K}$. Then, we obtain a set of approximate equations by substituting discrete variables with continuum ones. Under appropriate regularity assumptions, we can then employ Taylor expansions. Finally, some calculations and simplifications lead us to the formal derivation of the continuum model.

3.1 Derivation of the equation for the cancer cell density n

Recalling the rules governing cell dynamics presented in Section 2 for the individual-based model, the principle of mass balance gives for the cancer cell density:

$$
\begin{aligned}
n_{i,j}^{k+1} =& n_{i+1,j+1}^{k}\left\{\frac{\beta}{2}\left[1+\tau R\left(y_j,\rho_i^k,{m_K}_i^k\right)\right]\left[\frac{\eta\mu\left(y_j\right)}{2\rho_{\max}}\left(\rho_{i+1}^k-\rho_i^k\right)_+\right]\right\}\\
&+ n_{i-1,j+1}^{k}\left\{\frac{\beta}{2}\left[1+\tau R\left(y_j,\rho_i^k,{m_K}_i^k\right)\right]\left[\frac{\eta\mu\left(y_j\right)}{2\rho_{\max}}\left(\rho_{i-1}^k-\rho_i^k\right)_+\right]\right\}\\
&+ n_{i+1,j-1}^{k}\left\{\frac{\beta}{2}\left[1+\tau R\left(y_j,\rho_i^k,{m_K}_i^k\right)\right]\left[\frac{\eta\mu\left(y_j\right)}{2\rho_{\max}}\left(\rho_{i+1}^k-\rho_i^k\right)_+\right]\right\}\\
&+ n_{i-1,j-1}^{k}\left\{\frac{\beta}{2}\left[1+\tau R\left(y_j,\rho_i^k,{m_K}_i^k\right)\right]\left[\frac{\eta\mu\left(y_j\right)}{2\rho_{\max}}\left(\rho_{i-1}^k-\rho_i^k\right)_+\right]\right\}\\
&+ n_{i,j+1}^{k}\left\{\frac{\beta}{2}\left[1+\tau R\left(y_j,\rho_i^k,{m_K}_i^k\right)\right]\left[1-\frac{\eta\mu\left(y_j\right)}{2\rho_{\max}}\left[\left(\rho_i^k-\rho_{i+1}^k\right)_+ + \left(\rho_i^k-\rho_{i-1}^k\right)_+\right]\right]\right\}\\
&+ n_{i,j-1}^{k}\left\{\frac{\beta}{2}\left[1+\tau R\left(y_j,\rho_i^k,{m_K}_i^k\right)\right]\left[1-\frac{\eta\mu\left(y_j\right)}{2\rho_{\max}}\left[\left(\rho_i^k-\rho_{i+1}^k\right)_+ + \left(\rho_i^k-\rho_{i-1}^k\right)_+\right]\right]\right\}\\
&+ n_{i+1,j}^{k}\left\{(1-\beta)\left[1+\tau R\left(y_j,\rho_i^k,{m_K}_i^k\right)\right]\left[\frac{\eta\mu\left(y_j\right)}{2\rho_{\max}}\left(\rho_{i+1}^k-\rho_i^k\right)_+\right]\right\}\\
&+ n_{i-1,j}^{k}\left\{(1-\beta)\left[1+\tau R\left(y_j,\rho_i^k,{m_K}_i^k\right)\right]\left[\frac{\eta\mu\left(y_j\right)}{2\rho_{\max}}\left(\rho_{i-1}^k-\rho_i^k\right)_+\right]\right\}\\
&+ n_{i,j}^{k}\left\{(1-\beta)\left[1+\tau R\left(y_j,\rho_i^k,{m_K}_i^k\right)\right]\left[1-\frac{\eta\mu\left(y_j\right)}{2\rho_{\max}}\left[\left(\rho_i^k-\rho_{i+1}^k\right)_+ + \left(\rho_i^k-\rho_{i-1}^k\right)_+\right]\right]\right\}.
\end{aligned}
$$

This equation is built considering all the possible source terms, recalling that a spacial jump happens only if the local density is lower than the one in the neighbours, while the phenotypic one is random. The net growth between time steps t_k and t_{k+1} is also included. In particular, the mass could enter the balance through:

- both phenotipic and spatial jump from the neighbours y_{j-1} or y_{j+1} and x_{i-1} or x_{i+1} to the correct position x_i and phenotype y_j (first four rows)
- only phenotipic jump and no spatial movement(fifth and sixth rows)
- only spacial jump and no phenotipic changes (seventh and eighth rows)
- neither spacial movement nor phenotipic changes (ninth row)

Using the fact that for τ, Δ_x, and Δ_y sufficiently small the following relations hold:

$$
n_{i,j}^k \approx n(t,x,y) \equiv n, \quad n_{i,j}^{k+1} \approx n(t+\tau,x,y), \quad n_{i\pm1,j}^k \approx n\left(t,x\pm\Delta_x,y\right), \quad n_{i,j\pm1}^k \approx n\left(t,x,y\pm\Delta_y\right)
$$

$$
\rho_i^k \approx \rho(t,x) \equiv \rho, \quad \rho_{i\pm1}^k \approx \rho\left(t,x\pm\Delta_x\right), \quad \mu\left(y_j\right) \approx \mu(y) \equiv \mu, \quad R\left(y_j,\rho_i^k,{m_K}_i^k\right) \approx R(y,\rho,m_K) \equiv R,
$$

The discrete equation can be rewritten as:

$$
\begin{aligned}
n(t+\tau,x,y) = {} & n\left(t,x+\Delta_x,y+\Delta_y\right)\left\{\frac{\beta}{2}[1+\tau R]\left[\frac{\eta\mu}{2\rho_{\max}}\left(\rho\left(t,x+\Delta_x\right)-\rho\right)_+\right]\right\} \\
& + n\left(t,x-\Delta_x,y+\Delta_y\right)\left\{\frac{\beta}{2}[1+\tau R]\left[\frac{\eta\mu}{2\rho_{\max}}\left(\rho\left(t,x-\Delta_x\right)-\rho\right)_+\right]\right\} \\
& + n\left(t,x+\Delta_x,y-\Delta_y\right)\left\{\frac{\beta}{2}[1+\tau R]\left[\frac{\eta\mu}{2\rho_{\max}}\left(\rho\left(t,x+\Delta_x\right)-\rho\right)_+\right]\right\} \\
& + n\left(t,x-\Delta_x,y-\Delta_y\right)\left\{\frac{\beta}{2}[1+\tau R]\left[\frac{\eta\mu}{2\rho_{\max}}\left(\rho\left(t,x-\Delta_x\right)-\rho\right)_+\right]\right\} \\
& + n\left(t,x,y+\Delta_y\right)\left\{\frac{\beta}{2}[1+\tau R]\left[1-\frac{\eta\mu}{2\rho_{\max}}\left[\left(\rho-\rho\left(t,x+\Delta_x\right)\right)_+ + \left(\rho-\rho\left(t,x-\Delta_x\right)\right)_+\right]\right]\right\} \\
& + n\left(t,x,y-\Delta_y\right)\left\{\frac{\beta}{2}[1+\tau R]\left[1-\frac{\eta\mu}{2\rho_{\max}}\left[\left(\rho-\rho\left(t,x+\Delta_x\right)\right)_+ + \left(\rho-\rho\left(t,x-\Delta_x\right)\right)_+\right]\right]\right\} \\
& + n\left(t,x+\Delta_x,y\right)\left\{(1-\beta)[1+\tau R]\left[\frac{\eta\mu}{2\rho_{\max}}\left(\rho\left(t,x+\Delta_x\right)-\rho\right)_+\right]\right\} \\
& + n\left(t,x-\Delta_x,y\right)\left\{(1-\beta)[1+\tau R]\left[\frac{\eta\mu}{2\rho_{\max}}\left(\rho\left(t,x-\Delta_x-\rho\right)\right)_+\right]\right\} \\
& + n\left\{(1-\beta)[1+\tau R]\left[1-\frac{\eta\mu}{2\rho_{\max}}\left[\left(\rho-\rho\left(t,x+\Delta_x\right)\right)_+ + \left(\rho-\rho\left(t,x-\Delta_x\right)\right)_+\right]\right]\right\}.
\end{aligned}
$$

Assuming the function n to be sufficiently regular, we now expand using Taylor

$$
n\left(t,x,y\pm\Delta_y\right) = n \pm \Delta_y\frac{\partial n}{\partial y} + \frac{\Delta_y^2}{2}\frac{\partial^2 n}{\partial y^2} + \text{ h.o.t.}, \quad n\left(t,x\pm\Delta_x,y\right) = n \pm \Delta_x\frac{\partial n}{\partial x} + \frac{\Delta_x^2}{2}\frac{\partial^2 n}{\partial x^2} + \text{ h.o.t.},
$$

$$
n\left(t,x+\Delta_x,y\pm\Delta_y\right) = n + \Delta_x\frac{\partial n}{\partial x} \pm \Delta_y\frac{\partial n}{\partial y} + \frac{\Delta_x^2}{2}\frac{\partial^2 n}{\partial x^2} + \frac{\Delta_y^2}{2}\frac{\partial^2 n}{\partial y^2} \pm \Delta_x\Delta_y\frac{\partial^2 n}{\partial x\partial y} + \text{ h.o.t.},
$$

$$
n\left(t,x-\Delta_x,y\pm\Delta_y\right) = n - \Delta_x\frac{\partial n}{\partial x} \pm \Delta_y\frac{\partial n}{\partial y} + \frac{\Delta_x^2}{2}\frac{\partial^2 n}{\partial x^2} + \frac{\Delta_y^2}{2}\frac{\partial^2 n}{\partial y^2} \mp \Delta_x\Delta_y\frac{\partial^2 n}{\partial x\partial y} + \text{ h.o.t. }.
$$

In this way, the above equation can be rewritten as:

$$
\begin{aligned}
n(t+\tau,x,y) &= n\left\{\frac{\beta}{2}[1+\tau R]\left[\frac{\eta\mu}{2\rho_{\max}}\left(\rho\left(t,x+\Delta_x\right)-\rho\right)_+\right]\right\}+\Delta_x\frac{\partial n}{\partial x}\left\{\frac{\beta}{2}[1+\tau R]\left[\frac{\eta\mu}{2\rho_{\max}}\left(\rho\left(t,x+\Delta_x\right)-\rho\right)_+\right]\right\}\\
&+\Delta_y\frac{\partial n}{\partial y}\left\{\frac{\beta}{2}[1+\tau R]\left[\frac{\eta\mu}{2\rho_{\max}}\left(\rho\left(t,x+\Delta_x\right)-\rho\right)_+\right]\right\}+\Delta_x\Delta_y\frac{\partial^2 n}{\partial x\partial y}\left\{\frac{\beta}{2}[1+\tau R]\left[\frac{\eta\mu}{2\rho_{\max}}\left(\rho\left(t,x+\Delta_x\right)-\rho\right)_+\right]\right\}\\
&+\frac{\Delta_x^2}{2}\frac{\partial^2 n}{\partial x^2}\left\{\frac{\beta}{2}[1+\tau R]\left[\frac{\eta\mu}{2\rho_{\max}}\left(\rho\left(t,x+\Delta_x\right)-\rho\right)_+\right]\right\}+\frac{\Delta_y^2}{2}\frac{\partial^2 n}{\partial y^2}\left\{\frac{\beta}{2}[1+\tau R]\left[\frac{\eta\mu}{2\rho_{\max}}\left(\rho\left(t,x+\Delta_x\right)-\rho\right)_+\right]\right\}\\
&+n\left\{\frac{\beta}{2}[1+\tau R]\left[\frac{\eta\mu}{2\rho_{\max}}\left(\rho\left(t,x-\Delta_x\right)-\rho\right)_+\right]\right\}-\Delta_x\frac{\partial n}{\partial x}\left\{\frac{\beta}{2}[1+\tau R]\left[\frac{\eta\mu}{2\rho_{\max}}\left(\rho\left(t,x-\Delta_x\right)-\rho\right)_+\right]\right\}\\
&+\Delta_y\frac{\partial n}{\partial y}\left\{\frac{\beta}{2}[1+\tau R]\left[\frac{\eta\mu}{2\rho_{\max}}\left(\rho\left(t,x-\Delta_x\right)-\rho\right)_+\right]\right\}-\Delta_x\Delta_y\frac{\partial^2 n}{\partial x\partial y}\left\{\frac{\beta}{2}[1+\tau R]\left[\frac{\eta\mu}{2\rho_{\max}}\left(\rho\left(t,x-\Delta_x\right)-\rho\right)_+\right]\right\}\\
&+\frac{\Delta_x^2}{2}\frac{\partial^2 n}{\partial x^2}\left\{\frac{\beta}{2}[1+\tau R]\left[\frac{\eta\mu}{2\rho_{\max}}\left(\rho\left(t,x-\Delta_x\right)-\rho\right)_+\right]\right\}+\frac{\Delta_y^2}{2}\frac{\partial^2 n}{\partial y^2}\left\{\frac{\beta}{2}[1+\tau R]\left[\frac{\eta\mu}{2\rho_{\max}}\left(\rho\left(t,x-\Delta_x\right)-\rho\right)_+\right]\right\}\\
&+n\left\{\frac{\beta}{2}[1+\tau R]\left[\frac{\eta\mu}{2\rho_{\max}}\left(\rho\left(t,x+\Delta_x\right)-\rho\right)_+\right]\right\}+\Delta_x\frac{\partial n}{\partial x}\left\{\frac{\beta}{2}[1+\tau R]\left[\frac{\eta\mu}{2\rho_{\max}}\left(\rho\left(t,x+\Delta_x\right)-\rho\right)_+\right]\right\}\\
&-\Delta_y\frac{\partial n}{\partial y}\left\{\frac{\beta}{2}[1+\tau R]\left[\frac{\eta\mu}{2\rho_{\max}}\left(\rho\left(t,x+\Delta_x\right)-\rho\right)_+\right]\right\}-\Delta_x\Delta_y\frac{\partial^2 n}{\partial x\partial y}\left\{\frac{\beta}{2}[1+\tau R]\left[\frac{\eta\mu}{2\rho_{\max}}\left(\rho\left(t,x+\Delta_x\right)-\rho\right)_+\right]\right\}\\
&+\frac{\Delta_x^2}{2}\frac{\partial^2 n}{\partial x^2}\left\{\frac{\beta}{2}[1+\tau R]\left[\frac{\eta\mu}{2\rho_{\max}}\left(\rho\left(t,x+\Delta_x\right)-\rho\right)_+\right]\right\}+\frac{\Delta_y^2}{2}\frac{\partial^2 n}{\partial y^2}\left\{\frac{\beta}{2}[1+\tau R]\left[\frac{\eta\mu}{2\rho_{\max}}\left(\rho\left(t,x+\Delta_x\right)-\rho\right)_+\right]\right\}\\
&+n\left\{\frac{\beta}{2}[1+\tau R]\left[\frac{\eta\mu}{2\rho_{\max}}\left(\rho\left(t,x-\Delta_x\right)-\rho\right)_+\right]\right\}-\Delta_x\frac{\partial \eta}{\partial x}\left\{\frac{\beta}{2}[1+\tau R]\left[\frac{\eta\mu}{2\rho_{\max}}\left(\rho\left(t,x-\Delta_x\right)-\rho\right)_+\right]\right\}\\
&-\Delta_y\frac{\partial n}{\partial y}\left\{\frac{\beta}{2}[1+\tau R]\left[\frac{\eta\mu}{2\rho_{\max}}\left(\rho\left(t,x-\Delta_x\right)-\rho\right)_+\right]\right\}+\Delta_x\Delta_y\frac{\partial^2 n}{\partial x\partial y}\left\{\frac{\beta}{2}[1+\tau R]\left[\frac{\eta\mu}{2\rho_{\max}}\left(\rho\left(t,x-\Delta_x\right)-\rho\right)_+\right]\right\}\\
&+\frac{\Delta_x^2}{2}\frac{\partial^2 n}{\partial x^2}\left[\frac{\beta}{2}[1+\tau R]\left[\frac{\eta\mu}{2\rho_{\max}}\left(\rho\left(t,x\Delta_x\right)-\rho\right)_+\right]\right\}+\frac{\Delta_y^2}{2}\frac{\partial^2 n}{\partial y^2}\left\{\frac{\beta}{2}[1+\tau R]\left[\frac{\eta\mu}{2\rho_{\max}}\left(\rho\left(t,x-\Delta_x\right)-\rho\right)_++\right]\right.\\
&+n\left\{\frac{\beta}{2}[1+\tau R]\left[1-\frac{\eta\mu}{2\rho_{\max}}\left[\left(\rho-\rho\left(t,x+\Delta_x\right)\right)_++\left(\rho-\rho\left(t,x-\Delta_x\right)\right)_+\right]\right]\right\}\\
&+\Delta_y\frac{\partial n}{\partial y}\left\{\frac{\beta}{2}[1+\tau R]\left[1-\frac{\eta\mu}{2\rho_{\max}}\left[\left(\rho-\rho\left(t,x+\Delta_x\right)\right)_++\left(\rho-\rho\left(t,x-\Delta_x\right)\right)_+\right]\right]\right\}\\
&+\frac{\Delta_y^2}{2}\frac{\partial^2 n}{\partial y^2}\left\{\frac{\beta}{2}[1+\tau R]\left[1-\frac{\eta\mu}{2\rho_{\max}}\left[\left(\rho-\rho\left(t,x+\Delta_x\right)\right)_++\left(\rho-\rho\left(t,x-\Delta_x\right)\right)_+\right]\right]\right\}
\end{aligned}
$$

$$
\begin{aligned}
&+ n\left\{\frac{\beta}{2}[1+\tau R]\left[1-\frac{\eta\mu}{2\rho_{\max}}\left[(\rho-\rho\,(t,x+\Delta_x))_+ + (\rho-\rho\,(t,x-\Delta_x))_+\right]\right]\right\}\\
&- \Delta_y\frac{\partial n}{\partial y}\left\{\frac{\beta}{2}[1+\tau R]\left[1-\frac{\eta\mu}{2\rho_{\max}}\left[(\rho-\rho\,(t,x+\Delta_x))_+ + (\rho-\rho\,(t,x-\Delta_x))_+\right]\right]\right\}\\
&+ \frac{\Delta_y^2}{2}\frac{\partial^2 n}{\partial y^2}\left\{\frac{\beta}{2}[1+\tau R]\left[1-\frac{\eta\mu}{2\rho_{\max}}\left[(\rho-\rho\,(t,x+\Delta_x))_+ + (\rho-\rho\,(t,x-\Delta_x))_+\right]\right]\right\}\\
&+ n\left\{(1-\beta)[1+\tau R]\left[\frac{\eta\mu}{2\rho_{\max}}\left(\rho\,(t,x+\Delta_x)-\rho\right)_+\right]\right\}\\
&+ \Delta_x\frac{\partial n}{\partial x}\left\{(1-\beta)[1+\tau R]\left[\frac{\eta\mu}{2\rho_{\max}}\left(\rho\,(t,x+\Delta_x)-\rho\right)+\right]\right\}.\\
&+ \frac{\Delta_x^2}{2}\frac{\partial^2 n}{\partial x^2}\left\{(1-\beta)[1+\tau R]\left[\frac{\eta\mu}{2\rho_{\max}}\left(\rho\,(t,x+\Delta_x)-\rho\right)_+\right]\right\}\\
&+ n\left\{(1-\beta)[1+\tau R]\left[\frac{\eta\mu}{2\rho_{\max}}\left(\rho\,(t,x-\Delta_x)-\rho\right)_+\right]\right\}\\
&- \Delta_x\frac{\partial n}{\partial x}\left\{(1-\beta)[1+\tau R]\left[\frac{\eta\mu}{2\rho_{\max}}\left(\rho\,(t,x-\Delta_x)-\rho\right)_+\right]\right\}\\
&+ \frac{\Delta_x^2}{2}\frac{\partial^2 n}{\partial x^2}\left\{(1-\beta)[1+\tau R]\left[\frac{\eta\mu}{2\rho_{\max}}\left(\rho\,(t,x-\Delta_x)-\rho\right)_+\right]\right\}\\
&+ n\left\{(1-\beta)[1+\tau R]\left[1-\frac{\eta\mu}{2\rho_{\max}}\left[(\rho-\rho\,(t,x+\Delta_x))_+ + (\rho-\rho\,(t,x-\Delta_x))_+\right]\right]\right\} + \text{h.o.t.}
\end{aligned}
$$

Rearranging and collecting the derivatives of n, we have:

$$
\begin{aligned}
&n(t+\tau,x,y) =\\
&n\left\{\frac{\beta}{2}[1+\tau R]\left[\frac{\eta\mu}{2\rho_{\max}}\left(\rho\,(t,x+\Delta_x)-\rho\right)_+\right]\right\} + n\left\{\frac{\beta}{2}[1+\tau R]\left[\frac{\eta\mu}{2\rho_{\max}}\left(\rho\,(t,x-\Delta_x)-\rho\right)_+\right]\right\}\\
&+n\left\{\frac{\beta}{2}[1+\tau R]\left[\frac{\theta}{2}+\frac{\eta\mu}{2\rho_{\max}}\left(\rho\,(t,x+\Delta_x)-\rho\right)_+\right]\right\} + n\left\{\frac{\beta}{2}[1+\tau R]\left[\frac{\eta\mu}{2\rho_{\max}}\left(\rho\,(t,x-\Delta_x)-\rho\right)_+\right]\right\}\\
&+n\left\{\frac{\beta}{2}[1+\tau R]\left[1-\frac{\eta\mu}{2\rho_{\max}}\left[(\rho-\rho\,(t,x+\Delta_x))_+ + (\rho-\rho\,(t,x-\Delta_x))_+\right]\right]\right\}\\
&+n\left\{\frac{\beta}{2}[1+\tau R]\left[1-\frac{\eta\mu}{2\rho_{\max}}\left[(\rho-\rho\,(t,x+\Delta_x))_+ + (\rho-\rho\,(t,x-\Delta_x))_+\right]\right]\right\}\\
&+n\left\{(1-\beta)[1+\tau R]\left[\frac{\eta\mu}{2\rho_{\max}}\left(\rho\,(t,x+\Delta_x)-\rho\right)_+\right]\right\} + n\left\{(1-\beta)[1+\tau R]\left[\frac{\eta\mu}{2\rho_{\max}}\left(\rho\,(t,x-\Delta_x)-\rho\right)_+\right]\right\}\\
&+n\left\{(1-\beta)[1+\tau R]\left[1-\frac{\eta\mu}{2\rho_{\max}}\left[(\rho-\rho\,(t,x+\Delta_x))_+ + (\rho-\rho\,(t,x-\Delta_x))_+\right]\right]\right\}\\
&+\Delta_x\frac{\partial n}{\partial x}\left\{\frac{\beta}{2}[1+\tau R]\left[\frac{\eta\mu}{2\rho_{\max}}\left(\rho\,(t,x+\Delta_x)-\rho\right)_+\right]\right\} - \Delta_x\frac{\partial n}{\partial x}\left\{\frac{\beta}{2}[1+\tau R]\left[\frac{\eta\mu}{2E_{\max}}\left(\rho\,(t,x-\Delta_x)-\rho\right)_+\right]\right\}\\
&+\Delta_x\frac{\partial n}{\partial x}\left\{\frac{\beta}{2}[1+\tau R]\left[\frac{\eta\mu}{2\rho_{\max}}\left(\rho\,(t,x+\Delta_x)-\rho\right)_+\right]\right\} - \Delta_x\frac{\partial n}{\partial x}\left\{\frac{\beta}{2}[1+\tau R]\left[\frac{\eta\mu}{2\rho_{\max}}\left(\rho\,(t,x-\Delta_x)-\rho\right)_+\right]\right\}\\
&+\Delta_x\frac{\partial n}{\partial x}\left\{(1-\beta)[1+\tau R]\left[\frac{\eta\mu}{2\rho_{\max}}\left(\rho\,(t,x+\Delta_x)-\rho\right)_+\right]\right\}
\end{aligned}
$$

$$
\begin{aligned}
&- \Delta_x \frac{\partial n}{\partial x}\left\{(1-\beta)[1+\tau R]\left[\frac{\eta\mu}{2\rho_{\max}}\left(\rho\left(t,x-\Delta_x\right)-\rho\right)_+\right]\right\}\\
&+ \Delta_y \frac{\partial n}{\partial y}\left\{\frac{\beta}{2}[1+\tau R]\left[\frac{\eta\mu}{2\rho_{\max}}\left(\rho\left(t,x+\Delta_x\right)-\rho\right)_+\right]\right\} + \Delta_y \frac{\partial n}{\partial y}\left\{\frac{\beta}{2}[1+\tau R]\left[\frac{\eta\mu}{2E_{\max}}\left(\rho\left(t,x-\Delta_x\right)-\rho\right)_+\right]\right\}\\
&- \Delta_y \frac{\partial n}{\partial y}\left\{\frac{\beta}{2}[1+\tau R]\left[\frac{\eta\mu}{2\rho_{\max}}\left(\rho\left(t,x+\Delta_x\right)-\rho\right)_+\right]\right\} - \Delta_y \frac{\partial n}{\partial y}\left\{\frac{\beta}{2}[1+\tau R]\left[\frac{\eta\mu}{2\rho_{\max}}\left(\rho\left(t,x-\Delta_x\right)-\rho\right)_+\right]\right\}\\
&+ \Delta_y \frac{\partial n}{\partial y}\left\{\frac{\beta}{2}[1+\tau R]\left[1-\frac{\eta\mu}{2\rho_{\max}}\left[\left(\rho-\rho\left(t,x+\Delta_x\right)\right)_+ + \left(\rho-\rho\left(t,x-\Delta_x\right)\right)_+\right]\right]\right\}\\
&- \Delta_y \frac{\partial n}{\partial y}\left\{\frac{\beta}{2}[1+\tau R]\left[1-\frac{\eta\mu}{2\rho_{\max}}\left[\left(\rho-\rho\left(t,x+\Delta_x\right)\right)_+ + \left(\rho-\rho\left(t,x-\Delta_x\right)\right)_+\right]\right]\right\}\\
&+ \Delta_x\Delta_y \frac{\partial^2 n}{\partial x\partial y}\left\{\frac{\beta}{2}[1+\tau R]\left[\frac{\eta\mu}{2\rho_{\max}}\left(\rho\left(t,x+\Delta_x\right)-\rho\right)_+\right]\right\}\\
&- \Delta_x\Delta_y \frac{\partial^2 n}{\partial x\partial y}\left\{\frac{\beta}{2}[1+\tau R]\left[\frac{\eta\mu}{2\rho_{\max}}\left(\rho\left(t,x-\Delta_x\right)-\rho\right)_+\right]\right\}\\
&- \Delta_x\Delta_y \frac{\partial^2 n}{\partial x\partial y}\left\{\frac{\beta}{2}[1+\tau R]\left[\frac{\eta\mu}{2\rho_{\max}}\left(\rho\left(t,x+\Delta_x\right)-\rho\right)_+\right]\right\}\\
&+ \Delta_x\Delta_y \frac{\partial^2 n}{\partial x\partial y}\left\{\frac{\beta}{2}[1+\tau R]\left[\frac{\eta\mu}{2\rho_{\max}}\left(\rho\left(t,x-\Delta_x\right)-\rho\right)_+\right]\right\}\\
&+ \frac{\Delta_x^2}{2}\frac{\partial^2 n}{\partial x^2}\left\{\frac{\beta}{2}[1+\tau R]\left[\frac{\eta\mu}{2\rho_{\max}}\left(\rho\left(t,x+\Delta_x\right)-\rho\right)_+\right]\right\} + \frac{\Delta_x^2}{2}\frac{\partial^2 n}{\partial x^2}\left\{\frac{\beta}{2}[1+\tau R]\left[\frac{\eta\mu}{2\rho_{\max}}\left(\rho\left(t,x-\Delta_x\right)-\rho\right)_+\right]\right\}\\
&+ \frac{\Delta_x^2}{2}\frac{\partial^2 n}{\partial x^2}\left\{\frac{\beta}{2}[1+\tau R]\left[\frac{\eta\mu}{2\rho_{\max}}\left(\rho\left(t,x+\Delta_x\right)-\rho\right)_+\right]\right\} + \frac{\Delta_x^2}{2}\frac{\partial^2 n}{\partial x^2}\left\{\frac{\beta}{2}[1+\tau R]\left[\frac{\eta\mu}{2\rho_{\max}}\left(\rho\left(t,x-\Delta_x\right)-\rho\right)_+\right]\right\}\\
&+ \frac{\Delta_x^2}{2}\frac{\partial^2 n}{\partial x^2}\left\{(1-\beta)[1+\tau R]\left[\frac{\eta\mu}{2\rho_{\max}}\left(\rho\left(t,x+\Delta_x\right)-\rho\right)_+\right]\right\}\\
&+ \frac{\Delta_x^2}{2}\frac{\partial^2 n}{\partial x^2}\left\{(1-\beta)[1+\tau R]\left[\frac{\eta\mu}{2\rho_{\max}}\left(\rho\left(t,x-\Delta_x\right)-\rho\right)_+\right]\right\}\\
&+ \frac{\Delta_y^2}{2}\frac{\partial^2 n}{\partial y^2}\left\{\frac{\beta}{2}[1+\tau R]\left[\frac{\eta\mu}{2\rho_{\max}}\left(\rho\left(t,x+\Delta_x\right)-\rho\right)_+\right]\right\} + \frac{\Delta_y^2}{2}\frac{\partial^2 n}{\partial y^2}\left\{\frac{\beta}{2}[1+\tau R]\left[\frac{\eta\mu}{2\rho_{\max}}\left(\rho\left(t,x-\Delta_x\right)\ -\rho\right)_+\right]\right\}\\
&+ \frac{\Delta_y^2}{2}\frac{\partial^2 n}{\partial y^2}\left\{\frac{\beta}{2}[1+\tau R]\left[\frac{\eta\mu}{2\rho_{\max}}\left(\rho\left(t,x+\Delta_x\right)-\rho\right)_+\right]\right\} + \frac{\Delta_y^2}{2}\frac{\partial^2 n}{\partial y^2}\left\{\frac{\beta}{2}[1+\tau R]\left[\frac{\eta\mu}{2\rho_{\max}}\left(\rho\left(t,x-\Delta_x\right)-\rho\right)_+\right]\right\}\\
&+ \frac{\Delta_y^2}{2}\frac{\partial^2 n}{\partial y^2}\left\{\frac{\beta}{2}[1+\tau R]\left[1-\frac{\eta\mu}{2\rho_{\max}}\left[\left(\rho-\rho\left(t,x+\Delta_x\right)\right)_+ + \left(\rho-\rho\left(t,x-\Delta_x\right)\right)_+\right]\right]\right\}\\
&+ \frac{\Delta_y^2}{2}\frac{\partial^2 n}{\partial y^2}\left\{\frac{\beta}{2}[1+\tau R]\left[1-\frac{\eta\mu}{2\rho_{\max}}\left[\left(\rho-\rho\left(t,x+\Delta_x\right)\right)_+ + \left(\rho-\rho\left(t,x-\Delta_x\right)\right)_+\right]\right]\right\} + \text{h.o.t.}
\end{aligned}
$$

Further simplifying yields

$$
\begin{aligned}
&n(t+\tau,x,y) = \\
&n\left\{\beta[1+\tau R]\left[\frac{\eta\mu}{2\rho_{\max}}\left(\rho\left(t,x+\Delta_x\right)-\rho\right)_+\right]\right\} + n\left\{\beta[1+\tau R]\left[\frac{\eta\mu}{2\rho_{\max}}\left(\rho\left(t,x-\Delta_x\right)-\rho\right)_+\right]\right\} \\
&+n\left\{\beta[1+\tau R]\left[1-\frac{\eta\mu}{2E_{\max}}\left[\left(\rho-\rho\left(t,x+\Delta_x\right)\right)_+ + \left(\rho-\rho\left(t,x-\Delta_x\right)\right)_+\right]\right]\right\} \\
&+n\left\{(1-\beta)[1+\tau R]\left[\frac{\eta\mu}{2\rho_{\max}}\left(\rho\left(t,x+\Delta_x\right)-\rho\right)_+\right]\right\} + n\left\{(1-\beta)[1+\tau R]\left[\frac{\eta\mu}{2\rho_{\max}}\left(\rho\left(t,x-\Delta_x\right)-\rho\right)_+\right]\right\} \\
&+n\left\{(1-\beta)[1+\tau R]\left[1-\frac{\eta\mu}{2\rho_{\max}}\left[\left(\rho-\rho\left(t,x+\Delta_x\right)\right)_+ + \left(\rho-\rho\left(t,x-\Delta_x\right)\right)_+\right]\right]\right\} \\
&+\Delta_x\frac{\partial n}{\partial x}\left\{\beta[1+\tau R]\left[\frac{\eta\mu}{2\rho_{\max}}\left(\rho-\rho\left(t,x+\Delta_x\right)\right)_+\right]\right\} \\
&-\Delta_x\frac{\partial n}{\partial x}\left\{\beta[1+\tau R]\left[\frac{\eta\mu}{2\rho_{\max}}\left(\rho\left(t,x-\Delta_x\right)-\rho\right)_+\right]\right\} \\
&+\Delta_x\frac{\partial n}{\partial x}\left\{(1-\beta)[1+\tau R]\left[\frac{\eta\mu}{2\rho_{\max}}\left(\rho\left(t,x+\Delta_x\right)-\rho\right)_+\right]\right\} \\
&-\Delta_x\frac{\partial \eta}{\partial x}\left\{(1-\beta)[1+\tau R]\left[\frac{\eta\mu}{2\rho_{\max}}\left(\rho\left(t,x-\Delta_x\right)-\rho\right)_+\right]\right\} \\
&+\Delta_y\frac{\partial n}{\partial y}\left\{\beta[1+\tau R]\left[\frac{\eta\mu}{2\rho_{\max}}\left(\rho\left(t,x+\Delta_y\right)-\rho\right)_+\right]\right\} - \Delta_y\frac{\partial n}{\partial y}\left\{\beta[1+\tau R]\left[\frac{\eta\mu}{2\rho_{\max}}\left(\rho\left(t,x-\Delta_x\right)-\rho\right)_+\right]\right\} \\
&+\frac{\Delta_x^2}{2}\frac{\partial^2 n}{\partial x^2}\left\{\beta[1+\tau R]\left[\frac{\eta\mu}{2\rho_{\max}}\left(\rho\left(t,x+\Delta_x\right)-\rho\right)_+\right]\right\} \\
&+\frac{\Delta_x^2}{2}\frac{\partial^2 n}{\partial x^2}\left\{\beta[1+\tau R]\left[\frac{\eta\mu}{2\rho_{\max}}\left(\rho\left(t,x-\Delta_x\right)-\rho\right)_+\right]\right\}. \\
&+\frac{\Delta_x^2}{2}\frac{\partial^2 n}{\partial x^2}\left\{(1-\beta)[1+\tau R]\left[\frac{\eta\mu}{2\rho_{\max}}\left(\rho\left(t,x+\Delta_x\right)-\rho\right)_+\right]\right\} \\
&+\frac{\Delta_x^2}{2}\frac{\partial^2 n}{\partial x^2}\left\{(1-\beta)[1+\tau R]\left[\frac{\eta\mu}{2\rho_{\max}}\left(\rho\left(t,x-\Delta_x\right)-\rho\right)_+\right]\right\} \\
&+\frac{\Delta_y^2}{2}\frac{\partial^2 n}{\partial y^2}\left\{\beta[1+\tau R]\left[\frac{\eta\mu}{2\rho_{\max}}\left(\rho\left(t,x+\Delta_x\right)-\rho\right)_+\right]\right\} \\
&+\frac{\Delta_y^2}{2}\frac{\partial^2 n}{\partial y^2}\left\{\beta[1+\tau R]\left[\frac{\eta\mu}{2\rho_{\max}}\left(\rho\left(t,x-\Delta_x\right)-\rho\right)_+\right]\right\} \\
&+\frac{\Delta_y^2}{2}\frac{\partial^2 n}{\partial y^2}\left\{\beta[1+\tau R]\left[1-\frac{\eta\mu}{2\rho_{\max}}\left[\left(\rho-\rho\left(t,x+\Delta_x\right)\right)_+ + \left(\rho-\rho\left(t,x-\Delta_x\right)\right)_+\right]\right]\right\}
\end{aligned}
$$

Cancelling out terms in which β appears, we find

$$
\begin{aligned}
n(t+\tau,x,y) &= n\left\{[1+\tau R]\left[\frac{\eta\mu}{2\rho_{\max}}\left(\rho\left(t,x+\Delta_x\right)-\rho\right)_+\right]\right\} - n\left\{[1+\tau R]\left[\frac{\eta\mu}{2\rho_{\max}}\left(\rho-\rho\left(t,x+\Delta_x\right)\right)_+\right]\right\} \\
&+n\left\{[1+\tau R]\left[\frac{\eta\mu}{2\rho_{\max}}\left(\rho\left(t,x-\Delta_x\right)-\rho\right)_+\right]\right\} - n\left\{[1+\tau R]\left[\frac{\eta\mu}{2\rho_{\max}}\left(\rho-\rho\left(t,x-\Delta_x\right)\right)_+\right]\right\} + n\{[1+\tau R]\} \\
&+\Delta_x\frac{\partial n}{\partial x}\left\{[1+\tau R]\left[\frac{\eta\mu}{2\rho_{\max}}\left(\rho\left(t,x+\Delta_x\right)-\rho\right)_+\right]\right\} - \Delta_x\frac{\partial n}{\partial x}\left\{[1+\tau R]\left[\frac{\eta\mu}{2\rho_{\max}}\left(\rho\left(t,x-\Delta_x\right)-\rho\right)_+\right]\right\} \\
&+\Delta_y\frac{\partial n}{\partial y}\left\{\beta[1+\tau R]\left[\frac{\eta\mu}{2\rho_{\max}}\left(\rho\left(t,x+\Delta_x\right)-\rho\right)_+\right]\right\} - \Delta_y\frac{\partial n}{\partial y}\left\{\beta[1+\tau R]\left[\frac{\eta\mu}{2\rho_{\max}}\left(\rho\left(t,x-\Delta_x\right)-\rho\right)_+\right]\right\} \\
&+\frac{\Delta_x^2}{2}\frac{\partial^2 n}{\partial x^2}\left\{[1+\tau R]\left[\frac{\eta\mu}{2\rho_{\max}}\left(\rho\left(t,x+\Delta_x\right)-\rho\right)_+\right]\right\} + \frac{\Delta_x^2}{2}\frac{\partial^2 n}{\partial x^2}\left\{[1+\tau R]\left[\frac{\eta\mu}{2\rho_{\max}}\left(\rho\left(t,x-\Delta_x\right)-\rho\right)_+\right]\right\} \\
&+\frac{\Delta_y^2}{2}\frac{\partial^2 n}{\partial y^2}\{\beta[1+\tau R]\} + \text{ h.o.t.}
\end{aligned}
$$

Using the relation $(f)_+ - (-f)_+ = f$ which holds for real functions f, we obtain:

$$
\begin{aligned}
n(t+\tau,x,y) &= n\left\{[1+\tau R]\left[\frac{\eta\mu}{2\rho_{\max}}\left(\rho\left(t,x+\Delta_x\right)-\rho\right)\right]\right\} + n\left\{[1+\tau R]\left[\frac{\eta\mu}{2\rho_{\max}}\left(\rho\left(t,x-\Delta_x\right)-\rho\right)\right]\right\} \\
&+\Delta_x\frac{\partial n}{\partial x}\left\{[1+\tau R]\left[\frac{\eta\mu}{2\rho_{\max}}\left(\rho\left(t,x+\Delta_x\right)-\rho\right)_+\right]\right\} - \Delta_x\frac{\partial n}{\partial x}\left\{[1+\tau R]\left[\frac{\eta\mu}{2\rho_{\max}}\left(\rho\left(t,x-\Delta_x\right)-\rho\right)_+\right]\right\} \\
&+\Delta_y\frac{\partial n}{\partial y}\left\{\beta[1+\tau R]\left[\frac{\eta\mu}{2\rho_{\max}}\left(\rho\left(t,x+\Delta_x\right)-\rho\right)_+\right]\right\} - \Delta_y\frac{\partial n}{\partial y}\left\{\beta[1+\tau R]\left[\frac{\eta\mu}{2\rho_{\max}}\left(\rho\left(t,x-\Delta_x\right)-\rho\right)_+\right]\right\} \\
&+\frac{\Delta_x^2}{2}\frac{\partial^2 n}{\partial x^2}\left\{[1+\tau R]\left[\frac{\eta\mu}{2\rho_{\max}}\left(\rho\left(t,x+\Delta_x\right)-\rho\right)_+\right]\right\} + \frac{\Delta_x^2}{2}\frac{\partial^2 n}{\partial x^2}\left\{[1+\tau R]\left[\frac{\eta\mu}{2\rho_{\max}}\left(\rho\left(t,x-\Delta_x\right)-\rho\right)_+\right]\right\} \\
&+\frac{\Delta_y^2}{2}\frac{\partial^2 n}{\partial y^2}\{\beta[1+\tau R]\} + n\{[1+\tau R]\} + \text{ h.o.t.}
\end{aligned}
$$

Assuming the function ρ to be sufficiently regular, substituting the following Taylor expansion

$$\rho\left(t,x\pm\Delta_x\right) = \rho \pm \Delta_x\frac{\partial\rho}{\partial x} + \frac{\Delta_x^2}{2}\frac{\partial^2\rho}{\partial x^2} + \text{ h.o.t.}$$

we have:

$$
\begin{aligned}
n(t+\tau,x,y) &= n\left\{[1+\tau R]\left[+\frac{\Delta_x^2\eta\mu}{2\rho_{\max}}\frac{\partial^2\rho}{\partial x^2}\right]\right\} + n\{[1+\tau R]\} + \Delta_x\frac{\partial n}{\partial x}\left\{[1+\tau R]\left[\frac{\eta\mu}{2\rho_{\max}}\left(+\Delta_x\frac{\partial\rho}{\partial x}\right)_+\right]\right\} \\
&- \Delta_x\frac{\partial n}{\partial x}\left\{[1+\tau R]\left[\frac{\eta\mu}{2\rho_{\max}}\left(-\Delta_x\frac{\partial\rho}{\partial x}\right)_+\right]\right\} + \Delta_y\frac{\partial n}{\partial y}\left\{\beta[1+\tau R]\left[\frac{\eta\mu}{2\rho_{\max}}\left(+\Delta_x\frac{\partial\rho}{\partial x}\right)_+\right]\right\} \\
&- \Delta_y\frac{\partial n}{\partial y}\left\{\beta[1+\tau R]\left[\frac{\eta\mu}{2\rho_{\max}}\left(-\Delta_x\frac{\partial\rho}{\partial x}\right)_+\right]\right\} + \frac{\Delta_y^2}{2}\frac{\partial^2 n}{\partial y^2}\{\beta[1+\tau R]\} + \text{ h.o.t.}
\end{aligned}
$$

Considering terms of order $O\left(\tau\Delta_x^2\right)$ and $O\left(\tau\Delta_y^2\right)$ as h.o.t. yields

$$
\begin{aligned}
n(t+\tau,x,y) = n\left\{\left[+\frac{\Delta_x^2\eta\mu}{2\rho_{\max}}\frac{\partial^2\rho}{\partial x^2}\right]\right\} + n\{[1+\tau R]\} + \Delta_x\frac{\partial n}{\partial x}\left\{\left[\frac{\eta\mu}{2\rho_{\max}}\left(+\Delta_x\frac{\partial\rho}{\partial x}\right)_+\right]\right\} \\
- \Delta_x\frac{\partial n}{\partial x}\left\{\left[\frac{\eta\mu}{2\rho_{\max}}\left(-\Delta_x\frac{\partial\rho}{\partial x}\right)_+\right]\right\} + \Delta_y\frac{\partial n}{\partial y}\left\{\beta\left[\frac{\eta\mu}{2\rho_{\max}}\left(+\Delta_x\frac{\partial\rho}{\partial x}\right)_+\right]\right\} \\
- \Delta_y\frac{\partial n}{\partial y}\left\{\beta\left[\frac{\eta\mu}{2\rho_{\max}}\left(-\Delta_x\frac{\partial\rho}{\partial x}\right)_+\right]\right\} + \frac{\Delta_y^2\beta}{2}\frac{\partial^2 n}{\partial y^2} + \text{ h.o.t.}
\end{aligned}
$$

Once again, using the relation $(f)_+ - (-f)_+ = f$, we obtain:

$$
\begin{aligned}
n(t+\tau,x,y) =& n\left\{\left[+\frac{\Delta_x^2\eta\mu}{2\rho_{\max}}\frac{\partial^2\rho}{\partial x^2}\right]\right\} + n\{[1+\tau R]\} + \Delta_x^2\frac{\partial n}{\partial x}\left\{\left[+\frac{\eta\mu}{2\rho_{\max}}\frac{\partial\rho}{\partial x}\right]\right\} \\
&+ \Delta_y\Delta_x\frac{\partial n}{\partial y}\left\{\beta\left[+\frac{\eta\mu}{2\rho_{\max}}\frac{\partial\rho}{\partial x}\right]\right\} + \frac{\Delta_y^2\beta}{2}\frac{\partial^2 n}{\partial y^2} + \text{ h.o.t.}
\end{aligned}
$$

Further rearranging yields

$$
n(t+\tau,x,y) = \frac{\Delta_x^2\eta\mu}{2\rho_{\max}}\left[n\frac{\partial^2\rho}{\partial x^2} + \frac{\partial n}{\partial x}\frac{\partial\rho}{\partial x}\right] + n + \tau Rn + \frac{\Delta_y^2\beta}{2}\frac{\partial^2 n}{\partial y^2} + \beta\Delta_y\Delta_x\left[\frac{\eta\mu}{2\rho_{\max}}\frac{\partial\rho}{\partial x}\right]\frac{\partial n}{\partial y} + \text{ h.o.t.}
$$

Dividing both sides by τ we have

$$
\frac{n(t+\tau,x,y)-n}{\tau} = \frac{\Delta_x^2\eta\mu}{2\rho_{\max}\tau}\left[n\frac{\partial^2\rho}{\partial x^2} + \frac{\partial n}{\partial x}\frac{\partial\rho}{\partial x}\right] + Rn + \frac{\Delta_y^2\beta}{2\tau}\frac{\partial^2 n}{\partial y^2} + \frac{\beta\Delta_y\Delta_x}{\tau}\left[\frac{\eta\mu}{2\rho_{\max}}\frac{\partial\rho}{\partial x}\right]\frac{\partial n}{\partial y} + \text{ h.o.t.}
$$

Now we let the time-step $\tau \to 0$, the space-step $\Delta_x \to 0$ and the phenotype-step $\Delta_y \to 0$ in such a way that

$$
\frac{\Delta_x^2\eta}{2\rho_{\max}\tau} \to \alpha \in \mathbb{R}_*^+, \quad \text{and} \quad \frac{\Delta_y^2\beta}{2\tau} \to \omega \in \mathbb{R}_*^+
$$

we formally obtain

$$
\frac{\partial n}{\partial t} = \alpha\ \mu(y)\left[n\frac{\partial^2\rho}{\partial x^2} + \frac{\partial n}{\partial x}\frac{\partial\rho}{\partial x}\right] + Rn + \omega\frac{\partial^2 n}{\partial y^2},
$$

which simplifies to

$$
\frac{\partial n(t,x,y)}{\partial t} - \alpha\ \mu(y)\frac{\partial}{\partial x}\left(n(t,x,y)\frac{\partial\rho(t,x)}{\partial x}\right) = R(y,\rho,m_{_K})\ n(t,x,y) + \omega\frac{\partial^2 n(t,x,y)}{\partial y^2}.
$$

Using the definition (1.11) for the term $R(y,\rho,m_{_K})$ we recover:

$$
\partial_t n - \alpha\ \mu(y)\ \partial_x\ (n\ \partial_x\rho) = G(y,\rho)\ n + \omega\ \partial_{yy}^2 n - \gamma\ m_{_K} n,
$$

that is the PIDE $(2.10)_1$ for $n(t,x,y)$.

3.2 Derivation of the equation for the attranctant S

Using the fact that for τ, Δ_y and Δ_x sufficiently small it holds

$$n_{i,j}^k \approx n(t,x,y) \quad n_{i,j}^{k+1} \approx n(t+\tau,x) \quad \rho_i^k \approx \rho(t,x)$$

$$S_i^k \approx S(t,x) \quad S_i^{k+1} \approx S(t+\tau,x) \quad S_{i\pm1}^k = S(t,x\pm\Delta_x) \quad P(y_j) \approx P(y)$$

and the sum on j formally converge to integral for $\Delta_y \to 0$, we obtain the approximated equation:

$$S(t+\tau,x) = S(t,x)+\tau\left[\, D_S \frac{S(t,x+\Delta_x)+S(t,x-\Delta_x)-2S(t,x)}{\Delta_x^2} - \lambda S(t,x) + \frac{\mathbb{1}_{\mathrm{supp}(\rho)}}{\rho(t,x)} \int P(y)\; n(t,x,y)\; \mathrm{d}y \right] .$$

Dividing by τ and letting $\tau \to 0$ and $\Delta_x \to 0$, formally gives:

$$\partial_t S = \mathbb{1}_{\mathrm{supp}(\rho)} \int_0^Y \frac{P(y)}{\rho(t,x)}\; n(t,x,y)\; dy - \lambda S + D_s\; \partial_{xx}^2 S,$$

that is the PDE $(2.10)_3$ for the evolution of the attractant concentration S.

3.3 Derivation of the equation for the density of regulatory cells $m_{_R}$

For simplicity, we rename the spacial step as $\Delta_x = h$ and the density of regulatory cells as $m_{_R} = u$, and then we write the discrete equation based on the rules presented in Section 2.5 . The principle of mass conservation gives:

$$\begin{aligned} u_i^{k+1} = (1-\gamma_{_R}\;\tau)\;\Bigg\{ & u_i^k + \frac{\vartheta}{2}\Big(u_{i-1}^k + u_{i+1}^k\Big) - \vartheta\; u_i^k \\ & + \frac{\nu}{2S_M}\left[\Big(\; S_i^k - S_{i-1}^k\Big)_+ u_{i-1}^k + \Big(S_i^k - S_{i+1}^k\Big)_+ u_{i+1}^k\right] \\ & - \frac{\nu}{2S_M}\left[\Big(S_{i-1}^k - S_i^k\Big)_+ u_i^k + \Big(S_{i+1}^k - S_i^k\Big)_+ u_i^k\right] \Bigg\} + \tau\Lambda(S_i^k). \end{aligned}$$

In this equation appears the factor $(1-\gamma_{_R}\tau)$ representing the probability that a regulatory cell remains quiescent (without dying) between time t_k and t_{k+1}. The first three terms in the curly brackets represent the fact that the density of regulatory cells at a certain time in a certain position x_i is given by the density that is already in the correct position at a previous time plus the contribute of the mass that will jump in or out the position x_i from the neighbours due to random motion. The other two terms represent, respectively, the source and sink terms related to the chemotactic motion so that the mass in the neighbourhood tends to move in position x_i if there is a higher chemical concentration, and vice versa the mass undergoes the opposite movement, exiting from the balance. In addition, the last term represents an external source that produces regulatory cells depending on the concentration of the chemical attractor at the

specific location.
For spacial and time step h, τ sufficiently small it holds:

$$t_k \approx t \quad t_{k+1} \approx t+\tau \quad x_i \approx x \quad x_{i\pm1} \approx x \pm h$$
$$u_i^k \approx u(t,x) \quad u_i^{k+1} \approx u(t+\tau,x) \quad u_{i\pm1}^k \approx u(t,x\pm h)$$
$$S_i^k \approx S(t,x) \quad S_i^{k+1} \approx S(t+\tau,x) \quad S_{i\pm1}^k \approx S(t,x\pm h) \quad \Lambda(S_i^k) \approx \Lambda(S)$$

Substituting these relations into the discrete formulation, we obtain an approximated equation:

$$\begin{aligned} u(t+\tau,x) = (1-\gamma_{_R}\tau)\ \Big\{ & u(t,x) + \frac{\vartheta}{2}\Big(u(t,x-h)+u(t,x+h)\Big) - \vartheta\ u(t,x) \\ & + \frac{v}{2S_M}\Big[\Big(\ S(t,x)-S(t,x-h)\Big)_+ u(t,x-h) + \Big(S(t,x)-S(t,x+h)\Big)_+ u(t,x+h)\Big] \\ & - \frac{v}{2S_M}\Big[\Big(S(t,x-h)-S(t,x)\Big)_+ u(t,x) + \Big(S(t,x+h)-S(t,x)\Big)_+ u(t,x)\Big]\ \Big\} + \tau\Lambda(S). \end{aligned}$$

We suppose these functions to be sufficiently regular; in particular we ask $u(t,x)$ and $S(t,x)$ to be twice differentiable in space x and $u(t,x)$ differentiable also in time t so that we can write Taylor expansions in x and t:

$$u(t+\tau,x) = u + \tau\frac{\partial u}{\partial t} + \text{h.o.t}$$
$$u(t,x\pm h) = u\ \pm h\frac{\partial u}{\partial x} + \frac{h^2}{2}\frac{\partial^2 u}{\partial x^2} + \text{h.o.t}$$
$$S(t,x\pm h) = S\ \pm h\frac{\partial S}{\partial x} + \frac{h^2}{2}\frac{\partial^2 S}{\partial x^2} + \text{h.o.t}$$

Introducing these definitions into the above equation:

$$\begin{aligned} u+\tau\frac{\partial u}{\partial t} = (1-\gamma_{_R}\tau)\ \Big\{ & u + \frac{\vartheta}{2}\Big(u - h\frac{\partial u}{\partial x} + \frac{h^2}{2}\frac{\partial^2 u}{\partial x^2} + u + h\frac{\partial u}{\partial x} + \frac{h^2}{2}\frac{\partial^2 u}{\partial x^2}\Big) - \vartheta\ u \\ & + \frac{\nu}{2S_M}\Big[\Big(\ S - S + h\frac{\partial S}{\partial x} - \frac{h^2}{2}\frac{\partial^2 S}{\partial x^2}\Big)_+ \Big(u - h\frac{\partial u}{\partial x} + \frac{h^2}{2}\frac{\partial^2 u}{\partial x^2}\Big) \\ & + \Big(S - S - h\frac{\partial S}{\partial x} - \frac{h^2}{2}\frac{\partial^2 S}{\partial x^2}\Big)_+ \Big(u + h\frac{\partial u}{\partial x} + \frac{h^2}{2}\frac{\partial^2 u}{\partial x^2}\Big)\Big] \\ & - \frac{\nu}{2\ S_M}\Big[\Big(S - h\frac{\partial S}{\partial x} + \frac{h^2}{2}\frac{\partial^2 S}{\partial x^2} - S\Big)_+ u + \Big(S + h\frac{\partial S}{\partial x} + \frac{h^2}{2}\frac{\partial^2 S}{\partial x^2} - S\Big)_+ u\Big]\ \Big\} + \tau\Lambda(S) + \text{ h.o.t.} \end{aligned}$$

Simplifying some terms:

$$\begin{aligned} u+\tau\frac{\partial u}{\partial t} = (1-\gamma_{_R}\tau)\ \Big\{ & u + \vartheta\frac{h^2}{2}\frac{\partial^2 u}{\partial x^2} + \frac{\nu}{2S_M}\Big[\Big(\ +h\frac{\partial S}{\partial x} - \frac{h^2}{2}\frac{\partial^2 S}{\partial x^2}\Big)_+ \Big(u - h\frac{\partial u}{\partial x} + \frac{h^2}{2}\frac{\partial^2 u}{\partial x^2}\Big) \\ & + \Big(-h\frac{\partial S}{\partial x} - \frac{h^2}{2}\frac{\partial^2 S}{\partial x^2}\Big)_+ \Big(u + h\frac{\partial u}{\partial x} + \frac{h^2}{2}\frac{\partial^2 u}{\partial x^2}\Big)\Big] \\ & - \frac{\nu}{2\ S_M}\Big[\Big(-h\frac{\partial S}{\partial x} + \frac{h^2}{2}\frac{\partial^2 S}{\partial x^2}\Big)_+ u + \Big(+h\frac{\partial S}{\partial x} + \frac{h^2}{2}\frac{\partial^2 S}{\partial x^2}\Big)_+ u\Big]\ \Big\} + \tau\Lambda(S) + \text{ h.o.t.} \end{aligned}$$

Grouping some terms:

$$u+\tau\frac{\partial u}{\partial t}=(1-\gamma_{_R}\tau)\left\{u+\vartheta\frac{h^2}{2}\frac{\partial^2 u}{\partial x^2}+\frac{\nu}{2S_M}\left[\left(+h\frac{\partial S}{\partial x}-\frac{h^2}{2}\frac{\partial^2 S}{\partial x^2}\right)_+\left(u-h\frac{\partial u}{\partial x}+\frac{h^2}{2}\frac{\partial^2 u}{\partial x^2}\right)\right.\right.$$
$$+\left(-h\frac{\partial S}{\partial x}-\frac{h^2}{2}\frac{\partial^2 S}{\partial x^2}\right)_+\left(u+h\frac{\partial u}{\partial x}+\frac{h^2}{2}\frac{\partial^2 u}{\partial x^2}\right)$$
$$\left.\left.-\left(-h\frac{\partial S}{\partial x}+\frac{h^2}{2}\frac{\partial^2 S}{\partial x^2}\right)_+ u-\left(+h\frac{\partial S}{\partial x}+\frac{h^2}{2}\frac{\partial^2 S}{\partial x^2}\right)_+ u\right]\right\}+\tau\Lambda(S)+\text{ h.o.t.}$$

We now use for the terms in u the well known fact that for a generic function f holds $(f)_+-(-f)_+=f$:

$$u+\tau\frac{\partial u}{\partial t}=(1-\gamma_{_R}\tau)\left\{u+\vartheta\frac{h^2}{2}\frac{\partial^2 u}{\partial x^2}+\frac{\eta}{2S_M}\left[\left(+h\frac{\partial S}{\partial x}-\frac{h^2}{2}\frac{\partial^2 S}{\partial x^2}\right)_+\left(-h\frac{\partial u}{\partial x}+\frac{h^2}{2}\frac{\partial^2 u}{\partial x^2}\right)\right.\right.$$
$$+\left(-h\frac{\partial S}{\partial x}-\frac{h^2}{2}\frac{\partial^2 S}{\partial x^2}\right)_+\left(+h\frac{\partial u}{\partial x}+\frac{h^2}{2}\frac{\partial^2 u}{\partial x^2}\right)$$
$$\left.\left.+\left(+h\frac{\partial S}{\partial x}-\frac{h^2}{2}\frac{\partial^2 S}{\partial x^2}\right)u+\left(-h\frac{\partial S}{\partial x}-\frac{h^2}{2}\frac{\partial^2 S}{\partial x^2}\right)u\right]\right\}+\tau\Lambda(S)+\text{ h.o.t.}$$

Neglecting the term of order greater than 2 in h:

$$u+\tau\frac{\partial u}{\partial t}=(1-\gamma_{_R}\tau)\left\{u+\vartheta\frac{h^2}{2}\frac{\partial^2 u}{\partial x^2}+\frac{\nu}{2S_M}\left[\left(+h\frac{\partial S}{\partial x}\right)_+\left(-h\frac{\partial u}{\partial x}\right)\right.\right.$$
$$\left.\left.+\left(-h\frac{\partial S}{\partial x}\right)_+\left(+h\frac{\partial u}{\partial x}\right)-h^2\frac{\partial^2 S}{\partial x^2}\,u\right]\right\}+\tau\Lambda(S)+\text{ h.o.t.}$$

Once again we use the rule $(f)_+-(-f)_+=f$ for the term with $h\,\dfrac{\partial u}{\partial x}$:

$$u+\tau\frac{\partial u}{\partial t}=(1-\gamma_{_R}\tau)\left\{u+\vartheta\frac{h^2}{2}\frac{\partial^2 u}{\partial x^2}+\frac{\nu}{2S_M}\left[-h^2\frac{\partial S}{\partial x}\,\frac{\partial u}{\partial x}\,-h^2\frac{\partial^2 S}{\partial x^2}\,u\right]\right\}+\tau\Lambda(S)+\text{ h.o.t.}$$

Neglecting the term with τh^2 we finally have:

$$u+\tau\frac{\partial u}{\partial t}=\;u+\vartheta\frac{h^2}{2}\frac{\partial^2 u}{\partial x^2}+\frac{\nu}{2S_M}\left[-h^2\frac{\partial S}{\partial x}\,\frac{\partial u}{\partial x}\,-h^2\frac{\partial^2 S}{\partial x^2}\,u\right]-\gamma_{_R}\tau u+\;\tau\Lambda(S)+\text{ h.o.t.}$$

Recognizing in the brackets the derivative of a product with respect to x ad dividing by τ:

$$\frac{\partial u}{\partial t}=\;\vartheta\frac{h^2}{2\tau}\frac{\partial^2 u}{\partial x^2}-\frac{\nu\,h^2}{2\tau S_M}\,\frac{\partial}{\partial x}\left[\frac{\partial S}{\partial x}\,u\right]-\gamma_{_R}\,u+\;\Lambda(S)+\text{ h.o.t.}$$

Letting $\tau\to 0$ and $h\to 0$, in such a way that

$$\frac{\nu h^2}{2\tau S_M}\to\alpha_{_R}\chi_{_R}\in\mathbb{R}_*^+\;,\qquad\frac{\vartheta h^2}{2\tau}\to D_R\in\mathbb{R}_*^+$$

Returning to the original variable $u=m_{_R}$, the equation becomes:

$$\frac{\partial m_{_R}}{\partial t}+\alpha_{_R}\frac{\partial}{\partial x}\left[\chi_{_R}\frac{\partial S}{\partial x}\,m_{_R}\right]=\;D_R\frac{\partial^2 m_{_R}}{\partial x^2}\;+\Lambda(S)\;-\gamma_{_R}\,m_{_R}.$$

that is exactly the equation $(2.10)_4$ governing the evolution of $m_{_R}$.

3.4 Derivation of the equation for the density of killer cells $m_{_K}$

Using the same approach as the regulatory cell case, we write the discrete equation based on the rules presented in Section 2.4. Renaming the spacial step as $\Delta_x = h$ and the killer cell density as $m_{_k} = u$, the principle of mass conservation now gives:

$$\begin{aligned} u_i^{k+1} = (1-\gamma_{_K}\tau)\ \Bigg\{ & u_i^k + \frac{\vartheta}{2}\Big(u_{i-1}^k + u_{i+1}^k\Big) - \vartheta\ u_i^k \\ & + \frac{\sigma\chi_{_K}}{2\rho_{\max}}\Bigg[\Big(\ \rho_i^k - \rho_{i-1}^k\Big)_+ u_{i-1}^k + \Big(\rho_i^k - \rho_{i+1}^k\Big)_+ u_{i+1}^k\Bigg] \\ & - \frac{\sigma\chi_{_K}}{2\rho_{\max}}\Bigg[\Big(\rho_{i-1}^k - \rho_i^k\Big)_+ u_i^k + \Big(\rho_{i+1}^k - \rho_i^k\Big)_+ u_i^k\Bigg]\ \Bigg\} + \tau B(m_{_{Ri}}{}^k). \end{aligned}$$

This equation is composed of a right-hand-side that is multiplied by the factor $(1-\gamma_{_k}\tau)$ that represents the probability that a regulatory cell remains quiescent (without dying) between time t_k and t_{k+1}. The first three terms in the curly brackets represent the fact that the density of killer cells at a certain time in a certain position x_i is given by the density already in the correct position at a previous time plus the contribution of the mass that will jump in or out the position x_i from the neighbours due to random motion. The other two terms represent, respectively, the source and sink terms related to the motion towards higher tumour cell density so that the mass in the neighbourhood tends to move in position x_i if there's a higher cancer cell density, and vice versa the mass undergoes the opposite movement, exiting from the balance. In addition, the last term represents an external source that produces killer cells depending on the presence of regulatory cells at the specific location.
For spacial and time step h, τ sufficiently small it holds:

$$t_k \approx t \quad t_{k+1} \approx t+\tau \quad x_i \approx x \quad x_{i\pm1} \approx x \pm h$$

$$u_i^k \approx u(t,x) \quad u_i^{k+1} \approx u(t+\tau,x) \quad u_{i\pm1}^k \approx u(t, x\pm h)$$

$$\rho_i^k \approx \rho(t,x) \quad \rho_i^{k+1} \approx \rho(t+\tau,x) \quad \rho_{i\pm1}^k \approx \rho(t,x\pm h) \quad B(m_{_{Ri}}{}^k) \approx B(m_{_R})$$

Substituting these relations into the discrete equation, we obtain an approximated form:

$$\begin{aligned} u(t+\tau,x) = (1-\gamma_{_K}\tau)\ \Bigg\{ & u(t,x) + \frac{\vartheta}{2}\Big(u(t,x-h) + u(t,x+h)\Big) - \vartheta\ u(t,x) \\ & + \frac{\sigma\chi_{_K}}{2\rho_{\max}}\Bigg[\Big(\ \rho(t,x) - \rho(t,x-h)\Big)_+ u(t,x-h) + \Big(\rho(t,x) - \rho(t,x+h)\Big)_+ u(t,x+h)\Bigg] \\ & - \frac{\sigma\chi_{_K}}{2\rho_{\max}}\Bigg[\Big(\rho(t,x-h) - \rho(t,x)\Big)_+ u(t,x) + \Big(\rho(t,x+h) - \rho(t,x)\Big)_+ u(t,x)\Bigg]\ \Bigg\} + \tau B(m_{_R}). \end{aligned}$$

We suppose the involved functions to be sufficiently regular, in particular, $u(t,x)$ and $\rho(t,x)$ twice differentiable in space x and $u(t,x)$ differentiable in time t so that can be expanded using Taylor in x and t:

$$u(t+\tau,x) = u + \tau\frac{\partial u}{\partial t} + \text{h.o.t}$$

$$u(t, x \pm h) = u \ \pm h\frac{\partial u}{\partial x} + \frac{h^2}{2}\frac{\partial^2 u}{\partial x^2} + \text{h.o.t}$$
$$\rho(t, x \pm h) = \rho \ \pm h\frac{\partial \rho}{\partial x} + \frac{h^2}{2}\frac{\partial^2 \rho}{\partial x^2} + \text{h.o.t}$$

Introducing these definitions into the above equation:

$$\begin{aligned} u + \tau\frac{\partial u}{\partial t} = (1 - \gamma_{_K}\tau) \Big\{ & u + \frac{\vartheta}{2}\Big(u - h\frac{\partial u}{\partial x} + \frac{h^2}{2}\frac{\partial^2 u}{\partial x^2} + u + h\frac{\partial u}{\partial x} + \frac{h^2}{2}\frac{\partial^2 u}{\partial x^2}\Big) - \vartheta\ u \\ & + \frac{\sigma\chi_{_K}}{2\rho_{\max}}\Big[\Big(\ \rho - \rho + h\frac{\partial \rho}{\partial x} - \frac{h^2}{2}\frac{\partial^2 \rho}{\partial x^2}\Big)_+ \Big(u - h\frac{\partial u}{\partial x} + \frac{h^2}{2}\frac{\partial^2 u}{\partial x^2}\Big) \\ & + \Big(\rho - \rho - h\frac{\partial \rho}{\partial x} - \frac{h^2}{2}\frac{\partial^2 \rho}{\partial x^2}\Big)_+ \Big(u + h\frac{\partial u}{\partial x} + \frac{h^2}{2}\frac{\partial^2 u}{\partial x^2}\Big)\Big] \\ & - \frac{\sigma\chi_{_K}}{2\rho_{\max}}\Big[\Big(\rho - h\frac{\partial \rho}{\partial x} + \frac{h^2}{2}\frac{\partial^2 \rho}{\partial x^2} - \rho\Big)_+ u + \Big(\rho + h\frac{\partial \rho}{\partial x} + \frac{h^2}{2}\frac{\partial^2 \rho}{\partial x^2} - \rho\Big)_+ u\Big]\ \Big\} + \tau B(m_{_R}) + \ \text{h.o.t.} \end{aligned}$$

Simplifying some terms:

$$\begin{aligned} u + \tau\frac{\partial u}{\partial t} = (1 - \gamma_{_K}\tau) \Big\{ & u + \vartheta\frac{h^2}{2}\frac{\partial^2 u}{\partial x^2} + \frac{\sigma\chi_{_K}}{2\rho_{\max}}\Big[\Big(\ +h\frac{\partial \rho}{\partial x} - \frac{h^2}{2}\frac{\partial^2 \rho}{\partial x^2}\Big)_+ \Big(u - h\frac{\partial u}{\partial x} + \frac{h^2}{2}\frac{\partial^2 u}{\partial x^2}\Big) \\ & + \Big(-h\frac{\partial \rho}{\partial x} - \frac{h^2}{2}\frac{\partial^2 \rho}{\partial x^2}\Big)_+ \Big(u + h\frac{\partial u}{\partial x} + \frac{h^2}{2}\frac{\partial^2 u}{\partial x^2}\Big)\Big] \\ & - \frac{\sigma\chi_{_K}}{2\rho_{\max}}\Big[\Big(-h\frac{\partial \rho}{\partial x} + \frac{h^2}{2}\frac{\partial^2 \rho}{\partial x^2}\Big)_+ u + \Big(+h\frac{\partial \rho}{\partial x} + \frac{h^2}{2}\frac{\partial^2 \rho}{\partial x^2}\Big)_+ u\Big]\ \Big\} + \tau B(m_{_R}) + \ \text{h.o.t.} \end{aligned}$$

Grouping some terms:

$$\begin{aligned} u + \tau\frac{\partial u}{\partial t} = (1 - \gamma_{_K}\tau) \Big\{ & u + \vartheta\frac{h^2}{2}\frac{\partial^2 u}{\partial x^2} + \frac{\sigma\chi_{_K}}{2\rho_{M}}\Big[\Big(\ +h\frac{\partial \rho}{\partial x} - \frac{h^2}{2}\frac{\partial^2 \rho}{\partial x^2}\Big)_+ \Big(u - h\frac{\partial u}{\partial x} + \frac{h^2}{2}\frac{\partial^2 u}{\partial x^2}\Big) \\ & + \Big(-h\frac{\partial \rho}{\partial x} - \frac{h^2}{2}\frac{\partial^2 \rho}{\partial x^2}\Big)_+ \Big(u + h\frac{\partial u}{\partial x} + \frac{h^2}{2}\frac{\partial^2 u}{\partial x^2}\Big) \\ & - \Big(-h\frac{\partial \rho}{\partial x} + \frac{h^2}{2}\frac{\partial^2 \rho}{\partial x^2}\Big)_+ u - \Big(+h\frac{\partial \rho}{\partial x} + \frac{h^2}{2}\frac{\partial^2 \rho}{\partial x^2}\Big)_+ u\Big]\ \Big\} + \tau B(m_{_R}) + \ \text{h.o.t.} \end{aligned}$$

We now use for the terms in u the well known fact that for a generic function f holds $(f)_+ - (-f)_+ = f$:

$$\begin{aligned} u + \tau\frac{\partial u}{\partial t} = (1 - \gamma_{_K}\tau) \Big\{ & u + \vartheta\frac{h^2}{2}\frac{\partial^2 u}{\partial x^2} + \frac{\sigma\chi_{_K}}{2\rho_{\max}}\Big[\Big(\ +h\frac{\partial \rho}{\partial x} - \frac{h^2}{2}\frac{\partial^2 \rho}{\partial x^2}\Big)_+ \Big(-h\frac{\partial u}{\partial x} + \frac{h^2}{2}\frac{\partial^2 u}{\partial x^2}\Big) \\ & + \Big(-h\frac{\partial \rho}{\partial x} - \frac{h^2}{2}\frac{\partial^2 \rho}{\partial x^2}\Big)_+ \Big(+h\frac{\partial u}{\partial x} + \frac{h^2}{2}\frac{\partial^2 u}{\partial x^2}\Big) \\ & + \Big(+h\frac{\partial \rho}{\partial x} - \frac{h^2}{2}\frac{\partial^2 \rho}{\partial x^2}\Big)\ u + \Big(-h\frac{\partial \rho}{\partial x} - \frac{h^2}{2}\frac{\partial^2 \rho}{\partial x^2}\Big)\ u\Big]\ \Big\} + \tau B(m_{_R}) + \ \text{h.o.t.} \end{aligned}$$

Neglecting the term of order greater than 2 in h:

$$u+\tau\frac{\partial u}{\partial t}=(1-\gamma_{_K}\tau)\left\{u+\vartheta\frac{h^2}{2}\frac{\partial^2 u}{\partial x^2}+\frac{\sigma\chi_{_K}}{2\rho_{\max}}\Big[\left(+h\frac{\partial\rho}{\partial x}\right)_+\left(-h\frac{\partial u}{\partial x}\right)\right.$$
$$\left.+\left(-h\frac{\partial\rho}{\partial x}\right)_+\left(+h\frac{\partial u}{\partial x}\right)-h^2\frac{\partial^2\rho}{\partial x^2}\,u\Big]\right\}+\tau B(m_{_R})+\text{ h.o.t.}$$

Once again we use the rule $(f)_+-(-f)_+=f$ for $h\,\dfrac{\partial u}{\partial x}$:

$$u+\tau\frac{\partial u}{\partial t}=(1-\gamma_{_K}\tau)\left\{u+\vartheta\frac{h^2}{2}\frac{\partial^2 u}{\partial x^2}+\frac{\sigma\chi_{_K}}{2\rho_{\max}}\left[-h^2\frac{\partial\rho}{\partial x}\,\frac{\partial u}{\partial x}\,-h^2\frac{\partial^2\rho}{\partial x^2}\,u\right]\right\}+\tau B(m_{_R})+\text{ h.o.t.}$$

Neglecting the term with τh^2 we finally have:

$$u+\tau\frac{\partial u}{\partial t}=\;u+\vartheta\frac{h^2}{2}\frac{\partial^2 u}{\partial x^2}+\frac{\sigma\chi_{_K}}{2\rho_{_M}}\left[-h^2\frac{\partial\rho}{\partial x}\,\frac{\partial u}{\partial x}\,-h^2\frac{\partial^2\rho}{\partial x^2}\,u\right]-\gamma_{_K}\tau u+\;\tau B(m_{_R})+\text{ h.o.t.}$$

Recognizing in the brackets the derivative of a product with respect to x ad dividing by τ:

$$\frac{\partial u}{\partial t}=\;\vartheta\frac{h^2}{2\tau}\frac{\partial^2 u}{\partial x^2}-\frac{\sigma\chi_{_K}}{2\tau\rho_{_M}}\,h^2\,\frac{\partial}{\partial x}\left[\frac{\partial\rho}{\partial x}\,u\right]-\gamma_{_K}\,u+\;B(m_{_R})+\text{ h.o.t.}$$

Letting $\tau\to 0$ and $h\to 0$, we define the coefficients:

$$\frac{\sigma h^2}{2\tau\rho_{\max}}\to\alpha_{_K}\in\mathbb{R}_*^+\;,\quad\frac{\vartheta h^2}{2\tau}\to D_{_K}\in\mathbb{R}_*^+$$

So that, recalling also that $u=m_{_K}$ the final form of the equation is

$$\frac{\partial m_{_K}}{\partial t}+\alpha_{_K}\frac{\partial}{\partial x}\left[\chi_K\frac{\partial\rho}{\partial x}\,m_{_K}\right]=\;D_K\frac{\partial^2 m_{_K}}{\partial x^2}\;+\;B(m_{_R})\;-\gamma_k\,m_{_K},$$

that is exactly equation $(2.10)_5$ governing the evolution of $m_{_K}$.

Part II

Second Part

Chapter 4

The model object of study

In this chapter we give a short review of the continuum model formally derived in Chapter 3, explaining the physical meaning of the parameters and functions comprised in this model. Then we illustrate the approach used to tackle our model, and, relying on the previous literature, we present expected results and questions.

4.1 The continuum model

The model derived in Chapter 3 for cancer invasion is the following:

$$\begin{cases} \partial_t n - \alpha\, \mu(y)\, \partial_x \left(n\, \partial_x \rho(t,x) \right) \right) = G(y,\rho)\, n + \omega\, \partial^2_{yy} n - \ \gamma m_{_K} n \\ \\ \rho(t,x) := \displaystyle\int_0^Y n(t,x,y)\ dy, \qquad\qquad (x,y) \in \mathbb{R} \times (0,Y) \\ \\ \partial_t S = \mathbb{1}_{\text{supp}\,(\rho(t,x))} \displaystyle\int_0^Y \frac{P(y)}{\rho(t,x)}\ n(t,x,y)\ dy - \lambda S + D_s\ \partial^2_{xx} S \\ \\ \partial_t m_{_R} + \alpha_{_R}\ \partial_x (\ m_{_R}\ \chi_{_R}\ \partial_x S\ ) = \Lambda(S) - \gamma_{_R} m_{_R} + D_{_R}\ \partial^2_{xx} m_{_R} \\ \\ \partial_t m_{_K} + \alpha_{_K}\ \partial_x (\ m_{_K}\ \chi_{_K}\ \partial_x \rho\ ) = B(m_{_R}) - \gamma_{_K} m_{_K} + D_{_K}\ \partial^2_{xx} m_{_K} \end{cases} \tag{2.10}$$

Here, the structure variable $y \in [0, Y]$ represents the phenotypic state of each cancer cell. This allows us to include the intra-population heterogeneity that the tumor exhibits in terms of mobility, proliferation, and chemical production. As already mentioned, we associate higher values of y with a more mesenchymal behaviour and lower values of y with a more epithelial one.
The first equation $(2.10)_1$ is a partial-integro-differential equation (PIDE) governing the evolution of $n(t,x,y)$ that is the cancer cell population density with phenotype y at position $x \in \mathbb{R}$ and time $t \in [0, +\infty]$, subject to zero Neumann boundary conditions at $y = 0$ and $y = Y$. This equation involves $\rho(x,t)$ that is the cell density at position x and

time t, defined by $(2.10)_2$.
Looking at the left-hand side of $(2.10)_1$, the second term takes into account the tendency of cells to move towards less crowded regions (down to the cell density gradient) [6],[26] . The function $\alpha\mu(y)$ with $\alpha > 0$ models the cell mobility. Since mesenchymal cells exhibit greater motility than the epithelial ones, we have defined μ as an increasing function of the cell phenotypic state y (cf.(1.6)). The first term of the right-hand side of $(2.10)_1$ represents the change of the population density due to cell division and death. Here, the rate $G(y, \rho(t, x))$ embodies the fitness of cells in the phenotypic state y at time t and position x, surrounded by cell density $\rho(x, t)$. To include volume-filling effects and the "go or growth" dynamics, G has been defined as a decreasing function of y and ρ (see definition (1.12 a) and properties (1.12 b),(1.13)). The second term on the right-hand side of the PIDE $(2.10)_1$ reflects the spontaneous, heritable phenotypic changes [70] that a cancer cell can undergo at rate $\omega > 0$. Finally, the last term in $(2.10)_1$ represents the death of a cancer cell due to the encounter with a killer one that happens at rate $\gamma > 0$.
The third equation in (2.10) governs the evolution of $S(x, t)$, that is the concentration of the chemotactic factor. The integral term in the right-hand side of $(2.10)_3$ represents the weighted integral average production of the attractant S, which occurs at a phenotype-dependent rate $P(y)$. Since mesenchymal cells produce more attractant than the epithelial ones, we have defined $P(y)$ as an increasing function of y (c.f. (1.16)). The second term on the right-hand side of $(2.10)_3$ embodies the spontaneous degradation of the chemical factor , which occurs at rate λ. Finally, the last term of $(2.10)_3$ reflects the spacial diffusion of the attractor, following the classical Fick's Law, with diffusion coefficient D_s.
The remaining equations $(2.10)_4$ and $(2.10)_5$ govern the evolution of $m_{_R}$ and $m_{_K}$ that are, respectively, the density of regulatory and killer cells at position x and time t. Both equations have a similar right-hand side, consisting of spatial diffusion, production and elimination terms. The elements that change are the diffusion coefficient (respectively $D_{_R}$ and $D_{_K}$), the elimination rate (respectively $\gamma_{_R}$ and $\gamma_{_K}$) and the proliferation rate ($\Lambda(S)$ and $B(\ m_{_R})$). The proliferation term depends on S in the regulatory case while is a function of $m_{_R}$ in the killer case. This choice aims to model the antagonism of the two types of cells and their different sources. Since the chemical factor attracts regulatory cells, the chemical-dependent proliferation rate $\Lambda(S)$ is defined as an increasing function of S (see (1.23)). On the other hand, killer cells proliferate with a regulatory-dependent rate $B(m_{_R})$, whose definition changes according to the biological scenario of interest (see (1.31a),(1.31b),(1.31c) for some possible choices). Another difference between $(2.10)_4$ and $(2.10)_5$ is in the transport term on their left-hand side. This reflects the fact that two different physical causes dictate movement. The regulatory cells move by chemotaxis with chemotactic sensitivity coefficient $\chi_{_R}$, while the killer cells move up to the cell density gradient with sensitivity coefficient $\chi_{_K}$.

4.2 Expected results and questions

Relying on the pre-existing literature, we can study the asymptotic behaviour of the cell population density n through a rescaling operation followed by a travelling wave analysis on the equation $(2.10)_1$. We expect to find that the cell population density n converges

weakly in measures to a delta distribution centred in a dominant phenotype $\bar{y}$ multiplied by the cell density ρ. This procedure allows us to obtain a transport equation for the dominant phenotype $\overline{y}(z)$. Consistently with the experimental evidence, we expect $\overline{y}(z)$ to behave as a wave that links values near 0 in the rear (where the majority of cells are epithelial) to values near Y at the edge the front (where the prevalent phenotypic trait is mesenchymal). This reflects the emergence of phenotypically structured invading cell fronts, in which mesenchymal cells act as leaders while the epithelial cells behave as followers, similarly with [82, 83, 84]. Moreover, we expect the cell density ρ to be a wave which reaches maximum value $\rho_{\max}$ at the rear and tends to zero near the front. Employing the same rescaling approach to equation $(2.10)_3$ and substituting the asymptotic solution found for n, working in the travelling wave framework, we will find an explicit form for the wave associated with S in analogy with [82, 83]. A priori, we do not know how this wave will be since its behaviour depends on the combined effects of density growth rate and chemical factor production rate, which are both functions of the phenotype and depend on the modelling choices. Under the hypothesis that $P(Y) >> P(0)$ we can envisage that the wave has a peak at the front, where the more mesenchymal cells are located. Finally, using the known results for ρ and S into the travelling-wave rescaled version of $(2.10)_4$ and $(2.10)_5$, we obtain explicit expressions for $m_{_K}$ and $m_{_R}$. Due to their "antagonism", we expect them to be waves with opposite behaviour. In particular, we expect a peak of regulatory cells at the front since the wave for S exhibits a peak at that location. As a consequence, in this region the density of killer cells has to be very low. Furthermore, we expect that a tumor composed of more mesenchymal cells will show a greater concentration of attractant S, then a greater density of regulatory cells $m_{_R}$ which hinders the penetration of killer cells $m_{_K}$ into the tumor bulk. In this case, we expect the wave for $m_{_K}$ to be low within the tumor bulk, that is, for $z < l$ where $z = l$ is the position of the front edge. Conversely, a more epithelial tumor is supposed to face a heavier immune response due to the shortage of chemical attractant and regulatory cells within tumor. In the latter case, we expect $m_{_K}$ to be higher within the tumor than the previous one. Outside the tumour, i.e. for $z > l$, the lack of cancer cells results in limited chemical production and thus the absence of regulatory cells, which implies a massive presence of killer cells in both scenarios.

Chapter 5

Formal asymptotic analysis

In this section, we conduct a travelling wave analysis of an opportune rescalation of the system (2.10). We lean on the asymptotic method developed in [83, 84], which builds on the Hamilton-Jacobi approach employed in previous works [14, 41, 70, 86].

5.1 Rescaled model

We put ourselves in a biological scenario in which cancer cell proliferation and chemoattractor production/degradation play a stronger role in the system dynamics than cell density-directed movement and immune action of killer cells, which play a stronger role than spacial diffusion of chemicals and phenotypic changes [8, 10, 70, 101, 132]. Hence, introducing a small parameter $\varepsilon \in \mathbb{R}_*^+$, we rescale the equations for n and S, choosing:

$$\alpha := \varepsilon \quad \omega := \varepsilon^2 \quad D_{_S} := \varepsilon^2. \tag{3}$$

Regarding the dynamics of regulatory and killer cells, we focus on a biological scenario in which the spacial diffusion happens on a longer characteristic timescale than the cell movement that in turn plays a weaker role than cellular proliferation and death. This corresponds to the parameter scaling:

$$\alpha_{_K} := \varepsilon \quad \alpha_{_R} := \varepsilon \quad D_{_K} := \varepsilon^2 \quad D_{_R} := \varepsilon^2. \tag{3.1}$$

Finally, to study the long time behaviour of the solution, we employ a time rescaling: $t \to \frac{t}{\varepsilon}$, leading to :

$$n(\tfrac{t}{\varepsilon}, x, y) := n_\varepsilon(t, x, y) \ , \quad S(\tfrac{t}{\varepsilon}, x, y) := S_\varepsilon(t, x, y)$$

$$m_{_K}(\tfrac{t}{\varepsilon}, x, y) := m_{_{K,\varepsilon}}(t, x, y), \quad m_{_R}(\tfrac{t}{\varepsilon}, x, y) := m_{_{R,\varepsilon}}(t, x, y)$$

In so doing, we obtain the following rescaled version of system (2.10):

$$\begin{cases} \varepsilon\ \partial_t n_\varepsilon - \varepsilon\,\mu(y)\,\partial_x\left(n_\varepsilon\,\partial_x\rho_\varepsilon\right) = G(y,\rho_\varepsilon)\,n_\varepsilon + \varepsilon^2\,\partial^2_{yy} n_\varepsilon - \varepsilon\ m_{K,\varepsilon} n_\varepsilon \\ \rho_\varepsilon(t,x) := \displaystyle\int_0^Y n_\varepsilon(t,x,y)\ dy, \qquad (x,y)\in\mathbb{R}\times(0,Y) \\ \varepsilon\ \partial_t S_\varepsilon = \mathbb{1}_{\text{supp}\,(\rho_\varepsilon(t,x))} \displaystyle\int_0^Y \frac{P(y)}{\rho_\varepsilon(t,x)}\ n_\varepsilon(t,x,y)\ dy - \lambda S_\varepsilon + \varepsilon^2\ \partial^2_{xx} S_\varepsilon \\ \varepsilon\ \partial_t m_{R,\varepsilon} + \varepsilon\ \partial_x(\ m_{R,\varepsilon}\ \chi_R\ \partial_x S_\varepsilon\ ) = \Lambda(S_\varepsilon) - \gamma_R m_{R,\varepsilon} + \varepsilon^2\ \partial^2_{xx} m_{R,\varepsilon} \\ \varepsilon\ \partial_t m_{K,\varepsilon} + \varepsilon\ \partial_x(\ m_{K,\varepsilon}\ \chi_K(m_{R,\varepsilon})\ \partial_x\rho_\varepsilon\ ) = B(m_{R,\varepsilon}) - \gamma_K m_{K,\varepsilon} + \varepsilon^2\ \partial^2_{xx} m_{K,\varepsilon} \end{cases} \tag{3.3}$$

5.2 Formal limit for $\varepsilon \to 0$

On the basis of the Hamilton-Jacobi method in [14, 41, 86, 110, 111], we make the so-called real phase WKB ansatz [13, 44, 48]:

$$n_\varepsilon(t,x,y) = e^{\frac{u_\varepsilon(t,x,y)}{\varepsilon}}, \tag{3.4}$$

so :

$$\partial_t n_\varepsilon = \frac{\partial_t u_\varepsilon}{\varepsilon} n_\varepsilon, \quad \partial_x n_\varepsilon = \frac{\partial_x u_\varepsilon}{\varepsilon} n_\varepsilon, \quad \partial^2_{yy} n_\varepsilon = \left(\frac{1}{\varepsilon^2}(\partial_y u_\varepsilon)^2 + \frac{1}{\varepsilon}\partial^2_{yy} u_\varepsilon\right) n_\varepsilon. \tag{3.5}$$

Substituting the latter expressions into the PIDE for n_ε $(3.3)_1$, making explicit the product derivative on the left-hand side and simplifying, we obtain the following Hamilton-Jacobi equation for $u_\varepsilon(t,x,y)$:

$$\partial_t u_\varepsilon - \mu(y)\,(\partial_x u_\varepsilon\,\partial_x\rho_\varepsilon + \varepsilon\,\partial^2_{xx}\rho_\varepsilon\ ) = G(y,\rho_\varepsilon) + (\partial_y u_\varepsilon)^2 + \epsilon\,\partial^2_{yy} u_\varepsilon - \varepsilon\ m_{K,\varepsilon}, \quad (x,y)\in\ \mathbb{R}\times(0,Y). \tag{3.6}$$

We can express u_ε and ρ_ε through their asymptotic expansions in terms of ε:

$$u_\varepsilon = u + \varepsilon u_1 + \varepsilon^2 u_2 + ..., \quad \rho_\varepsilon = \rho + \varepsilon\rho_1 + \varepsilon^2\rho_2 + ... \quad \text{for } \varepsilon\to 0, \tag{3.7}$$

where u and ρ are the leading-order terms of the expansions. Substituting these expansions into (3.8) and taking the limit for $\varepsilon \to 0$, we obtain an equation for the principal term u :

$$\partial_t u - \mu(y)\ \partial_x\rho\ \partial_x u = G(y,\rho\ ) + (\partial_y u)^2, \quad (x,y)\in\mathbb{R}\times(0,Y). \tag{3.8}$$

Constraint on u

Let $x\in\mathbb{R}$ so that $\rho(t,x) > 0$ i.e.

$$x\in \text{supp}(\rho).$$

Let $\overline{y}(t,x)$ be a nondegenerate maximum point of $u(t,x,y)$ that is

$$\overline{y}(t,x) \in \arg\max_{y\in[0,Y]} u(t,x,y),$$

with $\partial^2_{yy}u(t,x,\overline{y}) < 0$ by definition of nondegenerate maximum point.
Note that if u_ε is a strictly concave function of y, then under assumptions (1.12 b) we can expect the same property to hold for u, which means that we can expect $u(t,x,y)$ to have a unique maximum point $\overline{y}(t,x)$.
Since for the growth function $G(y,\rho_\varepsilon)$ holds (1.12 a),(1.12 b), then we also expect

$$\rho_\varepsilon(t,x) < \infty \quad \text{for all} \quad \varepsilon > 0,$$

which implies that n_ε is bounded in $L^1([0,Y])$ for $\varepsilon \to 0$. Recalling the ansatz (3.4), this is possible only if the following constraint is satisfied for all $t > 0$:

$$u(t,x,\overline{y}(t,x)) = \max_{y\in[0,Y]} u(t,x,y) = 0, \quad x \in \mathrm{supp}(\rho), \tag{3.9}$$

which also implies:

$$\partial_y u(t,x,\overline{y}(t,x)) = 0 \quad \text{and} \quad \partial_x u(t,x,\overline{y}(t,x)) = 0, \quad x \in \mathrm{supp}(\rho). \tag{3.10}$$

Equation (3.8) together with the constraint (3.9) can be seen as a constrained Hamilton-Jacobi equation with $\rho(x,t) > 0$ that plays the role of the Lagrange multiplier associated to the constraint.

Relation between $\overline{y}(t,x)$ and $\rho(t,x)$

Evaluating now the equation (3.8) at $y = \overline{y}(t,x)$:

$$\partial_t u(t,x,\overline{y}) - \mu(y)\ \partial_x\rho\ \partial_x u(t,x,\overline{y}) = G(\overline{y},\rho\ ) + (\partial_y u(t,x,\overline{y})\ )^2,$$

and using the constraint (3.9) and the relations (3.10), we find:

$$G(\overline{y}(t,x),\rho(t,x)) = 0, \quad x \in \mathrm{supp}(\rho). \tag{3.11}$$

Recalling the definition of $G(y,\rho)$ given by (1.13) we have:

$$r(\overline{y}(t,x)) - \rho(t,x) = 0 \quad \Longrightarrow \quad \rho(t,x) = r(\overline{y}(t,x)) \quad x \in \mathrm{supp}(\rho). \tag{3.12}$$

The monotonicity assumptions (1.12 b) or (1.13) ensure that the maps $\rho \mapsto G(\cdot,\rho)$ and $\overline{y} \mapsto G(\overline{y},\cdot)$ are both invertible. As a consequence (3.12) is a biunivocal correspondence between $\overline{y}(t,x)$ and $\rho(t,x)$.

Expression for $S(t,x)$

Under the validity of the ansatz (3.4) for n_ε , if u_ε and u are strictly concave functions of y and u satisfyies the constraint (3.9), then the following asymptotic result holds:

$$n_\varepsilon(t,x,y) \xrightarrow[\varepsilon\to 0]{} \rho(t,x)\ \delta_{\overline{y}(t,x)}(y) \quad \text{weakly in measure,} \tag{3.13}$$

where $\delta_{\overline{y}(t,x)}(y)$ is the Dirac delta centred in $y = \overline{y}(t,x)$. This means that at position x and time t, all cells express the dominant phenotypic trait $y = \overline{y}(t,x)$, while other phenotypic variants are locally absent.
As previously done, we take the asymptotic expansion of the function S_ε representing the chemical attractant:

$$S_\varepsilon = S + \varepsilon S_1 + \varepsilon^2 S_2 + .., \tag{3.14}$$

where S is the leading-order term. Using (3.14) into the rescaled equation for S_ε $(3.3)_3$ and taking the limit for $\varepsilon \to 0$, using also the asymptotic result (3.13), we obtain an equation for the leading-order term S :

$$\mathbb{1}_{\text{supp}\,(\rho(t,x))} \int_0^Y P(y)\ \delta_{\overline{y}(t,x)}(y)\ dy = \lambda S \quad \Longrightarrow \quad S(t,x) = \frac{P(\overline{y}(t,x))}{\lambda}\mathbb{1}_{\text{supp}\,(\rho(t,\cdot))}(x), \tag{3.15}$$

where $\mathbb{1}_{(}\cdot)$ is the indicator function of the set $(\cdot)$. As expected, out of $\text{supp}(\rho)$, the chemical concentration S vanishes due to the absence of cancer cells producing it.

5.2.1 Behaviour of $m_{_K}$ and $m_{_R}$

Recalling the equations for $m_{_K}$ and $m_{_R}$ in (3.3) , properly rescaled with ε:

$$\partial_t m_{_{R,\varepsilon}}(t,x) + \ \partial_x(\ m_{_{R,\varepsilon}}(t,x)\ \chi_{_R}\ \partial_x S_\varepsilon(t,x)\ ) = \varepsilon\ \partial^2_{xx} m_{_{R,\varepsilon}}(t,x) + \Lambda(S_\varepsilon(t,x)) - \gamma_{_R} m_{_{R,\varepsilon}}(t,x)$$

$$\partial_t m_{_{K,\varepsilon}}(t,x) + \ \partial_x(\ m_{_{K,\varepsilon}}(t,x)\ \chi_{_K}\ \partial_x \rho_\varepsilon(t,x)\ ) = \varepsilon\ \partial^2_{xx} m_{_{K,\varepsilon}}(t,x) + B(m_{_{R,\varepsilon}}(t,x)) - \gamma_{_K} m_{_{K,\varepsilon}}(t,x) \tag{3.16}$$

As previously done, we assume that we can take asymptotic expansions of $m_{_{R,\varepsilon}}$ and $m_{_{K,\varepsilon}}$:

$$\begin{aligned} m_{_{R,\varepsilon}} &= m_{_R} + \varepsilon m_{_{R_1}} + \varepsilon^2 m_{_{R_2}} + .. \\ m_{_{K,\varepsilon}} &= m_{_K} + \varepsilon m_{_{K_1}} + \varepsilon^2 m_{_{K_2}} + .. \end{aligned} \tag{3.17}$$

where $m_{_R}$ and $m_{_K}$ are the leading terms.
Introducing expansions (3.7), (3.14), (3.17) into (3.16) and taking the limit for $\varepsilon \to 0$, we obtain the following expressions for the leading-order terms $m_{_R}$ and $m_{_K}$:

$$\Lambda(S(t,x)) - \gamma_{_R} m_{_R}(t,x) = 0$$

and

$$B(m_{_R}(t,x)) - \gamma_{_K} m_{_K}(t,x) = 0.$$

From these we obtain an explicit form for $m_{_R}(t,x)$

$$m_{_R}(t,x) = \frac{\Lambda(S(t,x))}{\gamma_{_R}}, \tag{3.18}$$

and for $m_{_K}(t,x)$:

$$m_{_K}(t,x) = \frac{B(m_{_R}(t,x))}{\gamma_{_K}}. \tag{3.19}$$

Since $S(t,x)$ is known from the previous asymptotic analysis (see (3.15)), then $m_{_R}$ can be derived directly through (3.18). Once $m_{_R}$ is also known, we can use its expression into (3.19) to determine $m_{_K}$ explicitly. In particular, outside $\mathrm{supp}(\rho(t,\cdot))(x)$ we know that $S(t,x)$ vanishes and consequently so does $m_{_R}(t,x)$ according to (3.18) and (1.23). This implies that $m_{_K}(t,x)$ is high due to (1.31c) and (3.19).

Transport equation for $\overline{y}$

Taking the derivative of (3.8) with respect to y and evaluating the resulting equation in $y = \overline{y}(t,x)$, we obtain

$$\partial^2_{yt}u(t,x,\overline{y}) - \left.\frac{d\mu}{dy}\right|_{y=\overline{y}} \partial_x\rho\ \partial_x u(t,x,\overline{y}) - \ \mu(\overline{y})\ \partial_x\rho\ \partial^2_{yx}u(t,x,\overline{y}) = \\ = \partial_y G(\overline{y},\rho) + 2\ \partial_y u(t,x,\overline{y})\ \partial^2_{yy}u(t,x,\overline{y}),$$

which, using constraint (3.9) and results (3.10), simplifies to:

$$\partial^2_{yt}u(t,x,\overline{y}) - \ \mu(\overline{y})\ \partial_x\rho\ \partial^2_{yx}u(t,x,\overline{y}) = \partial_y G(\overline{y},\rho) \quad x \in \mathrm{supp}(\rho). \tag{3.20a}$$

Differentiating now the first relation of (3.10) with respect to t, we find:

$$\partial^2_{yt}u(t,x,\overline{y}) + \partial^2_{yy}u(t,x,\overline{y})\ \partial_t\overline{y}(t,x) = 0 \ \Rightarrow\ \partial^2_{yt}u(t,x,\overline{y}) = -\partial^2_{yy}u(t,x,\overline{y})\ \partial_t\overline{y}(t,x).$$

If, instead, we differentiate the same equation with respect to x, we find:

$$\partial^2_{xy}u(t,x,\overline{y}) + \partial^2_{yy}u(t,x,\overline{y})\ \partial_x\overline{y}(t,x) = 0 \ \Rightarrow\ \partial^2_{yx}u(t,x,\overline{y}) = -\partial^2_{yy}u(t,x,\overline{y})\ \partial_x\overline{y}(t,x).$$

We have now expressions for $\partial^2_{yt}u(t,x,\overline{y})$ and $\partial^2_{yx}u(t,x,\overline{y})$ that we can substitute into (3.20a), together with $\partial^2_{yy}u(t,x,\overline{y}) < 0$ (because $\overline{y}$ is the unique maximum point of u that is a strictly concave function of y). The result is the following transport equation for $\overline{y}(t,x)$:

$$\partial_t\overline{y} - \mu(\overline{y})\ \partial_x\rho\ \partial_x\overline{y}(t,x) = \frac{1}{-\partial^2_{yy}u(t,x,\overline{y})}\partial_y G(\overline{y},\rho), \quad x \in \mathrm{supp}(\rho), \tag{3.20}$$

that is a generalised Burgers equation with source term, given that $\rho(t,x)$ is linked to $\overline{y}(t,x)$ through (3.11) or is given explicitly by (3.12).

5.3 Travelling-wave analysis

Formulation of the travelling wave problem

Introducing the travelling wave ansatz

$$u(t,x,y) = u(z,y), \quad \rho(t,x) = \rho(z), \quad \overline{y}(t,x) = \overline{y}(z), \quad S(t,x) = S(z),$$

$$m_{_R}(t,x) = m_{_R}(z), \quad m_{_K}(t,x) = m_{_K}(z)$$

with

$$z := x - c\,t, \quad c \in \mathbb{R}_*^+$$

into

- the equation for u (3.8):
$$-(c + \mu(y)\rho')\partial_z u = G(y,\rho) + (\partial_y u)^2, \quad (z,y) \in \mathbb{R} \times (0,Y), \tag{3.21}$$
- the constraint on u (3.9):
$$u(z,\overline{y}(z)) = \max_{y\in[0,Y]} u(z,y) = 0, \quad z \in \mathrm{supp}(\rho), \tag{3.22}$$
- the relations (3.10) consequences of the constraint:
$$\partial_y u(z,\overline{y}(z)) = 0, \quad \partial_z u(z,\overline{y}(z)) = 0, \quad z \in \mathrm{supp}(\rho), \tag{3.23}$$
- the relation (3.12):
$$G(\overline{y}(z),\rho(z)) = 0 \quad \Rightarrow \quad \rho(z) = r(\overline{y}(z)), \quad z \in \mathrm{supp}(\rho), \tag{3.24}$$
- the equation for S (3.15):
$$S(z) = \frac{P(\overline{y}(z))}{\lambda}\mathbb{1}_{\mathrm{supp}(\rho)}(z), \tag{3.25}$$
- the equation for $m_{_R}$ (3.18):
$$m_{_R}(z) = \frac{\Lambda(S(z))}{\gamma_{_R}}, \tag{3.26}$$
- the equation for $m_{_K}$ (3.19):
$$m_{_K}(z) = \frac{B(m_{_R}(z))}{\gamma_{_K}}, \tag{3.27}$$
- the transport equation for $\overline{y}$ (3.20) :
$$\begin{aligned} -(\ c + \mu(\overline{y})\ \rho')\ \overline{y}' &= \frac{1}{-\partial^2_{yy}u(z,\overline{y})}\partial_y G(\overline{y},\rho), \quad x \in \mathrm{supp}(\rho), \\ (\ c + \mu(\overline{y})\ \rho')\ \overline{y}' &= \frac{\partial_y r(\overline{y})}{\partial^2_{yy}u(z,\overline{y})}, \quad x \in \mathrm{supp}(\rho). \end{aligned} \tag{3.28}$$

We are looking for a wave-like solution $\overline{y}(z)$ satisfying (3.28) and the following asymptotic condition:

$$\lim_{z\to-\infty} \overline{y}(z) = 0, \tag{3.29}$$

which is introduced since $r(0) = \rho_{\max}$ (see (1.13)) and thus

$$\lim_{z\to-\infty} \rho(z) = \rho_{\max}. \tag{3.30}$$

Monotonicity of the wave

Taking the derivative of the constraint (3.24) with respect to z, we obtain

$$\partial_y G(\overline{y}(z),\rho(z))\ \overline{y}'(z) + \partial_\rho G(\overline{y}(z),\rho(z))\ \rho'(z) = 0, \quad z \in \mathrm{supp}(\rho), \tag{3.31a}$$

from which we find an expression for $\rho'(z)$:

$$\rho'(z) = -\frac{\partial_y G(\overline{y}(z),\rho(z))\overline{y}'(z)}{\partial_\rho G(\overline{y}(z),\rho(z))} \quad z \in \mathrm{supp}(\rho). \tag{3.31b}$$

Substituting (3.31b) into (3.28)

$$-\ c\ \overline{y}' + \mu(\overline{y})\ \frac{\partial_y G(\overline{y},\rho)}{\partial_\rho G(\overline{y},\rho)}(\overline{y}')^2 = \frac{1}{-\partial^2_{yy}u(z,\overline{y})}\partial_y G(\overline{y},\rho),$$

that is,

$$\overline{y}' = \frac{-\partial_y G(\overline{y},\rho)}{c}\left(\frac{1}{\partial^2_{yy}u(z,\overline{y})} + \frac{\mu(\overline{y})(\overline{y}')^2}{-\partial_\rho G(\overline{y},\rho)}\right), \quad z \in \mathrm{supp}(\rho). \tag{3.31}$$

Since $\partial^2_{yy}u(z,\overline{y}) < 0$ and $\partial_y G(y,\cdot) < 0, \quad \partial_\rho G(\cdot,\ \rho) < 0$ for $(y,\rho) \in (0,Y] \times \mathbb{R}^+$ (see (1.12 a), (1.12 b)), relations (3.31) and (3.31b) allow us to conclude that:

$$\overline{y}'(z) > 0 \quad \text{and} \quad \rho'(z) < 0, \quad z \in \mathrm{supp}(\rho). \tag{3.32}$$

Biologically speaking, these results are consistent with experimental evidence. Firstly, the prevalence of epithelial cells is observed in the bulk of the tumor, while more mesenchymal cells are highlighted at the front. Therefore, it makes sense that the dominant phenotype $\overline{y}$ is an increasing function of z. At the same time, most cells reside in the bulk of the cancer mass while only a few occupy the front, so it is correct that the cancer density ρ decreases with z.

Position of the front

Putting together relation (3.24) with the monotonicity results (3.32) and the modeling assumptions (1.12 b) and (1.13), we can conclude that the position of the front of $\overline{y}(z)$, satisfying transport equation (3.28) and asymptotic condition (3.29), coincides with

$$\text{the unique point } l \in \mathbb{R} \text{ so that } \overline{y}(l) = Y \text{ and } \overline{y}(z) < Y \text{ on } (-\infty, l)\ . \tag{3.33a}$$

This implies $\mathrm{supp}(\rho) = (-\infty, l)$ from which (3.25) becomes:

$$S(z) = \frac{P(\overline{y}(z))}{\lambda}\ \mathbb{1}_{(-\infty,\ l)}(z). \tag{3.33}$$

Outside $\mathrm{supp}(\rho)(z)$ (i.e. for $z \in]l, +\infty)$) we conclude that $S(z)$ vanishes. According to (3.26) and (1.23) also $m_{_R}(z)$ vanishes and this implies that $m_{_K}(z)$ is high due to (1.31c) and (3.27). These results perfectly reflect our modelling assumptions and make sense biologically. Indeed, we are considering an asymptotical scenario in which chemical

diffusion is neglected, and the only factor determining the concentration of the attractor is the presence of cancer cells producing it. Given that outside $\text{supp}(\rho)(z)$ there are no cancer cells, the chemical concentration here must be zero. Since regulatory cells are recruited where the attractant concentration is sufficiently high, the density of regulatory cells is also zero outside $\text{supp}(\rho)(z)$. As the absence of regulatory cells means no inhibition of killer cells, the density of killer cells must be high outside $\text{supp}(\rho)$.

Mimimum wave speed

Differentiating (3.21) with respect to y gives

$$-(c+\mu(y)\rho')\ \partial^2_{yz}u(z,y) - \frac{\mathrm{d}\mu(y)}{\mathrm{d}y}\ \rho'\ \partial_z u(z,y) = \partial_y G(y,\rho) + 2\ \partial_y u(z,y)\ \partial^2_{yy}u(z,y).$$

Then, evaluating in $y=\overline{y}(z)$ and using the properties (3.22), (3.23), we find:

$$-(c+\mu(\overline{y})\rho')\ \partial^2_{yz}u(z,\overline{y}) - \partial_y G(\overline{y},\rho) = 0. \tag{3.34}$$

The result (3.19) in the travelling wave framework, gives:

$$\partial^2_{yz}u(z,\overline{y}) = -\partial^2_{yy}u(z,\overline{y})\overline{y}'.$$

Substituting into the latter equation the expression for $\overline{y}'$ from (3.31a), it results:

$$\partial^2_{yz}u(z,\overline{y}) = \partial^2_{yy}u(z,\overline{y})\frac{\partial_\rho G(\overline{y},\rho)}{\partial_y G(\overline{y},\rho)}\ \rho'.$$

Now that we have an explicit form for the term $\partial^2_{yz}u(z,\overline{y})$, we use it into (3.34) and, in so doing, we obtain:

$$\mu(y)\ \partial^2_{yy}u(z,\overline{y})\ \partial_\rho G(\overline{y},\rho)\ (\rho')^2 + c\ \partial^2_{yy}u(z,\overline{y})\ \partial_\rho G(\overline{y},\rho)\ \rho' + (\partial_y G(\overline{y},\rho))^2 = 0.$$

In the particular case in which $G(y,\rho)$ is defined through (1.13), it holds:

$$\partial_\rho G(\cdot,\rho) = -1 \quad \text{and} \quad \partial_y G(\overline{y},\cdot) = \frac{\mathrm{d}r(\overline{y})}{\mathrm{d}y}.$$

Hence, the previous equation becomes:

$$\mu(\overline{y})\ \partial^2_{yy}u(z,\overline{y})\ (\rho')^2 + c\ \partial^2_{yy}u(z,\overline{y})\ \rho' - \left(\frac{\mathrm{d}r(\overline{y})}{\mathrm{d}y}\right)^2 = 0. \tag{3.35}$$

We can look at (3.35) as a quadratic equation of ρ' that has real negative roots, consistently with the monotonicity result (3.32). In order to have real roots the following condition has to be satisfied:

$$(\ c\ \partial^2_{yy}u(z,\overline{y})\ )^2\ + 4\ \mu(\overline{y})\ \partial^2_{yy}u(z,\overline{y})\left(\frac{\mathrm{d}r(\overline{y})}{\mathrm{d}y}\right)^2 \geq 0,$$

that is,

$$c^2 \geq \ -4\ \mu(\overline{y})\ \frac{\partial^2_{yy}u(z,\overline{y})}{(\partial^2_{yy}u(z,\overline{y}))^2}\left(\ \frac{\mathrm{d}r(\overline{y})}{\mathrm{d}y}\right)^2.$$

Since

$$\partial^2_{yy}u(z,\overline{y}) < 0 \quad \Rightarrow \quad \partial^2_{yy}u(z,\overline{y}) = -|\ \partial^2_{yy}u(z,\overline{y})\ |,$$

recalling also that $c \geq 0$, we can thus conclude:

$$c \geq\ 2\ \sqrt{\frac{\mu(\overline{y})}{\partial^2_{yy}u(z,\overline{y})}}\ \left|\frac{\mathrm{d}r(\overline{y})}{\mathrm{d}y}\right|.$$

So there is a minimum wave speed c^* satisfying:

$$c^* = \sup_{z\in \mathrm{supp}(r(\overline{y}))} 2\ \sqrt{\frac{\mu(\overline{y}(z))}{\partial^2_{yy}u(z,\overline{y}(z))}}\ \left|\frac{\mathrm{d}r(\overline{y}(z))}{\mathrm{d}y}\right|, \tag{3.36}$$

where we have used the relation between $\rho(z)$ and $r(\overline{y}(z))$ given by (3.24).
As a consequence of (3.36), if

$$\sqrt{\mu(Y)}\left|\frac{\mathrm{d}r(Y))}{\mathrm{d}y}\right| \to \infty \quad \text{for} \quad Y \to \infty, \tag{3.37}$$

then $c^* \to \infty$ for $Y \to \infty$ and thus front acceleration may occur.

5.4 Illustration of the asymptotic results

In this section, we first choose coefficients and suitable functions for the model (3.3) (i.e. satisfying the modelling assumptions), then we use these to produce some plots in the travelling-wave framework to illustrate the asymptotic results obtained in the previous sections.
For the sake of simplicity, we assume $Y = 1$ so that $y \in [0,1]$. According to (1.6) we can take the phenotypic-dependent mobility as:

$$\mu(y) := y^2. \tag{4.1}$$

To satisfy assumptions (1.12 a),(1.12 b) on the cancer cells growth function $G(y,\rho)$ in the particular case given by (1.13) we define:

$$r(y) := 1 - y^2. \tag{4.2}$$

We assume $\lambda = 1$ In order to satisfy assumptions (1.16) on $P(y)$ we also define:

$$P(y) := \frac{1+y}{2}. \tag{4.3}$$

Since $\Lambda(S)$ has to satisfy assumption (1.23), at first instance we can define it as:

$$\Lambda(S) = S. \tag{4.4}$$

This modelling assumption is now made for the sake of simplicity but it can be modified, choosing a suitable function respecting the assumption (1.23). Another modelling assumption is the choice of $B(m_R)$, which has to be made carefully depending on which behaviour we want to model. Since $0 \leq y(z) \leq 1 \quad \forall z \in [-\infty, l]$, definition (4.3) together with (3.25) ensure that $0 \leq S(z) \leq 1 \quad \forall z \in [-\infty, l]$. Then, definition (4.4) together with (3.26) ensure that $0 \leq m_R(z) \leq 1 \quad \forall z \in [-\infty, l]$. Hence, the following definition for $B(m_R)$ is well posed and satisfies assumptions (1.31c):

$$B(m_R) = 1 - m_R. \tag{4.5}$$

Now, we postulate the shape of the solution $\overline{y}(z)$ according to the asymptotical conditions (3.32), (3.33a) and (3.29). In this way, we can consider $\overline{y}(z)$ as given and subsequently derive the other quantities using the asymptotical results. At first, we arbitrarily assume the position of the front at $z = l$. Then, the solution $\overline{y}(z)$ has to be an increasing function of z, linking the two extremes: $\overline{y} = 0$ at the rear, i.e. for $z \to -\infty$ and $\overline{y} = 1$ at the wave-front, i.e. for $z = l$. For representative purposes, we must consider z in a finite interval, we take $z \in [0, l]$. As a consequence, the behaviour at $z = 0$ in the following illustrations reflects the behaviour for $z \to -\infty$ in the travelling wave framework.
For simplicity, we assume $\overline{y}(z)$ to be a sigmoid function:

$$\overline{y}(z) = \frac{1}{1 + e^{-k(z - z_0)}}, \tag{4.6}$$

where k and z_0 are parameters influencing respectively the slope of the sigmoid and the point at which it reaches half of its maximum value. At first, we can choose $k = 0.42$ and $z_0 = 0.59 * l$. In the following, we will refer to this choice of parameters as the "mid-sigmoid" case. Now, knowing the explicit form of $\overline{y}(z)$, we can determine the shape

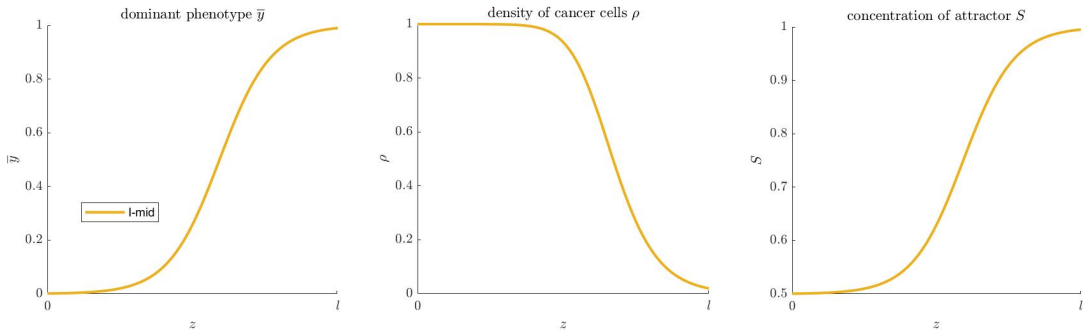

Figure 5.1. Plot of the phenotypic dominant trait $\overline{y}(z)$ assumed as the "mid-sigmoid" (4.6) (left), the density of cancer cells $\rho(z)$ obtained through (3.24) (center) and the concentration of the chemical attractant $S(z)$ obtained through (3.25) (right).

of the density $\rho(z)$ using the asymptotic result (3.24) and the assumption (4.2). At this point, we can employ the explicit formula (3.25) together with the definitions (4.2) and (4.3) to obtain the shape of the attractant concentration $S(z)$. Putting this result for $S(z)$ and the definition (4.4) into (3.26) and choosing a suitable coefficient γ_R, we obtain

an explicit expression for the density of regulatory cells $m_R(z)$. Once $m_R(z)$ is known and the coefficient γ_K is fixed, the formula (3.27) gives us the shape of the density of killer cells, under the modelling assumption (4.5). In the following, we will always consider $\gamma_R = \gamma_K = 1$.

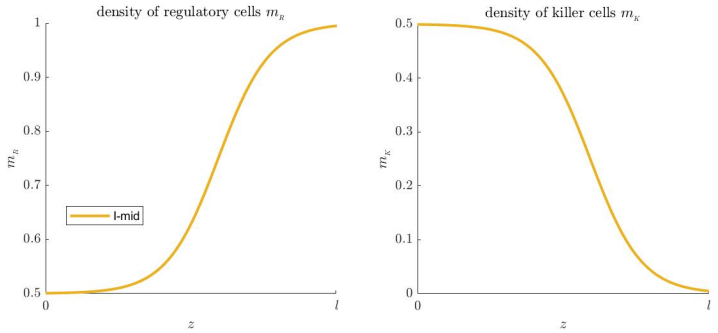

Figure 5.2. Plot of the density of regulatory cells $m_R(z)$ obtained through (3.26) (left) and the density of killer cells $m_K(z)$ obtained through (3.27) (right).

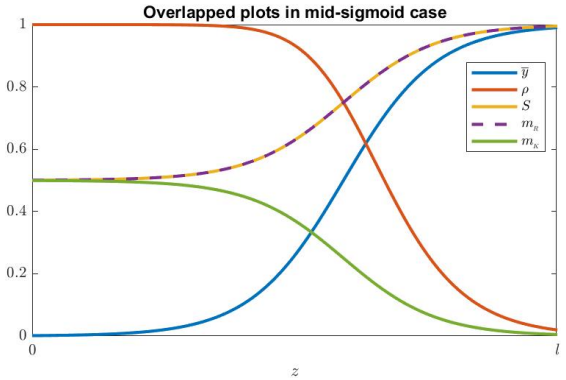

Figure 5.3. The overlapping plots of all the quantities involved in our analysis under the mid-sigmoid assumption (4.6) for $\overline{y}$. Due to our modeling choices, $S \equiv m_R$.

In this first basic example, we notice that the phenotypic spatial organization emerging in $\overline{y}(z)$ reflects on the concentration of the chemical factor S that impacts the shape of the density of regulatory cells m_R which in turn influence the production of killer cells m_K (Figure 5.1 and Figure 5.2). Near the leading edge, where the dominant phenotypic trait is mesenchymal, we can see a higher concentration of chemicals, which results in enhanced production of regulatory cells and reduced presence of killer ones. The situation is the opposite in the bulk, where more epithelial cells reside: indeed, at this location, more killer cells are attracted due to the lack of regulatory cells. These results, although simple, reflect biological evidence and simulate the scenario we expect, consistently with the modelling assumptions on which our model relies.

After this basic example, we explore other modelling choices for the shape of the dominant phenotypic trait $\overline{y}(z)$. Assuming the two growth functions $B(m_{_R})$ and $\Lambda(S)$ to be fixed as in the previous case (see (4.4) and (4.5)), we now investigate how the other involved quantities are affected by changing the shape of the dominant phenotypic trait $\overline{y}$. We expect a cascade effect in which a change in $\overline{y}$ will produce significant changes in its dependent quantities. This study can be seen as a sort of parametric study perturbing the solution of the transport equation (3.28).
Firstly, we change the shape and speed of the phenotypic switch between epithelial and mesenchymal traits, observing how it affects the degree of infiltration of killer cells within the tumour mass. We chose three shapes for $\overline{y}(z)$ that are two sigmoids and a power function. The mid-sigmoid case has already been investigated as the first basic example. In particular, we take:

$$\overline{y}(z) = \frac{1}{1 + e^{-k_m(z - c_m l))}}, \qquad \text{(mid-sigmoid)}$$

where l is the position of the front edge while k_m and c_m are parameters which determine the shape of the sigmoid. In particular, we chose $k_m = 0.42$ and $c_m = 0.59$.
Then,

$$\overline{y}(z) = \frac{1}{1 + e^{-k_s(z - c_s l)}}, \qquad \text{(sigmoid)}$$

where l is the position of the front edge while k_s and c_s are parameters that determine the shape of the sigmoid. In particular, we chose $k_m = 0.4$ and $c_s = 0.50$.
Finally,

$$\overline{y}(z) = \left(\frac{z}{l}\right)^n, \qquad \text{(power)}$$

where l is the position of the front edge and n is a parameter influencing the steepness of the power function. Here, we chose $n = 3$, which is the cubic case.

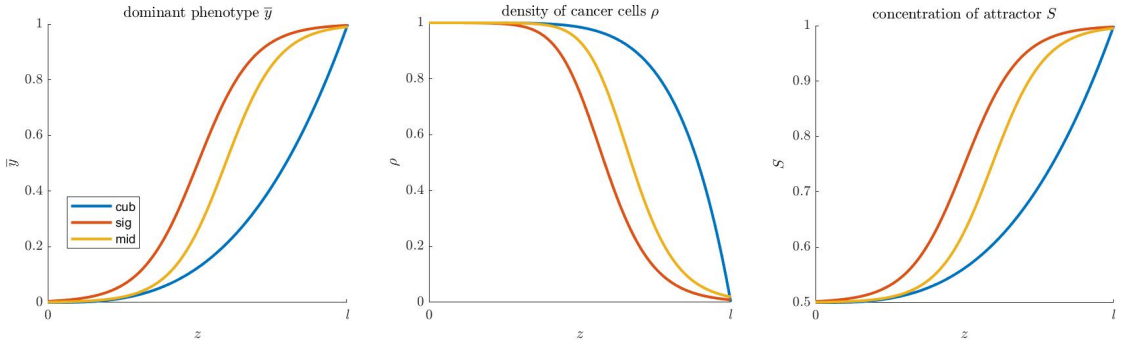

Figure 5.4. Plot of the dominant phenotypic trait $\overline{y}(z)$ and the asymptotic forms of the cancer density $\rho(z)$ and the concentration of the attractor $S(z)$ resulting from $\overline{y}$ taken as (mid-sigmoid), (sigmoid) or (power) function.

Focusing on the comparison of sigmoid, mid-sigmoid and cubic case (Figure 5.4 and Figure 5.5), we notice that a steeper slope of $\overline{y}(z)$ influences the shape of $\rho(z)$ and following even $S(z)$ changes. In particular, we can see that a faster transition towards $y = 1$, which

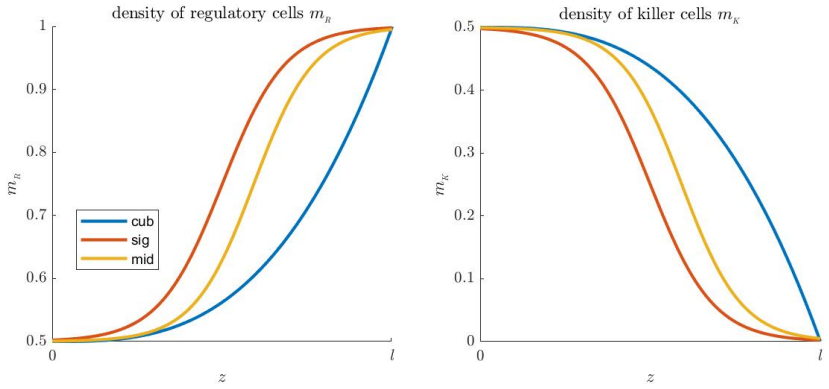

Figure 5.5. Plot of the asymptotic forms of the densities of regulatory m_R and killer m_K cells resulting from $\overline{y}$ taken as (mid-sigmoid), (sigmoid) or (power) function.

means a greater number of mesenchymal cells originated by the EMT transition, results in a global increase in the concentration of the chemical factor S within the tumor. This results in greater recruitment of regulatory cells m_R in the bulk of the tumor, leading to enhanced immunosuppression and less penetration of killer cells m_K. Numerically, this observation is confirmed if we look at the total number of killer cells penetrating the bulk of the tumour by calculating the integral under the curve m_K in the three different cases. We have:

$$\int_0^l m_K(z)\, dz = 6.74 \quad \text{in the sigmoid case,}$$

$$\int_0^l m_K(z)\, dz = 7.98, \quad \text{in the mid-sigmoid case,}$$

and

$$\int_0^l m_K(z)\, dz = 10.12 \quad \text{in the cubic case.}$$

As expected, the scenario leading to a lower presence of killer cells within the tumour is the one linked to the sigmoid case, which in our work is the modelling choice with a more rapid transition to the mesenchymal phenotype. We can conclude that a faster transition towards the mesenchymal trait results in a lower presence of killer cells within the tumor mass which means enhanced protection from the immune action. Of note, the penetration of killer cells into the cancer mass could not be blocked totally due to the "diffuse source" assumption for m_R and m_K. Indeed, this modelling assumption will always lead to a non-null density of killer cells in the bulk of the tumour, where the dominant phenotypic trait is epithelial, and the chemical concentration and the density of regulatory cells are near zero. Fixing the modelling choice for $\overline{y}(z)$, Figure 5.6 shows the overall situation obtained by the superposition of the plots of all the quantities involved in our study, further confirming the considerations just exposed.

At this point, we can compare the cases of tumours arising from a pool of more mesenchymal or epithelial cells, highlighting the difference that emerges in the derived quantities. In particular, we assume the more mesenchymal tumor to be composed of cells in the

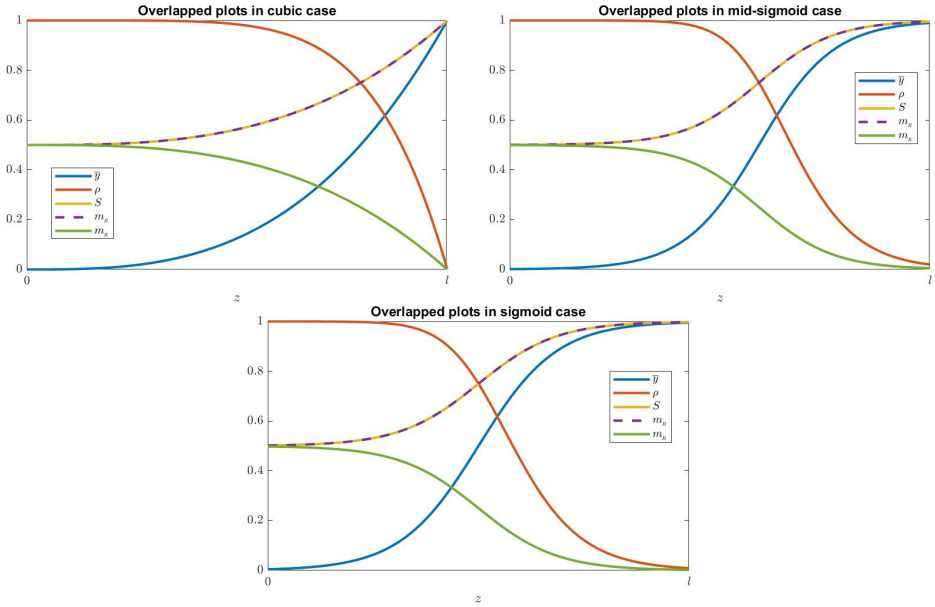

Figure 5.6. Overlapped plot of all the involved quantities resulting from $\overline{y}$ taken as (power) , (mid-sigmoid) or (sigmoid) function respectively.

phenotypic range $y \in [a,1]$ while the more epithelial neoplasm covers the range $y \in [0,b]$ with a, b fixed. We also investigate the case of an intermediate tumor originating from cells in the phenotypic range $y \in [0,1]$. For simplicity, we always choose $\overline{y}(z)$ as a function like the "mid-sigmoid" one, changing parameters appropriately to reflect what we want to model. In particular, we consider three different states that we denote as Epithelial, Mesenchymal and Intermediate.
Firstly,

$$\overline{y}(z) = \frac{1}{1+e^{-k_I(z-\ c_I l)}}, \qquad \text{(Intermediate)}$$

that is the usual "mid-sigmoidal" case with coefficients $c_I = 0.42$ and $k_I = 0.59$.
Then,

$$\overline{y}(z) = a + \frac{1-a}{1+e^{-k_M(z-\ c_M l)}}, \qquad \text{(Mesenchymal)}$$

with coefficients $c_M = 0.35$ and $k_M = 0.54$ and a that is a parameter representing the minimum value of the phenotypic dominant trait $\overline{y}(z)$ (reached in the bulk at $z = 0$). We will assume $a = 0.8$ in the following.
Finally,

$$\overline{y}(z) = \frac{b}{1+e^{-k_E(z-\ c_E l)}}, \qquad \text{(Epithelial)}$$

with coefficients $c_E = 0.37$ and $k_E = 0.57$ and b that is a parameter representing the maximum value of the phenotypic dominant trait $\overline{y}(z)$ (reached in the leading edge at $z = l$). We will assume $b = 0.2$ in the following.
Of note, our results still hold in the case of a tumor in which the dominant phenotype is

not zero in the bulk (i.e. if $\lim_{z\to-\infty}\overline{y}(z) \neq 0$), provided we change assumption (3.31a) consistently with the scenario we are studying (in our work this happens in the mesenchymal case in which the value at the rear is $\overline{y} = 0.8$).
As expected, the tumour initiated from more mesenchymal cells shows a lower density of cancer cells ρ but a greater production of attractant S than the one starting from the more epithelial pool (Figure 5.7). These results also affect the number of regulatory cells $m_{_R}$ attracted, which is very high in the more mesenchymal case, inducing very low recruitment of killer cells $m_{_K}$ and so a powerful immunosuppressive action (Figure 5.8). Due to its low chemical secretion, the tumor composed of more epithelial cells is not able to recall enough regulatory cells to effectively counteract the immune action of killer cells, which can therefore penetrate the tumour mass in large quantities.
Numerically, these observations are confirmed if we compute the total number of killer cells penetrating the bulk of the tumour by calculating the integral under the curve m_K in the three different cases. More in detail, we have:

$$\int_0^l m_{_K}(z)\, dz = 12.30 \quad \text{in the Epithelial case,}$$

$$\int_0^l m_{_K}(z)\, dz = 7.98 \quad \text{in the Intermediate case}$$

and

$$\int_0^l m_{_K}(z)\, dz = 1.74 \quad \text{in the Mesenchymal case.}$$

As expected, the scenario with the lower penetration of killer cells and, consequently, the greater immunosuppressive response is the one related to the modelling choice of a tumour composed of more mesenchymal cells. Conversely, the higher penetration of killer cells and, consequently, the stronger immune response is observed in the case of a tumor arising from more epithelial cells. Fixing the modelling choice for $\overline{y}(z)$, Figure 5.9 shows the overall situation obtained by the superposition of the plots of all the quantities involved in the model, further confirming the observations just discussed.

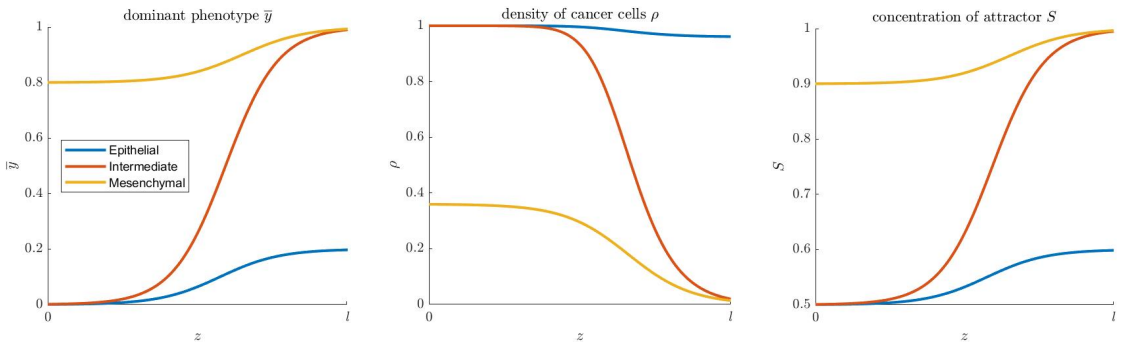

Figure 5.7. Plot of the dominant phenotypic trait $\overline{y}(z)$, the asymptotic forms of the cancer density $\rho(z)$ and the attractor concentration $S(z)$ resulting from $\overline{y}$ taken as (Intermediate), (Mesenchymal) or (Epithelial) function .

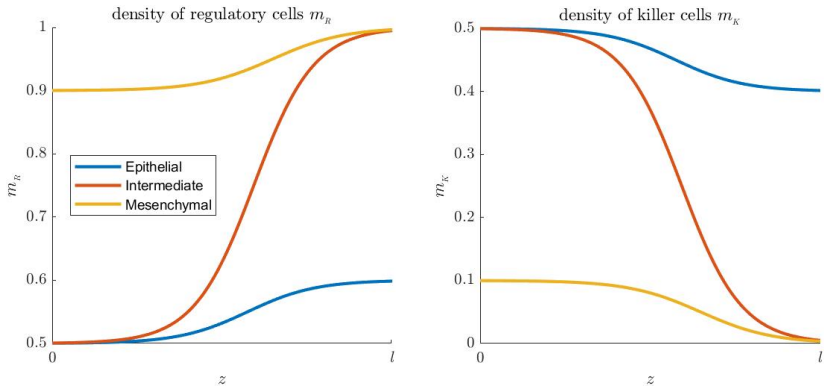

Figure 5.8. Plot of the asymptotic forms of the densities of regulatory m_R and killer m_K cells resulting from $\overline{y}$ taken as (Intermediate), (Mesenchymal) or (Epithelial) function .

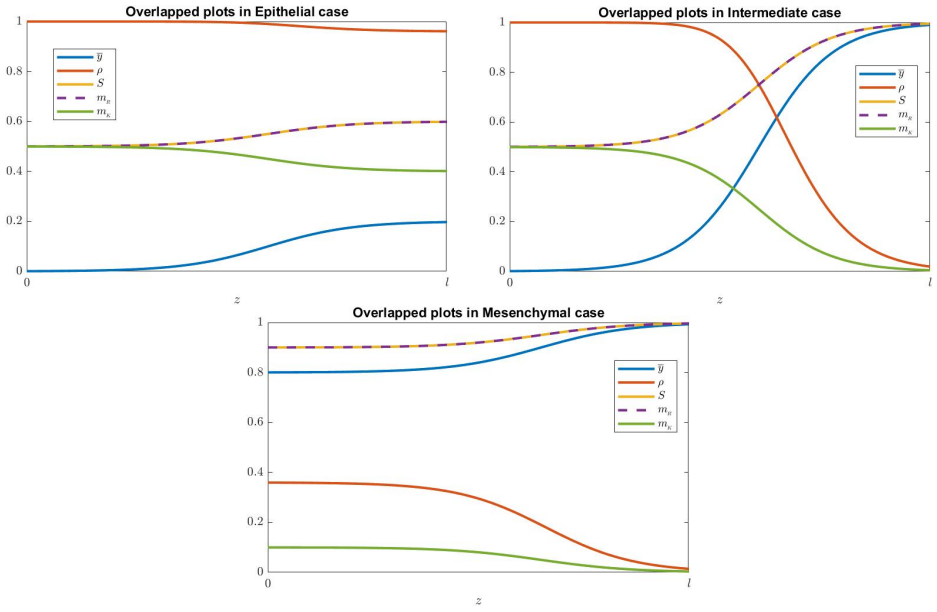

Figure 5.9. Overlapped plot of all the involved quantities resulting from $\overline{y}$ taken as (Epithelial) , (Intermediate) and (Mesenchymal) function respectively.

Part III

Third Part

Chapter 6

Conclusions and research perspectives

6.1 Conclusions and Biological Implications

This thesis deals with the derivation and travelling wave analysis of partial integro-differential equation models for EMT-mediated immunosuppression in cancer with phenotypic heterogeneity, including also the dynamics of killer and regulatory immune cells. Experimental evidence shows that mesenchymal cancer cells recruit regulatory cells, which suppress killer cell activity, creating a protective environment for the tumour. On the other hand, epithelial cancer cells experience higher immune activity due to the greater presence of killer cells. Cancer cells could have a phenotypic state ranging from totally epithelial to completely mesenchymal, modelled by the structure variable y. Specifically, a mesenchymal phenotype is characterized by high mobility and low proliferative ability, while an epithelial phenotype prioritizes reproduction over movement, reflecting the biological principle of "go or grow". Mesenchymal cells also show a high production of chemical attractant, which is responsible for recruiting regulatory cells which migrate due to chemotaxis. On the other hand, killer cells move up the density gradient of cancer cells and their activity is inhibited by regulatory cells. These biological considerations are expressed mathematically by choosing suitable functions to model the phenotype-dependent, mobility, production, and growth of cancer cells, as well as the chemical-dependent growth of regulatory and killer cells. After this, we can define jump probabilities in branching random walks on a lattice in physical and phenotypic space, formulating three coupled discrete agent-based models for the densities of cancer, regulatory and killer cells that are also coupled with a discrete finite difference equation for the concentration of the attractant. Through limit procedures, we formally derive the corresponding continuous model, composed of two partial integro-differential equations (IPDE) for the density of cancer and killer cells, coupled with two partial differential equations for the concentration of the chemical attractant and the density of regulatory cells. Despite the system's complexity, we show through formal asymptotic techniques that a detailed analysis within the framework of the travelling wave can be performed, obtaining invasion fronts with phenotypic

structure. As a preliminary step, we rescale the continuous model with appropriate powers of a small parameter ε, according to the biological relevance of the terms within the equations. Combining WKB ansatz for the density of cancer cells with asymptotic expansions, we derive an equation and a constraint for the new function u as $\varepsilon \to 0$. Through several mathematical steps, we obtain a transport equation for $\overline{y}(t, x)$, which is the dominant phenotypic trait at position x and time t. Shifting our focus to the traveling wave framework, we investigate the monotonicity of traveling front solutions, the wavefront position and the minimum propagation speed. We conclude that the maximum phenotypic trait $\overline{y}$ presents a monotonically increasing profile along the wave variable $z = x - ct$ while the density of cancer cells ρ has a decreasing behaviour. Finally, we can derive the profiles of the chemical concentration and densities of killer and regulatory cells using these results. As expected, mesenchymal cells dominate the wavefront while epithelial cells reside at the rear, following leader cell dynamics. Various scenarios are proposed to investigate how this spatial organisation influences the degree of infiltration of killer cells into the tumor. In particular, a tumour originating from a set of more mesenchymal cells shows less infiltration of killer cells and thus limited immune action than a tumour originating from more epithelial cells. The speed with which EMT is able to convert epithelial cells into mesenchymal cells also affects the penetration of killer cells. In this sense, a greater switiching rate implies a greater slope of the dominant phenotype curve $\overline{y}$ and thus the creation of a more protective immunosuppressive environment.

6.2 Research perspectives

The model presented here could be extended in many ways. Under the same assumptions, the model could be refined by choosing more suitable functions and parameters to fit with real data. For example, exploring various scenarios by choosing "ad hoc" proliferation functions for the regulatory and killer cells. Performing a sort of parametric study on these functions, one could investigate how these changes affect the penetration of killer cells and the position and speed of the wavefront. An interesting modelling alternative could be to neglect sources within the equations for regulatory and killer cells, giving more importance to the transport terms as the only ones dictating the migration. Rather than a "diffuse source" approach, we can consider an initial pool of regulatory and killer cells which move towards the tumour following chemical or physical stimuli (chemotaxis and density-driven migration). This approach has been investigated in Appendix, but it still needs to be refined in order to obtain reasonable outcomes.
Changing the model, we could also include haptotaxis as one of the causes of motion and study how the presence of regulatory/killer cells will affect this phenomenon. In this sense, a more mesenchymal phenotype would be linked with a greater secretion of MMP (metalloproteinases), which degrades the surrounding ECM (extracellular matrix) and helps the invasion process. From a mathematical point of view, this means adding to the system (2.10) two coupled evolutionary equations for the concentration of MMP and the density of ECM, resulting in some changes in the shapes of the solutions.
Another possibility would be to refine the current study by including intra-population phenotypic heterogeneity for regulatory and killer cells, leading to the differentiation of

the abilities of individual cells. This way, regulatory and killer cells would have different powers to eliminate cancer cells and to inhibit killer cells depending on their phenotypic state. Following this idea, we can also include phenotypic heterogeneity in the proliferation process, considering also the case in which cancer cells divide into daughter cells with a different phenotype.
Regarding the EMT-induced immunosuppression, it would be intriguing to study mathematically some other aspects revealed by experimental evidence [150]. Among them is the emergence of a mutant phenotypic variant that the selection mechanism establishes as the dominant trait within a tumour due to its high fitness and enhanced resistance to therapies. Of note is also the EMT-related phenomenon of "receptor switching" that makes targeted therapies fail, especially in breast tumours. In this sense, more specific models could be formulated to investigate the role of the EMT transcriptor factors (like Slug and Snail, ZEB-1 and TWIST) and EMT biomarkers (like E-cadherin and N-cadherin) which are involved in invasion and immune processes in certain types of cancers (breast, melanoma, mammary and lung tumour) [150].
Another attractive option would be to extend this model to a 2D domain in both physical and phenotypic space. In the physical space, this allows us to investigate the emergence of symmetric structures like spheroids and to study more in-depth the factors leading to a symmetry break with the arising of the so-called "tumour fingering". In the phenotypic space, a higher dimensionality enables decoupling some processes, which are taken as simultaneous in a 1D scenario, like the increase in motility and chemical secretion ability for mesenchymal cells. Of note, the model proposed in our work for carcinoma cells could be adapted to simulate other specific leader-follower cell dynamics, like the fibronectin-VEGF signalling in NSCLC (non-small cell lung cancer) [75].
A natural generalisation of this model is obtained by including pressure as the determining factor for migration in the equation $(2.10)_1$. Equations $(2.10)_1$ and $(2.10)_2$ would thus be replaced by the system

$$\begin{cases} \partial_t n - \alpha\, \mu(y)\, \partial_x \left(n\, \partial_x \mathcal{P}(t,x) \right) \right) = G(y, \mathcal{P}(t,x))\, n + \beta\, \partial^2_{yy} n - \gamma m_k n \\ \\ \mathcal{P} \equiv \Phi(\rho), \quad \rho(t,x) := \displaystyle\int_0^Y n(t,x,y)\, dy, \qquad\qquad (x,y) \in \mathbb{R} \times (0,Y) \end{cases} \tag{2.10mod}$$

imposing zero Neumann conditions at $y = 0$ and $y = Y$. In this formulation, $\mathcal{P}(t,x)$ is the pressure applied by cells residing at position x and time t, linked to the cell density $\rho(t,x)$ by the constitutive law $\Phi(\rho)$. In this sense, the model becomes more mechanistic and, under certain assumptions on the function $\Phi(\rho)$ [112], we recognise a porous medium equation governing the evolution of $\mathcal{P}$.
Ultimately, this work provides a starting point for the formulation of increasingly complex and precise models of tumour invasion which also take into account EMT-induced immunosuppressive effects given by the combined action of multiple types of agents, such as regulatory and killer cells in the specific cases of melanomas and carcinomas. We hope this work will provide interesting insights and enable further developments for future research in this area.

Chapter 7

Appendix

7.1 Another approach to the behaviour of m_K and m_R

Here, we present the initial approach that we have employed to study the behaviour of m_K and m_R that lead us to some unexpected conclusions. Firstly, we discuss a modelling assumption that differs from our actual work and then show how it affects the results. The essential difference is that now we switch from a "diffuse source" method to an approach that gives more importance to the transport component in the equations for m_R and m_K

Movement towards regions with higher density of cancer cells

The approach is similar to the one employed in Section 2.6.1 for the density-dependent movement of killer cells. To include the fact that the cancer gains a certain level of immunity when enough regulatory cells are present, we introduce the function $\chi_K(m_{R_i}^k)$ so that:

$$\frac{\mathrm{d}\chi_K}{\mathrm{d}m_R} < 0,$$

which represents the regulatory-dependent motility function of killer cells. We model χ_K as a decreasing function of m_R to reflect the tendency of killer cells to lose motility and reduce their migration towards cancer when lots of regulatory cells surround it. In other words, high m_R implies low m_K, which, in turn, results in an immunosuppressive action since only a few cancer cells are eliminated.
In particular, we can take:

$$\chi_K(m_R) = \psi_0 - \psi_1 \frac{m_R}{1 + m_R} \tag{2.9}$$

with ψ_0 that is the maximum mobility of a killer cell, reached when $m_R \to 0$ while ψ_1 is related with the minimum velocity of migration, that is $\psi_0 - \psi_1 > 0$ when $m_R \to \infty$. Calling $P_{FL_i}^k$ the probability that a regulatory cell in position x_i at time t_k ends up in

position x_{i-1} and $P^k_{FR_i}$ the probability to jump in position x_{i+1}, we have:

$$P^k_{FL_i} := \sigma\, \chi_K(m_{Ri}^k)\, \frac{(\rho^k_{i-1}-\rho^k_i)_+}{2\rho_{\max}}, \quad P^k_{FR_i} := \sigma\, \chi_k(m_{Ri}^k)\, \frac{(\rho^k_{i+1}-\rho^k_i)_+}{2\rho_{\max}} \text{with } (\cdot)_+ = \max(0,\cdot). \tag{1.26bis}$$

where $\sigma > 0$ is a scaling factor so that $\sigma\chi_K(m_{Ri}^k) \leq 1$ and $\rho_{\max}$ is the carrying capacity of the tumoral cell density. Obviously, the probability of not moving is given by:

$$P^k_{FS_i} = 1 - P^k_{FL_i} - P^k_{FR_i} \tag{1.27bis}$$

Using these newly defined probabilities, we derive the continuum model and switch to the travelling-wave framework. For the sake of simplicity, we neglect growth terms in the equations for m_K and m_R:

$$\Gamma_R(m_R, S) = 0, \quad \Gamma_K(m_R,\ m_K) = 0. \tag{3.2bis}$$

This is the case in which an initial concentration of regulatory and killer cells, located in a certain region, remains constant in number but can change its spatial distribution by moving towards cancer.Recalling the equations for m_K and m_R in (3.3) , properly rescaled with ε and assuming null growth (c.f. (3.2bis)):

$$\begin{aligned} \partial_t m_{R,\varepsilon}(x,t) + \ \partial_x(\ m_{R,\varepsilon}(x,t)\ \chi_R\ \partial_x S_\varepsilon(x,t)\ ) &= \varepsilon\ \partial^2_{xx} m_{R,\varepsilon}(x,t) \\ \partial_t m_{K,\varepsilon}(x,t) + \ \partial_x(\ m_{K,\varepsilon}(x,t)\ \chi_K(m_{R,\varepsilon})\ \partial_x \rho_\varepsilon(x,t)\ ) &= \varepsilon\ \partial^2_{xx} m_{K,\varepsilon}(x,t) \end{aligned} \tag{3.38bis}$$

Introducing expansions (3.7), (3.14), (3.17) into (3.38bis) and taking the limit for $\varepsilon \to 0$, we obtain equations for the leading-order term m_R and m_K:

$$\partial_t m_R(x,t) + \partial_x(\ m_R(x,t)\ \chi_R\ \partial_x S(x,t)\ ) = 0$$

and

$$\partial_t m_K(x,t) + \partial_x(\ m_K(x,t)\ \chi_K(m_K)\ \partial_x \rho(x,t)\ ) = 0$$

whose the travelling wave formulation is:

$$-c\ m_R'(z) + (m_R(z)\ \chi_R\ S'(z))' = 0 \tag{3.40bis}$$

and

$$-c\ m_K'(z) + (m_K(z)\ \chi_K(m_R)\ \rho'(z))' = 0 \tag{3.41bis}$$

We are searching for travelling waves $m_K(z)$ and $m_R(z)$ satisfying the asymptotic conditions :

$$\lim_{z\to+\infty} m_R(z) = m^0_R, \quad \lim_{z\to+\infty} m_K(z) = m^0_K, \tag{3.42bis}$$

that is like assuming a source of regulatory and killer cells for $z \to +\infty$ Therefore, by definition a travelling wave links two equilibriuum solution so

$$\lim_{z\to+\infty} S'(z) = 0, \quad \lim_{z\to+\infty} \rho'(z) = 0 \tag{3.43bis}$$

Integrating then (3.40bis) and (3.41bis) between z and $+\infty$, using (3.42bis) e (3.43bis), it results:

$$\int_z^{+\infty} \left(-c\, m_{_R}'(z) + (m_{_R}(z)\ \chi_{_R}\ S'(z))' \right)\ dz = 0 \quad \Rightarrow\ -c\, m_{_R}^0 + c\, m_{_R}(z) - m_{_R}(z)\chi_{_R}\ S'(z) = 0 \quad ,$$

$$\int_z^{+\infty} \left(-c\, m_{_K}'(z) + (m_{_K}(z)\ \chi_{_K}(m_{_R})\ \rho'(z))' \right)\ dz = 0 \quad \Rightarrow$$

$$-c\, m_{_K}^0 + c\, m_{_K}(z) - m_{_K}(z)\chi_{_K}(m_{_R}(z))\ \rho'(z) = 0 \quad .$$

From which we obtain an explicit form for $m_{_R}(z)$:

$$m_{_R} = \frac{m_{_R}^0}{1 - \frac{\chi_R}{c} S'(z)} \tag{3.44bis}$$

and for $m_{_K}(z)$:

$$m_{_K} = \frac{m_{_K}^0}{1 - \frac{\chi_K(\ m_{_R}(z))}{c} \rho'(z)} \tag{3.45bis}$$

These quantities are linked with S and ρ, whose behaviour is known from the asymptotic analysis previously executed. Expressions (3.44bis) and (3.45bis) lead us to unexpected conclusions. Firstly, to study the behaviour of $m_{_R}(z)$, we have to investigate how $S'(z)$ is. For some suitable choices of parameters and functions in (3.25), the shape of the wave representing the chemical factor $S(z)$ is a function reaching its maximum roughly at the front $z = l$. In light of these considerations, we expect $m_{_R}(z)$ to have a similar asymptotic behaviour as $S(z)$ since the only mechanism acting is the chemotactic movement that causes the regulatory cells to concentrate where $S(z)$ is greater.
Since $P(0) > 0$ (see (1.16)), we have

$$\lim_{z\to-\infty} S(z) = S^0 > \lim_{z\to+\infty} S(z) = 0.$$

Furthermore, it holds

$$\lim_{z\to\pm\infty} S'(z) = 0 \quad \Rightarrow \lim_{z\to\pm\infty} m_{_R}(z) = m_{_R}^0$$

This is the first surprising fact: we expect to have a larger accumulation of regulatory cells at $z \to -\infty$ rather than the source value $m_{_R}^0$ given at $+\infty$. Then, looking at the monotonicity of S, we can observe that the peak located in $z = l$ is preceded by a region in which S is increasing ($S'(z) > 0$) and followed by a region in which S is null since we are out of supp(ρ). According to the formula (3.44bis), this means that $m_R(z)$ is discontinuous at the front $z = l$, jumping from $m_{_R}^B > m_{_R}^0$ before the front to $m_{_R}^A = m_{_R}^0$ after. Similar considerations can be made looking at the formula (3.45bis). In this case, we physically expect to have a very low density in the bulk for $z \to -\infty$ because killer cells don't have any reason to penetrate due to the shielding effect of the barrier of regulatory cells at the front $z = l$. For $z \to +\infty$, we expect $m_{_K}$ to reach the maximum value since the regulatory density is low there (this coincides with the source $m_{_K}^0$ assumed at $z \to +\infty$). Clearly this is not happening in (3.45bis), because $\rho'(z) \to 0$ for $z \to -\infty$ implies $m_{_K}'(z) \to 0$ for

$z \to -\infty$. Therefore, from (3.32) we can conclude that $m_{_K} < m^0_{_K}$ for $z \in \text{supp}(\rho)$, while $m_{_K} = m^0_{_K}$ otherwise . So the profile of $m_{_K}$ starts from the value $m^0_{_K}$ for $z \to \infty$, then decreases for $z \in \text{supp}(\rho)$ until $z = l$ where it jumps to the constant value $m_{_K} = m^0_{_K}$ for $z \in (l, +\infty)$. By the way this behaviour is not totally wrong; the only strange fact is that the maximum value $m^0_{_K}$ is also attained at the bulk ($z \to -\infty$). Biologically speaking, this makes no sense: killer cells have no reason to be found deeply into the bulk, since their migration will be previously inhibited and blocked by the barrier made of regulatory cells at the front $z = l$. These results are consequences of the modelling choice of not including source terms in the evolutionary equations (3.38bis). This implies that the dynamics of $m_{_R}$ and $m_{_K}$ are dictated only by the transport terms and, as a consequence, are too strongly influenced by the initial condition given for $z \to +\infty$. This results in giving us outcomes that do not match biological expectations. For these reasons, in our work, we set aside this approach, including source terms into (3.38bis).

Bibliography

[1] N. Aceto, A. Bardia, and M. D. et al. Circulating tumor cell clusters are oligoclonal precursors of breast cancer metastasis. *Cell*, 158(5):1110–1122, 2014.

[2] N. Aiello, T. Brabletz, and K. Y. et al. Upholding a role for emt in pancreatic cancer metastasis. *Nature*, 547(7661):E7–E8, 2017.

[3] I. Akalay, B. Janji, and H. M. et al. Epithelial-to-mesenchymal transition and autophagy induction in breast carcinoma promote escape from t-cell-mediated lysis. *Cancer Res.*, 73(8):2418–2427, 2013.

[4] C. Aktipis, A. Boddy, R. Gatenby, J. Brown, and C. Maley. Life history trade-offs in cancer evolution. *Nat. Rev. Cancer*, 13:883, 2013.

[5] J. Alfonso, M. Talkenberger, and S. M. et al. The biology and mathematical modelling of glioma invasion: A review. *J. R. Soc. Interface* 2017, 14 (136):20170490, 2017.

[6] D. Ambrosi and L. Preziosi. On the closure of mass balance models for tumor growth. *Math. Mod. and Meth. in Appl. Sci.*, 12:737–754, 2002.

[7] V. Andasari, A. Gerisch, and L. G. et al. Mathematical modeling of cancer cell invasion of tissue: Biological insight from mathematical analysis and computational simulation. *J. Math. Biol.*, 63(1):141–171, 2011.

[8] A. Anderson and M. Chaplain. Continuous and discrete mathematical models of tumor-induced angiogenesis. *Bull. Math. Biol.*, 60(5):857–899, 1998.

[9] A. Anderson, A. Weaver, P. Cummings, and V. Quaranta. Tumor morphology and phenotypic evolution driven by selective pressure from the microenvironment. *Cell*, 127(5):905–915, 2006.

[10] A. R. A. Anderson, M. A. J. Chaplain, and E. L. Newman. Mathematical modelling of tumour invasion and metastasis. *Comput. Math. Meth. Med.*, 2(2):129–154, 2000.

[11] A. Arnold, L. Desvillettes, and C. Prevost. Existence of nontrivial steady states for populations structured with respect to space and a continuous trait. *Comm. on Pure and App. An.*, 11:83, 2012.

[12] D. Barkan, H. Kleinman, J. Simmons, H. Asmussen, and K. A. et al. Inhibition of metastatic outgrowth from single dormant tumor cells by targeting the cytoskeleton. *Cancer Res.*, 68:6241–6250, 2008.

[13] G. Barles, L. Evans, and P. Souganidis. Wavefront propagation for reaction-diffusion systems of pde. *Duke Math. Journ.*, 61:835–858, 1989.

[14] G. Barles, S. Mirrahimi, and B. Perthame. Concentration in lotka-volterra parabolic or integral equations: A general convergence result. *Meth. Appl. Anal.*, 16(3):321–340, 2009.

[15] O. Benichou, V. Calvez, N. Meunier, and R. Voituriez. Front acceleration by dynamic selection in fisher population waves. *Physical Review E* 2012, 86:041908, 2012.

[16] N. Berestycki, C. Mouhot, and G. Raoul. Existence of self-accelerating fronts for a non-local reaction-diffusion equations. *arXiv: Analysis of PDEs*, 2015.

[17] G. Berx, A. Cleton-Jansen, and S. K. et al. E-cadherin is inactivated in a majority of invasive human lobular breast cancers by truncation mutations throughout its extracellular domain. *Oncogene*, 13(9):1919–1925, 1996.

[18] A. Bortuli, I. Freire, and N. Maidana. Group classification and analytical solutions of a radially symmetric avascular cancer model. *Stud. Appl. Math.*, 147(3):978–1006, 2021.

[19] E. Bouin and V. Calvez. Travelling waves for the cane toads equation with bounded traits. *Nonlinearity*, 27:2233, 2014.

[20] E. Bouin, V. Calvez, N. Meunier, S. Mirrahimi, B. Perthame, G. Raoul, and R. Voituriez. Invasion fronts with variable motility: phenotype selection, spatial sorting and wave acceleration. *Comp. Rend. Math.*, 350:761–766, 2012.

[21] E. Bouin, C. Henderson, and L. Ryzhik. The bramson logarithmic delay in the cane toads equations. *Quart. of Appl. Math.*, 75:599–634, 2017.

[22] E. Bouin, C. Henderson, and L. Ryzhik. Super-linear spreading in local and non-local cane toads equations. *Jour. de Math. Pur. et Appl.*, 108:724–750, 2017.

[23] T. Brabletz, A. Jung, S. Spaderna, F. Hlubek, and T. Kirchner. Opinion: migrating cancer stem cells — an integrated concept of malignant tumour progression. *Nat Rev Cancer*, 5(9):744–749, 2005.

[24] F. Bubba, T. Lorenzi, and F. Macfarlane. From a discrete model of chemotaxis with volume filling to a generalized patlak–keller–segel model. *Proc. R. Soc. A*, 476(2237):20190871, 2020.

[25] L. Byers, L. Diao, and W. J. et al. An epithelial-mesenchymal transition gene signature predicts resistance to egfr and pi3k inhibitors and identifies axl as a therapeutic target for overcoming egfr inhibitor resistance. *Clin. Cancer Res.*, 19(1):279–290, 2013.

[26] H. M. Byrne and D. Drasdo. Individual-based and continuum models of growing cell populations: a comparison. *Journ. of Math. Biol.*, 58:657, 2009.

[27] P. Carmeliet and R. Jain. Principles and mechanisms of vessel normalization for cancer and other angiogenic diseases. *Nat. Rev. Drug Discov.*, 10:417–427, 2011.

[28] E. Carver, R. Jiang, Y. Lan, K. Oram, and T. Gridley. The mouse snail gene encodes a key regulator of the epithelial-mesenchymal transition. *Mol. Cell. Biol.*, 21(23):8184–8188, 2001 Dec.

[29] C. Chaffer, I. Brueckmann, C. Scheel, A. Kaestli, P. Wiggins, L. Rodrigues, M. Brooks, F. Reinhardt, Y. Su, K. Polyak, L. Arendt, C. Kuperwasser, B. Bierie, and R. Weinberg. Normal and neoplastic nonstem cells can spontaneously convert to a stemlike state. *Proc. Natl. Acad. Sci.*, 108(19):7950–7955, 2011.

[30] C. Chaffer, N. Marjanovic, T. Lee, G. Bell, C. Kleer, F. Reinhardt, A. D'Alessio, R. Young, and R. Weinberg. Poised chromatin at the zeb1 promoter enables breast cancer cell plasticity and enhances tumorigenicity. *Cell*, 154(1):61–74, 2013.

[31] A. Chambers, A. Groom, and I. MacDonald. Dissemination and growth of cancer cells in metastatic sites. *Nat. Rev. Cancer*, 2:563–572., 2002.

[32] M. Chaplain and G. Lolas. Mathematical modelling of cancer cell invasion of tissue: The role of the urokinase plasminogen activation system. *Math. Model. Meth. Appl. Sci.*, 15(11):1685–1734, 2005.

[33] M. Chaplain, T. Lorenzi, and F. Macfarlane. Bridging the gap between individual-based and continuum models of growing cell populations. *J. Math. Biol.*, 80:343–371, 2020.

[34] L. Chen, D. Gibbons, and G. S. et al. Metastasis is regulated via microrna-200/zeb1 axis control of tumour cell pd-l1 expression and intratumoral immunosuppression. *Nat. Commun.*, 5(1):5241, 2014.

[35] Z. Chen and R. Behringer. Twist is required in head mesenchyme for cranial neural tube morphogenesis. *Genes. Dev.*, 9(6):686–699, 1995.

[36] K. Cheung, V. Padmanaban, and S. V. et al. Polyclonal breast cancer metastases arise from collective dissemination of keratin 14-expressing tumor cell clusters. *Proc. Natl. Acad. Sci.* USA, 113(7):E854–E863, 2016.

[37] P. Ciarletta, L. Foret, and M. Ben Amar. The radial growth phase of malignant melanoma: Multi-phase modelling, numerical simulations and linear stability analysis. *J. R. Soc. Interface*, 8(56):345–368, 2011.

[38] I. Dagogo-Jack and A. Shaw. Tumour heterogeneity and resistance to cancer therapies. *Nat. Rev. Clin. Oncol.* 2018, 15(2):81–94, 2018.

[39] Y. Del Pozo Martin, D. Park, A. Ramachandran, L. Ombrato, F. Calvo, P. Chakravarty, B. Spencer-Dene, S. Derzsi, C. Hill, E. Sahai, and I. Malanchi. Mesenchymal cancer cell-stroma crosstalk promotes niche activation, epithelial reversion, and metastatic colonization. *Cell Rep.*, 13(11):2456–2469, 2015.

[40] J. Dembinski and S. Krauss. Characterization and functional analysis of a slow cycling stem cell-like subpopulation in pancreas adenocarcinoma. *Clin. Exp. Met.*, 26(7):611–623, 2009.

[41] O. Diekmann, P. E. Jabin, S. Mischler, and B. Perthame. The dynamics of adaptation: An illuminating example and a hamilton–jacobi approach. *Theor. Popul. Biol*, 67(4):257–271, 2005.

[42] A. Dongre, M. Rashidian, and R. F. et al. Epithelial-to-mesenchymal transition contributes to immunosuppression in breast carcinomas. *Cancer Res.*, 77(15):3982–3989, 2017.

[43] . *NCI Dictionary of Cancer Terms*. Nat. Canc. Inst., .

[44] L. Evans and P. Souganidis. A pde approach to geometric optics for certain semilinear parabolic equations. *Indiana Univ. Math. Jour.*, 38:141–172, 1989.

[45] G. Fiandaca, S. Bernardi, M. Scianna, and M. Delitala. A phenotype-structured model to reproduce the avascular growth of a tumor and its interaction with the surrounding environment. *J. Theor. Biol.*, 535:110980, 2022.

[46] G. Fiandaca, M. Delitala, and T. Lorenzi. A mathematical study of the influence of hypoxia and acidity on the evolutionary dynamics of cancer. *Bull. Math. Biol.*, 83(7):83, 2021.

[47] I. Fidler. The pathogenesis of cancer metastasis: the 'seed and soil' hypothesis revisited. *Nat. Rev. Cancer*, 3:453–458, 2003.

[48] W. Fleming and P. Souganidis. Pde-viscosity solution approach to some problems of large deviations. *Annali della Sc. Norm. Sup. di Pisa-Classe di Scienze*, 13:171–192, 1986.

[49] L. Franssen, T. Lorenzi, and M. Burgess, AEF et Chaplain. A mathematical framework for modelling the metastatic spread of cancer. *Bull. Math. Biol.*, 81(6):1965–2010, 2019.

[50] P. Friedl and D. Gilmour. Collective cell migration in morphogenesis, regeneration and cancer. *Nat. Rev. Mol. Cell. Biol.*, 10(7):445–457, 2009.

[51] P. Friedl, J. Locker, S. E, and J. Segall. Classifying collective cancer cell invasion. *Nat. Cell Biol.*, 14(8):777–783, 2012.

[52] J. Gallaher, J. Brown, and A. Anderson. The impact of proliferation-migration tradeoffs on phenotypic evolution in cancer. *Sci. Rep.*, 9:1–10, 2019.

[53] A. Gerisch and M. Chaplain. Mathematical modelling of cancer cell invasion of tissue: Local and non-local models and the effect of adhesion. *J. Theor. Biol.*, 250(4):684–704., 2008.

[54] P. Gerlee and A. Anderson. Evolution of cell motility in an individual-based model of tumour growth. *Jour. of Theor. Biol.*, 259:67–83, 2009.

[55] P. Gerlee and S. Nelander. The impact of phenotypic switching on glioblastoma growth and invasion. *PLoS Comp. Biol.*, 8:e1002556, 2012.

[56] M. Gerlinger, A. Rowan, and H. S. et al. Intratumor heterogeneity and branched evolution revealed by multiregion sequencing. *N. Engl. J. Med.*, 366(10):883–892, 2012.

[57] A. Giese, R. Bjerkvig, M. Berens, and W. Westphal. Cost of migration: invasion of malignant gliomas and implications for treatment. *Jour. of Clin. Onc.*, 21:1624–1636, 2003.

[58] A. Giese, M. Loo, N. Tran, D. Haskett, S. Coons, and M. Berens. Dichotomy of astrocytoma migration and proliferation. *Inter. Jour. of Canc.*, 67:275–282, 1996.

[59] C. Gjerdrum, C. Tiron, and H. T. et al. Axl is an essential epithelial-to-mesenchymal transition-induced regulator of breast cancer metastasis and patient survival. *Proc. Natl. Acad. Sci.* USA, 107(3):1124–1129, 2010.

[60] W. Guo and F. Giancotti. Integrin signalling during tumour progression. *Nat. Rev. Mol. Cell Biol.*, 5:816–826, 2004.

[61] W. Guo, Z. Keckesova, J. Donaher, T. Shibue, V. Tischler, F. Reinhardt, S. Itzkovitz, A. Noske, U. Zürrer-Härdi, G. Bell, W. Tam, S. Mani, A. van Oudenaarden, and R. Weinberg. Slug and sox9 cooperatively determine the mammary stem cell state. *Cell*, 148(5):1015–1028, 2012.

[62] G. Gupta, D. Nguyen, A. Chiang, and B. P. et al. Mediators of vascular remodelling co-opted for sequential steps in lung metastasis. *Nature*, 446:765–770, 2007.

[63] F. Hamel and L. Ryzhik. On the nonlocal fisher-kpp equation: steady states, spreading speed and global bounds,. *Nonlinearity*, 27:2735, 2014.

[64] D. Hamilton, B. Huang, and F. R. et al. Wee1 inhibition alleviates resistance to immune attack of tumor cells undergoing epithelial-mesenchymal transition. *Cancer Res.*, 74(9):2510–2519, 2014.

[65] A. Hata, M. Niederst, and A. H. et al. Tumour cells can follow distinct evolutionary paths to become resistant to epidermal growth factor receptor inhibition. *Nat. Med.*, 22(3):262–269, 2016.

[66] H. Hatzikirou, D. Basanta, M. Simon, K. Schaller, and A. Deutsch. 'go or grow': the key to the emergence of invasion in tumour progression? *Math. Med. and Biol.* 2012, 29:49–65, 2012.

[67] M. Heiss, H. Allgayer, and G. K. et al. Individual development and upa-receptor expression of disseminated tumour cells in bone marrow: a reference to early systemic disease in solid cancer. *Nat. Med.*, 1(10):1035–1039, 1995.

[68] S. Herbertz, J. Sawyer, and S. A. et al. Clinical development of galunisertib (ly2157299 monohydrate), a small molecule inhibitor of transforming growth factor-β signaling pathway. *Drug Des. Devel. Ther.*, 9:4479–4499, 2015.

[69] Y. Higashi, H. Moribe, T. Takagi, R. Sekido, K. Kawakami, H. Kikutani, and H. Kondoh. Impairment of t cell development in δEF1 mutant mice. *J. Exp. Med.*, 185(8):1467–1479, 1997.

[70] S. Huang. Genetic and non-genetic instability in tumor progression: link between the fitness landscape and the epigenetic landscape of cancer cells. *Canc. and Met. Rev.*, 32:423–448, 2013.

[71] R. Jiang, Y. Lan, C. Norton, J. Sundberg, and T. Gridley. The slug gene is not essential for mesoderm or neural crest development in mice. *Dev. Biol.*, 198(2):277–285, 1998.

[72] J. Joyce and J. Pollard. Microenvironmental regulation of metastasis. *Nat. Rev. Cancer*, 9:239–252, 2009.

[73] S. Kang, O. Halvorsen, K. Gravdal, and B. N. et al. Prosaposin inhibits tumor metastasis via paracrine and endocrine stimulation of stromal p53 and tsp-1. *Proc. Natl. Acad. Sci. USA*, 106:12115–12120, 2009.

[74] N. Kolbe, N. Sfakianakis, and S. C. et al. Modeling multiple taxis: Tumor invasion with phenotypic heterogeneity, haptotaxis, and unilateral interspecies repellence. *Disc. Contin. Dyn. Syst.*, 26(1):443–481, 2021.

[75] J. Konen, E. Summerbell, and D. B. et al. Image-guided genomics of phenotypically heterogeneous populations reveals vascular signalling during symbiotic collective cancer invasion. *Nat. Comm.*, 8(1):1–15, 2017.

[76] A. Krebs, J. Mitschke, and L. L. M. et al. The emt-activator zeb1 is a key factor for cell plasticity and promotes metastasis in pancreatic cancer. *Nat. Cell Biol.*, 19(5):518–529, 2017.

[77] C. Kudo-Saito, H. Shirako, and T. T. et al. Cancer metastasis is accelerated through immunosuppression during snail-induced emt of cancer cells. *Canc. Cell*, 15(3):195–206, 2009.

[78] A. Lambert, D. Pattabiraman, and R. Weinberg. Emerging biological principles of metastasis. *Cell*, 168(4):670–691, 2017.

[79] S. Lamouille, J. Xu, and R. Derynck. Molecular mechanisms of epithelial-mesenchymal transition. *Nat. Rev. Mol. Cell Biol.*, 15(3):178–196, 2014.

[80] D. Lawson, N. Bhakta, K. Kessenbrock, K. Prummel, Y. Yu, K. Takai, A. Zhou, H. Eyob, S. Balakrishnan, C. Wang, P. Yaswen, A. Goga, and Z. Werb. Single-cell analysis reveals a stem-cell program in human metastatic breast cancer cells. *Nature*, 526(7571):131–135, 2015.

[81] J. Lim and J. Thiery. Epithelial-mesenchymal transitions: insights from development. *Development*, 139(19):3471–3486, 2012.

[82] T. Lorenzi, F. Macfarlane, and K. Painter. Derivation and travelling wave analysis of phenotype-structured haptotaxis models of cancer invasion. *Europ. Jour. of Appl. Math.*, pages 1–33, 2024.

[83] T. Lorenzi and K. Painter. Trade-offs between chemotaxis and proliferation shape the phenotypic structuring of invading waves. *Int. J. Non-Linear Mech.*, 139:103885, 2022.

[84] T. Lorenzi, B. Perthame, and X. Ruan. Invasion fronts and adaptive dynamics in a model for the growth of cell populations with heterogeneous mobility. *Eur. J. Appl. Math.*, pages 1–18, 2021.

[85] T. Lorenzi, C. Venkataraman, A. Lorz, and M. Chaplain. The role of spatial variations of abiotic factors in mediating intratumour phenotypic heterogeneity. *J. Theor. Biol.*, 451:101–110, 2018.

[86] A. Lorz, S. Mirrahimi, and B. Perthame. Dirac mass dynamics in multidimensional nonlocal parabolic equations. *Commun. Partial. Differ. Equ.*, 36(6):1071–1098, 2011.

[87] F. Macfarlane, X. Ruan, and T. Lorenzi. Individual-based and continuum models of phenotypically heterogeneous growing cell populations. *AIMS Bioeng.*, 9(1):68–92, 2022.

[88] S. Mani, W. Guo, M. Liao, E. Eaton, A. Ayyanan, A. Zhou, M. Brooks, F. Reinhard, C. Zhang, M. Shipitsin, L. Campbell, K. Polyak, C. Brisken, J. Yang, and R. Weinberg. The epithelial-mesenchymal transition generates cells with properties of stem cells. *Cell*, 133(4):704–715, 2008.

[89] T. Martin, L. Ye, and A. e. a. Sanders. Cancer invasion and metastasis: Molecular and cellular perspective. *Mad. Curie Bio. Dat. Austin (TX): Lan. Bio.*, :, 2000-2013.

[90] C. Meacham and S. Morrison. Tumour heterogeneity and cancer cell plasticity. *Nature*, 501(7467):328–337, 2013.

[91] P. Mehlen and A. Puisieux. Metastasis: a question of life or death. *Nat Rev Cancer* 2006, 6(6):449–458, 2006.

[92] S. Meng, D. Tripathy, and F. E. et al. Circulating tumor cells in patients with breast cancer dormancy. *Clin. Canc. Res.*, 10(24):8152–8162, 2004.

[93] S. Meng, D. Tripathy, E. Frenkel, S. Shete, E. Naftalis, J. Huth, P. Beitsch, M. Leitch, S. Hoover, and E. D. et al. Circulating tumor cells in patients with breast cancer dormancy. *Clin. Cancer Res.*, 10:8152–8162, 2004.

[94] D. Micalizzi, S. Farabaugh, and H. Ford. Epithelial-mesenchymal transition in cancer: parallels between normal development and tumor progression. *J. Mammary Gland. Biol. Neoplasia*, 15(2):117–134, 2010.

[95] G. Naumov, I. MacDonald, and W. P. et al. Persistence of solitary mammary carcinoma cells in a secondary site: a possible contributor to dormancy. *Cancer Res.*, 62(7):2162–2168, 2002.

[96] M. Nieto, R. Huang, R. Jackson, and J. Thiery. EMT. *Cell.*, 166(1):21–45, 2016 Jun 30.

[97] M. Noman, B. Janji, and A. A. et al. The immune checkpoint ligand pd-l1 is upregulated in emt-activated human breast cancer cells by a mechanism involving zeb-1 and mir-200. *Oncoimmunology*, 6(1):e1263412, 2017.

[98] O. Ocaña, R. Córcoles, A. Fabra, G. Moreno-Bueno, H. Acloque, S. Vega, A. Barrallo-Gimeno, A. Cano, and M. Nieto. Metastatic colonization requires the repression of the epithelial-mesenchymal transition inducer prrx1. *Cancer Cell*, 22(6):709–724, 2012.

[99] B. Oliveira, C. Dalmaz, and Zeidán-Chuliá. Network-based identification of altered stem cell pluripotency and calcium signaling pathways in metastatic melanoma. *F. Med. Sci.*, 6(1):23, 2018.

[100] P. Orlando, R. Gatenby, and J. Brown. Tumor evolution in space: the effects of competition colonization tradeoffs on tumor invasion dynamics. *Front. in Onc.*, 3:45, 2013.

[101] B. Orsolits, Z. Kovács, J. Kriston-Vizi, B. Merkely, and G. Földes. New modalities of 3d pluripotent stem cell-based assays in cardiovascular toxicity. *Front. Pharmacol.*, 12:603016, 2021.

[102] D. Padua, X. Zhang, Q. Wang, C. Nadal, and G. W. et al. Tgfbeta primes breast tumors for lung metastasis seeding through angiopoietin-like 4. *Cell*, 133:66–77, 2008.

[103] K. Painter. Mathematical models for chemotaxis and their applications in self-organisation phenomena. *J. Theor. Biol.*, 481:162–182, 2019.

[104] K. Painter, N. Armstrong, and J. Sherratt. The impact of adhesion on cellular invasion processes in cancer and development. *J. Theor. Biol.*, 264(3):1057–1067, 2010.

[105] I. Pastushenko, A. Brisebarre, and S. A. et al. Identification of the tumour transition states occurring during emt. *Nature*, 556(7702):463–468, 2018.

[106] D. Pattabiraman, B. Bierie, and K. K. et al. Activation of pka leads to mesenchymal-to-epithelial transition and loss of tumor-initiating ability. *Science*, 351(6277):aad3680, 2016.

[107] D. Pattabiraman and R. Weinberg. Tackling the cancer stem cells—what challenges do they pose? *Nat. Rev. Drug. Discov.*, 13(7):497–512, 2014.

[108] H. Peinado, D. Olmeda, and A. Cano. Snail, zeb and bhlh factors in tumour progression: an alliance against the epithelial phenotype? *Nat. Rev. Canc.*, 7(6):415–428, 2007.

[109] C. Penington, B. Hughes, and K. Landman. Building macroscale models from microscale probabilistic models: A general probabilistic approach for nonlinear diffusion and multispecies phenomena. *Phys. Rev. E*, 84(4):041120, 2011.

[110] B. Perthame. *Transport equations in biology* 2006. Springer Science and Business Media, 2006.

[111] B. Perthame and G. Barles. Dirac concentrations in lotka-volterra parabolic pdes. *Indiana Univ. Math. J.*, 57(7):3275–3301, 2008.

[112] B. Perthame, F. Quiros, and J. L. Vazquez. The hele-shaw asymptotics for mechanical models of tumor growth. *Archive for Rational Mechanics and Analysis* 2014, 212:93–127, 2014.

[113] K. Pham, A. Chauviere, and H. Hatzikirou. Density-dependent quiescence in glioma invasion: Instability in a simple reaction–diffusion model for the migration/proliferation dichotomy. *J. Biol. Dyn. (sup1)*, 6:54–71, 2012.

[114] B. Phillips, G. Brown, J. Webb, and R. Shine. Invasion and the evolution of speed in toads. *Nature*, 439:803, 2006.

[115] B. Psaila and D. Lyden. The metastatic niche: adapting the foreign soil. *Nat. Rev. Cancer*, 9:285–293, 2009.

[116] S. Puram, I. Tirosh, and P. A. et al. Single-cell transcriptomic analysis of primary and metastatic tumor ecosystems in head and neck cancer. *Cell*, 171(7):1611–1624 e24, 2017.

[117] B. Qian and J. Pollard. Macrophage diversity enhances tumor progression and metastasis. *Cell*, 141:39–51, 2010.

[118] D. Quail and J. Joyce. Microenvironmental regulation of tumor progression and metastasis. *Nat. Med.*, 19(11):1423–1437, 2013.

[119] C. Revenu and D. Gilmour. Emt 2.0: shaping epithelia through collective migration. *Curr. Opin. Genet. Dev.*, 19(4):338–342, 2009.

[120] M. Saxena, M. Stephens, H. Pathak, and A. Rangarajan. Transcription factors that mediate epithelial-mesenchymal transition lead to multidrug resistance by upregulating abc transporters. *Cell Death Dis.*, 2(7):e179–e179, 2011.

[121] N. Sfakianakis and M. Chaplain. Mathematical modelling of cancer invasion: A review. *International Conference by Center for Mathematical Modeling and Data Science, Osaka University*, pages 153–172 , Springer, 2020.

[122] M. Shackleton, E. Quintana, and F. E. et al. Heterogeneity in cancer: cancer stem cells versus clonal evolution. *Cell*, 138(5):822–829, 2009.

[123] L. Shangerganesh, N. Nyamoradi, and S. G. et al. Finite-time blow-up of solutions to a cancer invasion mathematical model with haptotaxis effects. *Comput. Math. Appl.*, 77(8):2242–2254, 2019.

[124] T. Shaw and P. Martin. Wound repair: a showcase for cell plasticity and migration. *P. Curr. Opin. Cell. Biol.*, 42:29–37, 2016.

[125] T. Shibue and R. Weinberg. Emt, cscs, and drug resistance: the mechanistic link and clinical implications. *Nat. Rev. Clin. Oncol.*, 14(10):611–629, 2017.

[126] R. Shine. A review of ecological interactions between native frogs and invasive cane toads in australia,. *Aust. Ecology*, 39:1–16, 2014.

[127] R. Shine, G. Brown, and B. Phillips. An evolutionary process that assembles phenotypes through space rather than through time,. *Proc. of the Nat. Acad. of Sc.*, 108:5708–5711, 2011.

[128] T. Stepien, E. Rutter, and Y. Kuang. Traveling waves of a go-or-grow model of glioma growth. *SIAM J. Appl. Math.*, 78(3):1778–1801, 2018.

[129] A. Stevens and H. Othmer. Aggregation, blowup, and collapse: The abc's of taxis in reinforced random walks. *SIAM J. Appl. Math.*, 57(4):1044–1081, 1997.

[130] M. Strobl, A. Krause, and D. M. et al. Mix and match: Phenotypic coexistence as a key facilitator of cancer invasion. *Bull. Math. Biol.*, 82:1–26, 2020.

[131] S. Terry, P. Savagner, and O.-C. S. et al. New insights into the role of emt in tumor immune escape. *Mol. Oncol.*, 11(7):824–846, 2017.

[132] J. Textor, M. Sinn, and R. J. De Boer. Analytical results on the beauchemin model of lymphocyte migration. *BMC Bioinf. Biomed. Centr.*, 14:1–15, 2013.

[133] J. Thiery. Epithelial-mesenchymal transitions in tumour progression. *Nat. Rev. Canc.*, 2(6):442–454, 2002.

[134] J. Thiery, H. Acloque, and H. R. et al. Epithelial-mesenchymal transitions in development and disease. *Cell*, 139(5):871–890, 2009.

[135] L. Thompson, B. Chang, and S. Barsky. Monoclonal origins of malignant mixed tumors (carcinosarcomas). evidence for a divergent histogenesis. *Am. J. Surg. Pathol.*, 20(3):277–285, 1996.

[136] J. Tsai, J. Donaher, D. Murphy, S. Chau, and J. Yang. Spatiotemporal regulation of epithelial-mesenchymal transition is essential for squamous cell carcinoma metastasis. *Cancer Cell*, 22(6):725–736, 2012.

[137] O. Turanova. On a model of a population with variable motility. *Math. Mod. and Meth. in Appl. Sci.*, 25:1961–2014, 2015.

[138] M. Urban, B. Phillips, D. Skelly, and R. Shine. A toad more traveled: the heterogeneous invasion dynamics of cane toads in australia. *The Am. Nat.*, 171:E134–E148, 2008.

[139] S. Valastyan and R. Weinberg. Tumor metastasis: molecular insights and evolving paradigms. *Cell*, 147(2):275–92, 2011.

[140] T. Van de Putte, M. Maruhashi, A. Francis, L. Nelles, H. Kondoh, D. Huylebroeck, and Y. Higashi. Mice lacking zfhx1b, the gene that codes for smad-interacting protein-1, reveal a role for multiple neural crest cell defects in the etiology of hirschsprung diseasemental retardation syndrome. *Am. J. Hum. Genet.*, 72(2):465–470, 2003.

[141] S. Vega, A. Morales, and O. O. et al. Snail blocks the cell cycle and confers resistance to cell death. *Genes. Dev.*, 18(10):1131–1143, 2004.

[142] S. A. Vilchez Mercedes, F. Bocci, H. Levine, J. N. Onuchic, M. K. Jolly, and P. K. Wong. Decoding leader cells in collective cancer invasion. *Nat. Rev. Cancer*, 9:21, 2021.

[143] C. Villa, M. Chaplain, and T. Lorenzi. Modeling the emergence of phenotypic heterogeneity in vascularized tumors. *SIAM J. Appl. Math.* 2021, 81(2):434–453, 2021.

[144] W. Wang, S. Goswami, K. Lapidus, A. Wells, J. Wyckoff, E. Sahai, R. Singer, J. Segall, and Condeelis. Identification and testing of a gene expression signature of invasive carcinoma cells within primary mammary tumors. *J. Cancer Res.*, 64:8585–8594, 2004.

[145] Z. Wang, J. Butner, and K. R. et al. Simulating cancer growth with multiscale agent-based modeling. *In Sem. Cancer Biol. Elsevier*, 30:70–78, 2015.

[146] J. West, M. Robertson-Tessi, and A. Anderson. Agent-based methods facilitate integrative science in cancer. *Trends Cell Biol.*, 33(4):300–311, 2022.

[147] J. Westcott, A. Prechtl, and E. Maine. An epigenetically distinct breast cancer cell subpopulation promotes collective invasion. *J. Clin. Invest.*, 125(5):1927–1943, 2015.

[148] X. Ye, W. Tam, and S. T. et al. Distinct emt programs control normal mammary stem cells and tumour-initiating cells. *Nature*, 525(7568):256–260, 2015.

[149] M. Yu, A. Bardia, and W. B. et al. Circulating breast tumor cells exhibit dynamic changes in epithelial and mesenchymal composition. *Science*, 339(6119):580–584, 2013.

[150] Y. Zhang and R. Weinberg. Epithelial-to-mesenchymal transition in cancer: complexity and opportunities. *Front. Med.*, 12:361–373, 2018.

[151] X. Zheng, J. Carstens, and K. J. et al. Epithelial-to-mesenchymal transition is dispensable for metastasis but induces chemoresistance in pancreatic cancer. *Nature*, 527(7579):525–530, 2015.